

Chiral spectrum of the universal tuned $(\text{SU}(3) \times \text{SU}(2) \times \text{U}(1))/\mathbb{Z}_6$ 4D F-theory model

Patrick Jefferson,[†] Washington Taylor,[†] and Andrew P. Turner[‡]

[†]*Center for Theoretical Physics
Department of Physics
Massachusetts Institute of Technology
77 Massachusetts Avenue
Cambridge, MA 02139, USA*

[‡]*Department of Physics and Astronomy
University of Pennsylvania
Philadelphia, PA 19104, USA*

E-mail: `pjeffers at mit.edu`, `wati at mit.edu`, `turnerap at sas.upenn.edu`

ABSTRACT:

We use the recently developed methods of [2108.07810](#) to analyze vertical flux backgrounds and associated chiral matter spectra in the 4D universal $(\text{SU}(3) \times \text{SU}(2) \times \text{U}(1))/\mathbb{Z}_6$ model introduced in [1912.10991](#), which is believed to describe the most generic family of F-theory vacua with tuned $(\text{SU}(3) \times \text{SU}(2) \times \text{U}(1))/\mathbb{Z}_6$ gauge symmetry. Our analysis focuses on a resolution of a particular presentation of the $(\text{SU}(3) \times \text{SU}(2) \times \text{U}(1))/\mathbb{Z}_6$ model in which the elliptic fiber is realized as a cubic in \mathbb{P}^2 fibered over an arbitrary smooth threefold base. We show that vertical fluxes can produce nonzero multiplicities for all chiral matter families that satisfy 4D anomaly cancellation, which include as a special case the chiral matter families of the Minimal Supersymmetric Standard Model.

Contents

1	Introduction	1
2	Summary of results	4
2.1	Resolution of singularities and 4D kinematics	4
2.2	Vertical flux backgrounds and chiral matter spectrum	7
3	Basic setup and resolution	9
4	Codimension one: gauge symmetry	13
4.1	$u(1)$	13
4.2	$\mathfrak{su}(3) \oplus \mathfrak{su}(2)$	14
5	Codimension two: local matter	15
5.1	Kaluza–Klein charges	15
5.2	$(\mathbf{1}, \mathbf{1})_{w_{\bar{1}}}$	17
5.3	$(\mathbf{1}, \mathbf{2})_{w_{\bar{1}}}$	18
5.4	$(\mathbf{3}, \mathbf{1})_{w_{\bar{1}}}$	19
5.5	$(\mathbf{3}, \mathbf{2})_{w_{\bar{1}}}$	21
6	Codimension three: Yukawa interactions	23
6.1	$(\mathbf{3}^*, \mathbf{2})_{w_{\bar{1}}} \times (\mathbf{3}, \mathbf{1})_{w'_{\bar{1}}} \times (\mathbf{1}, \mathbf{2})_{w''_{\bar{1}}}$	26
6.2	$(\mathbf{3}^*, \mathbf{1})_{w_{\bar{1}}} \times (\mathbf{3}, \mathbf{1})_{w'_{\bar{1}}} \times (\mathbf{1}, \mathbf{1})_{w''_{\bar{1}}}$	28
6.3	$(\mathbf{1}, \mathbf{2})_{w_{\bar{1}}} \times (\mathbf{1}, \mathbf{2})_{w'_{\bar{1}}} \times (\mathbf{1}, \mathbf{1})_{w''_{\bar{1}}}$	30
7	Intersection theory, 3D Chern–Simons couplings, and chiral matter multiplicities	31
7.1	Quadruple intersection numbers and the reduced intersection matrix	31
7.2	Fluxes preserving 4D $(SU(3) \times SU(2) \times U(1))/\mathbb{Z}_6$ gauge symmetry	36
7.2.1	Fluxes through vertical surfaces	36
7.2.2	Symmetry constraints	37
7.2.3	Integrality of the second Chern class	37
7.3	3D Chern–Simons couplings	40
7.4	Chiral indices	43
7.5	Chiral spectrum	45
7.6	Alternative treatment of the symmetry constraints	49

8	Examples	50
8.1	$B = \mathbb{P}^3$	50
8.1.1	$B = \mathbb{P}^3$ as a special case of the general formalism	50
8.1.2	Rational solution	51
8.1.3	Polynomial expressions and chiral multiplicities	52
8.2	Special cases $Y = 0$ (F_{11} model)	54
8.2.1	General F_{11} models	54
8.2.2	Specialized “SU(5)” F_{11} models	55
9	Quantization of multiplicities	55
10	Conclusions	59
A	Converting between the geometric and gauge bases	60

1 Introduction

One of the hallmarks of the Standard Model is the presence of chiral fermions transforming in representations of the gauge symmetry group $(\mathrm{SU}(3) \times \mathrm{SU}(2) \times \mathrm{U}(1))/\Gamma$, where $\Gamma \in \{1, \mathbb{Z}_2, \mathbb{Z}_3, \mathbb{Z}_6\}$ is a possibly trivial discrete subgroup of the center of $\mathrm{SU}(3) \times \mathrm{SU}(2) \times \mathrm{U}(1)$. Chiral fermions charged under the Standard Model gauge group have been realized in numerous string theory constructions—see [1] for a review of recent developments. The purpose of this paper is to analyze the chiral matter spectrum and aspects of the Yukawa interactions of the universal tuned F-theory model with gauge group $(\mathrm{SU}(3) \times \mathrm{SU}(2) \times \mathrm{U}(1))/\mathbb{Z}_6$ introduced in [2].

There are obvious motivations for finding specific, dynamically stable solutions of string theory that reproduce all observed aspects of the Standard Model. However, rather than aiming for a complete string-theoretic construction of the Standard Model, we instead take a top-down approach and focus on sets of solutions in the space of string vacua that exhibit the gross features of the Standard Model, specifically the gauge group and allowed representations in the chiral matter spectrum. One reason for this approach is that taking a bird’s eye view can give us a comprehensive picture of the set of candidate string vacua, which may help to address broad questions about how the fundamental interactions of the Standard Model can be reproduced by a self-consistent theory of quantum gravity (many examples of which we expect to come from string theory). Some obvious questions of this sort are how common or uncommon various realizations of the Standard Model are in the space of string theory solutions with given supersymmetry, and what kinds of physics beyond the Standard Model are associated with these different realizations. Another, related, question is what, if any, constraints are imposed on the kinematics of Standard Model-like theories,

and whether or not these constraints can teach us anything about more general constraints imposed by consistency with quantum gravity that we might expect to be manifest at low energies. The set of string theory vacua with prescribed low-energy data is sometimes referred to as part of the string *landscape*, while low-energy effective theories with similar kinematic structure that do not admit a UV completion in string theory (and therefore, perhaps not in quantum gravity more generally) are said to belong to the *swampland* [3, 4]. Adopting this terminology, the questions described above can be rephrased as questions about, respectively, the prevalence of Standard Model-like vacua within the string landscape, and identification of the “boundary” between the landscape and the swampland as viewed from the perspective of Standard Model-like constructions. Taking the broad approach of constructing large classes of Standard Model-like theories also provides the more pragmatic opportunity of comparing how natural or phenomenologically-relevant different classes of such constructions may be, and for identifying more specific features of observed physics that may arise in subsets of the classes of constructed models.

The questions described above could in principle be explored in the context of various different types of constructions belonging to different branches of string theory. In this paper, however, we focus exclusively on Standard Model-like constructions in F-theory [5–7]. F-theory provides a remarkably effective set of tools for exploring the landscape of 4D $\mathcal{N} = 1$ string vacua. The reason for this is that F-theory relates nonperturbative type IIB flux compactifications on compact Kähler threefolds with 7-branes to the geometry of singular elliptically-fibered Calabi–Yau (CY) fourfolds, and this relationship has in turn led to the development of a systematic procedure for constructing 4D $\mathcal{N} = 1$ string vacua with desired kinematics simply by tuning the mathematical properties of the elliptic CY singularities using celebrated results in algebraic geometry. An enormous number of string vacua have been constructed following this procedure, and although F-theory is dual in certain regimes to other constructions such as heterotic string compactifications, F-theory is believed to give the broadest global picture currently available of the supersymmetric string landscape in terms of a unified space of elliptic CY fourfolds that are connected through various topology-changing transitions (see, e.g., [8–11]).

An extensive literature on 4D F-theory flux compactifications has been produced over the past fifteen years, with most papers on standard model-like F-theory vacua focusing on GUT models whose gauge group is broken, giving the Standard Model gauge group at low energies, see, e.g., [12–28], and [29] for a review of the extensive literature on $SU(5)$ F-theory GUT constructions. The topic of this paper is a somewhat less extensively explored type of construction, namely F-theory vacua with exact $(SU(3) \times SU(2) \times U(1))/\Gamma$ gauge symmetry and no larger geometric GUT symmetry. Specifically, we study the family of F-theory vacua engineered by the universal tuned $(SU(3) \times SU(2) \times U(1))/\mathbb{Z}_6$ model described in [2]. The $(SU(3) \times SU(2) \times U(1))/\mathbb{Z}_6$ model describes a universal class of F-theory Weierstrass models with tuned¹ $(SU(3) \times SU(2) \times U(1))/\mathbb{Z}_6$ gauge symmetry that has geometrically generic

¹A tuned gauge group is one that is directly tuned in the Weierstrass model defining the F-theory com-

matter for this gauge group,² which includes the matter representations of the Minimal Supersymmetric Standard Model (MSSM) and three additional exotic matter representations; these representations can combine into three independent anomaly-free families (one of which is that of the MSSM). Note that a subclass of these models, which arise naturally through a toric fiber (“ F_{11} ”) construction [32], contains the exact matter spectrum of the MSSM with no exotics; relatedly, chiral matter in F_{11} models was investigated in [33, 34], and vector-like matter in these models (which we do not address here) has been explored in [35–38].

One of the primary questions we address in this paper is whether the tuned $(\text{SU}(3) \times \text{SU}(2) \times \text{U}(1))/\mathbb{Z}_6$ model over an arbitrary base that allows this tuning naturally contains chiral matter in the other two allowed families, or whether the other two families are for some reason forbidden by F-theory geometry and hence belong to the swampland. To this end we use the recently developed approach of [39] to determine the lattice of vertical fluxes of the $(\text{SU}(3) \times \text{SU}(2) \times \text{U}(1))/\mathbb{Z}_6$ model defined over an arbitrary smooth base and in the presence of a non-trivial flux background. By computing the full set of linear dependences of the vertical fluxes, we show that all three independent families of anomaly-free chiral matter are realized, and hence that the linear constraints imposed by F-theory geometry on chiral multiplicities precisely match those imposed by 4D anomaly cancellation. Furthermore, we examine aspects of the quantization of the fluxes (and hence, of the chiral indices) both in general and for specific choices of F-theory base, and comment on the implications for the numbers of allowed chiral families.

More precisely, we compute an explicit resolution of a presentation of the $(\text{SU}(3) \times \text{SU}(2) \times \text{U}(1))/\mathbb{Z}_6$ model in which the elliptic fiber is realized as a general cubic in \mathbb{P}^2 . We use this resolution to confirm that the gauge symmetries, matter representations, and Yukawa interactions anticipated in [2] are realized geometrically by the singular elliptic CY fourfold associated to the $(\text{SU}(3) \times \text{SU}(2) \times \text{U}(1))/\mathbb{Z}_6$ model. We then use the methods of [39] to show that the lattice of vertical fluxes preserving the 4D local Lorentz and gauge symmetry, which gives at least a subset of the full set of chiral multiplicities realized by the F-theory model, spans the full linear space of anomaly-free chiral spectra transforming under $(\text{SU}(3) \times \text{SU}(2) \times \text{U}(1))/\mathbb{Z}_6$. The analysis carried out here is performed in a (mostly) base-independent fashion so that the results can be applied to a large number of F-theory vacua with a wide range of

pactification, corresponding to fixing some specific complex structure moduli, as opposed to one that arises on a rigid divisor as a generic feature of the F-theory base geometry, or which arises from breaking a larger such rigid group. In this sense, the standard $\text{SU}(5)$ F-theory GUT constructions reviewed in [29] also rely on tuning of the $\text{SU}(5)$ structure, while the more recent flux-breaking GUT constructions of [27, 28] and the direct SM construction of [30] use rigid gauge factors, which may be more prevalent in the landscape.

²The notion of genericity for matter representations in 6D and 4D F-theory was defined and explored in [31]. Note that while universal tuned Weierstrass models will exist for other choices of global gauge group structure associated with other quotient factors Γ , the Standard Model chiral matter is only generic for $\Gamma = \mathbb{Z}_6$. Note also that generic matter types are associated with the geometry of general Weierstrass tuning of any given gauge group; while in 6D this definition can be naturally understood as a feature of the low-energy theory (where generic matter is associated with the largest-dimensional branch of the moduli space for fixed gauge group), this distinction is less transparent in 4D, and other constructions such as that of [28] do not seem to share the same natural structure of generic matter in 4D.

bases. Note, however, that not all base geometries admit tuning of this gauge structure. In particular, at large Hodge numbers, there are many rigid gauge factors and it can become difficult to find room in the geometry for tuning additional features.

The remainder of this paper is structured as follows: In [Section 2](#), we give a brief summary of the main results of the paper. In [Section 3](#), we outline the basic setup and describe explicitly the resolution of the universal tuned $(\text{SU}(3) \times \text{SU}(2) \times \text{U}(1))/\mathbb{Z}_6$ model. In [Sections 4 to 6](#), we study the explicit resolutions of singularities at codimension one, two, three, corresponding to the gauge factors, matter representations, and Yukawa interactions. In [Section 7](#), we analyze the chiral matter multiplicities in the presence of (vertical) fluxes using the formalism of [\[39\]](#), and in [Section 8](#) we consider explicit examples. In [Section 9](#) we discuss some more detailed aspects of the quantization of chiral multiplicities. We conclude in [Section 10](#) with a discussion of the results and further directions for future work.

2 Summary of results

Our analysis of the chiral spectrum of the tuned $G_{\text{SM}} = (\text{SU}(3) \times \text{SU}(2) \times \text{U}(1))/\mathbb{Z}_6$ model is divided into two parts. First, we resolve the singular F-theory background X_0 in order to study the kinematics of the corresponding low-energy effective 4D theory for an arbitrary choice of base and characteristic data where the tuned G_{SM} structure is possible. Second, we switch on a generic vertical flux background and use the geometry of the resolved model to compute the corresponding chiral excesses induced in the 4D spectrum. We summarize the results of these two parts of the analysis in the subsections below.

2.1 Resolution of singularities and 4D kinematics

Let $X_0 \rightarrow B$ be the singular elliptic CY variety defining the $(\text{SU}(3) \times \text{SU}(2) \times \text{U}(1))/\mathbb{Z}_6$ model, where B is the base of the elliptic fibration. In [Section 3](#), we use well-established methods³ to study the geometry of a particular resolution $X_5 \rightarrow X_0$ in order to explore the kinematic structure of the low-energy effective 4D theory. Although for the purposes of computing the chiral spectrum following the approach of [\[39\]](#) it is sufficient to simply resolve the singularities of X_0 and use the structure of the codimension-one singular fibers of X_5 to write the intersection numbers of X_5 in terms of a basis of Cartan divisors, we nevertheless provide a comprehensive description of the singular fibers over the codimension-one, codimension-two, and codimension-three components of the discriminant locus in B . Our analysis of the singular fibers of X_5 shows that the 4D effective theory exhibits the

³A distinctive feature of our analysis is the fact that the singular $(\text{SU}(3) \times \text{SU}(2) \times \text{U}(1))/\mathbb{Z}_6$ model is constructed using a general cubic in \mathbb{P}^2 as opposed to the more standard Weierstrass equation. As a result, the resolution $X_5 \rightarrow X_0$ exhibits a rational, rather than holomorphic, zero section, which indicates the presence of primitive BPS particles with non-trivial KK charge in the spectrum of the low-energy 3D theory corresponding to X_5 . The presence of non-trivial KK charges changes the way in which the 4D spectrum is “imprinted” on the spectrum of its 3D KK reduction, and thus some care is required in recovering the 4D kinematics from the 3D KK theory. We stress that the methods we use in our analysis here are not novel; other models sharing this feature have been similarly analyzed in the literature, see, e.g., [\[40, 32, 41\]](#).

\mathfrak{g}	locus	fiber
$\mathfrak{su}(3)$	$b_1 e_2 e_3 = 0$	
$\mathfrak{su}(2)$	$d_0 e_1 = 0$	

R	locus	fiber
$(\mathbf{3}, \mathbf{2})_{\frac{1}{6}}$	$b_1 e_2 e_3 = d_0 e_1 = 0$	
$(\mathbf{3}, \mathbf{1})_{\frac{2}{3}}$	$b_1 e_2 e_3 = s_8 s_2^2 - s_5 s_2 s_6 + s_1 s_6^2 = 0$	
$(\mathbf{3}, \mathbf{1})_{-\frac{1}{3}}$	$b_1 e_2 e_3 = d_2 s_6^2 - d_1 s_6 s_8 + d_0 e_1 s_8^2 = 0$	
$(\mathbf{3}, \mathbf{1})_{-\frac{4}{3}}$	$b_1 e_2 e_3 = s_2 = 0$	
$(\mathbf{1}, \mathbf{2})_{\frac{1}{2}}$	$d_0 e_1 = \Delta_{(a)} = 0$	
$(\mathbf{1}, \mathbf{2})_{\frac{3}{2}}$	$d_0 e_1 = s_2 = 0$	
$(\mathbf{1}, \mathbf{1})_1$	$V_{g=1} = 0$	
$(\mathbf{1}, \mathbf{1})_2$	$s_1 = s_2 = 0$	

Table 1. Singular elliptic fibers of the resolution $X_5 \rightarrow X_0$ (see Eq. (3.10)) of the $(\mathrm{SU}(3) \times \mathrm{SU}(2) \times \mathrm{U}(1))/\mathbb{Z}_6$ model over codimension-one and codimension-two components of the discriminant locus $\Delta = 0$; these singular fibers correspond to (resp.) gauge symmetries and charged matter representations. The nodes of the graphs in the right-most columns represent irreducible components of the singular elliptic fibers, while the edges of the graphs correspond to points of intersection between pairs of irreducible components. Each irreducible component is birational to \mathbb{P}^1 . A blue (red) ‘ \times ’ in the center of a node indicates that the curve represented by that node intersects the zero section (generating section) at a point away from the points of intersection with other \mathbb{P}^1 components. A blue node is an exceptional \mathbb{P}^1 wrapped by the zero section; such curves correspond in the M-theory frame to primitive BPS particles whose KK central charges are approximately the same scale as their Coulomb branch central charges. (Note that we express the loci in terms of the parameters of the resolution X_5 , so that $d_0 e_1 = 0, b_1 e_2 e_3 = 0$ are, respectively, the $\mathrm{SU}(2), \mathrm{SU}(3)$ gauge divisors $\Sigma_2, \Sigma_3 \subset B$.)

$R \times R' \times R''$	locus	fiber
$(\mathbf{3}^*, \mathbf{2})_{-\frac{1}{6}} \times (\mathbf{3}, \mathbf{1})_{-\frac{4}{3}} \times (\mathbf{1}, \mathbf{2})_{\frac{3}{2}}$	$b_1 e_2 e_3 = d_0 e_1 = s_2 = 0$	
$(\mathbf{3}^*, \mathbf{2})_{-\frac{1}{6}} \times (\mathbf{3}, \mathbf{1})_{\frac{2}{3}} \times (\mathbf{1}, \mathbf{2})_{-\frac{1}{2}}$	$b_1 e_2 e_3 = d_0 e_1 = s_8 s_2^2 - s_5 s_2 s_6 + s_1 s_6^2 = 0$	
$(\mathbf{3}^*, \mathbf{2})_{-\frac{1}{6}} \times (\mathbf{3}, \mathbf{1})_{-\frac{1}{3}} \times (\mathbf{1}, \mathbf{2})_{\frac{1}{2}}$	$b_1 e_2 e_3 = d_0 e_1 = d_2 s_6^2 - d_1 s_6 s_8 + d_0 e_1 s_8^2 = 0$	
$(\mathbf{3}^*, \mathbf{1})_{\frac{4}{3}} \times (\mathbf{3}, \mathbf{1})_{\frac{2}{3}} \times (\mathbf{1}, \mathbf{1})_{-2}$	$b_1 e_2 e_3 = s_2 = s_1 = 0$	
$(\mathbf{3}^*, \mathbf{1})_{-\frac{2}{3}} \times (\mathbf{3}, \mathbf{1})_{-\frac{1}{3}} \times (\mathbf{1}, \mathbf{1})_1$	$b_1 e_2 e_3 = d_2 s_6^2 - d_1 s_6 s_8 + d_0 e_1 s_8^2 = s_8 s_2^2 - s_2 s_5 s_6 + s_1 s_6^2 = 0$	
$(\mathbf{3}^*, \mathbf{1})_{\frac{4}{3}} \times (\mathbf{3}, \mathbf{1})_{-\frac{1}{3}} \times (\mathbf{1}, \mathbf{1})_{-1}$	$b_1 e_2 e_3 = s_2 = d_2 s_6^2 - d_1 s_6 s_8 + d_0 e_1 s_8^2 = 0$	
$(\mathbf{1}, \mathbf{2})_{\frac{1}{2}} \times (\mathbf{1}, \mathbf{2})_{-\frac{3}{2}} \times (\mathbf{1}, \mathbf{1})_1$	$d_0 e_1 = s_2 = \frac{\Delta_{(a)}}{s_1} = 0$	
$(\mathbf{1}, \mathbf{2})_{\frac{1}{2}} \times (\mathbf{1}, \mathbf{2})_{\frac{3}{2}} \times (\mathbf{1}, \mathbf{1})_{-2}$	$d_0 e_1 = s_2 = s_1 = 0$	
$(\mathbf{1}, \mathbf{2})_{\frac{1}{2}} \times (\mathbf{1}, \mathbf{2})_{\frac{3}{2}} \times (\mathbf{1}, \mathbf{1})_{-1}$	$d_0 e_1 = \Delta_{(a)} = V_{q=1} = 0$	

Table 2. Table of singular elliptic fibers of the resolution $X_5 \rightarrow X_0$ of the $(\text{SU}(3) \times \text{SU}(2) \times \text{U}(1))/\mathbb{Z}_6$ model over codimension-three components of the discriminant locus $\Delta = 0$; these singular fibers correspond to Yukawa interactions. The left-most column describes the triples of chiral representations that are contracted to gauge-singlets in each Yukawa interaction. See the caption of [Table 1](#) for an explanation of the graphs in the right-most column and the definitions of the singular loci.

gauge symmetries and charged matter spectrum listed in the left-hand columns of [Table 1](#). The gauge symmetries and charged matter spectrum we find agree with the analysis of the singular limit X_0 in [\[2\]](#), and hence our analysis provides a check of the predictions made in [\[2\]](#) regarding the gauge symmetries and matter spectrum of the $(\mathrm{SU}(3) \times \mathrm{SU}(2) \times \mathrm{U}(1))/\mathbb{Z}_6$ model. Our analysis also includes detailed geometric information relevant for further investigation of structures such as the Yukawa interactions of the theory—see [Table 2](#).

2.2 Vertical flux backgrounds and chiral matter spectrum

We next use the resolution $X_5 \rightarrow X_0$ to compute the multiplicities of 4D $\mathcal{N} = 1$ chiral multiplets in the $(\mathrm{SU}(3) \times \mathrm{SU}(2) \times \mathrm{U}(1))/\mathbb{Z}_6$ model induced by a non-trivial vertical flux background. The multiplicities of 4D $\mathcal{N} = 1$ chiral multiplets can be expressed in terms of the chiral indices

$$\chi_r = n_r - n_{r^*}, \quad (2.1)$$

where n_r, n_{r^*} are the numbers of chiral and anti-chiral multiplets transforming in the complex representations r, r^* . We direct the reader to [Section 7.2](#) for a detailed review of the terminology and concepts discussed below.

Computing the chiral multiplicities for a 4D F-theory compactification in terms of the geometry of a resolved elliptic CY is a well-studied problem in F-theory, reviewed in [\[42\]](#). Base-independent analyses of this problem for specific gauge groups have also been worked out in, e.g., [\[43–46\]](#). In [\[39\]](#), we developed a base-independent analysis, in which the intersection numbers of a resolved elliptic CY X are used to compute the integral pairing on the vertical homology subgroup,

$$M: H_{2,2}^{\mathrm{vert}}(X, \mathbb{Z}) \times H_{2,2}^{\mathrm{vert}}(X, \mathbb{Z}) \rightarrow \mathbb{Z}. \quad (2.2)$$

After homological equivalences on vertical cycles are modded out, this nondegenerate intersection pairing M_{red} was found to be independent of the choice of resolution in many cases, and conjectured to be resolution-independent in general. If true, the resolution-independence of the matrix M_{red} suggests that the integral pairing on vertical cohomology is intrinsic to the singular F-theory limit that directly encodes information about the low-energy 4D theory; this is physically natural since all physical features such as the chiral spectrum should be resolution-independent, but this kind of cohomology of singular spaces is not fully understood mathematically. Other recent work aimed at a direct characterization of the physics of F-theory models in terms of the singular geometry described by type IIB string theory includes [\[47–49\]](#).

The chiral multiplicities of any theory of interest can be computed from simple linear algebra using M_{red} , where schematically $\Theta_{IJ} = M_{(IJ)(KL)} \phi^{KL}$ in terms of a (homologically redundant) basis of surfaces $S_{IJ} = \hat{D}_I \cap \hat{D}_J$, ϕ^{IJ} parameterizes the allowed (vertical) fluxes, and the chiral multiplicities can be related to certain Θ_{IJ} , while other Θ_{IJ} are constrained to vanish by various symmetry principles. For example, for an F-theory Tate model with a nonabelian gauge group (defined over an arbitrary base, and with generic complex parameters,

with no additional Kodaira singularities at higher codimension), the reduced matrix M_{red} takes the schematic form

$$M_{\text{red}} = \begin{pmatrix} D_{\alpha'} \cdot K \cdot D_{\alpha} & D_{\alpha'} \cdot D_{\alpha} \cdot D_{\beta} & 0 & 0 \\ D_{\alpha'} \cdot D_{\beta'} \cdot D_{\alpha} & 0 & 0 & * \\ 0 & 0 & -\kappa^{ij} \Sigma \cdot D_{\alpha} \cdot D_{\alpha'} & * \\ 0 & * & * & * \end{pmatrix}, \quad (2.3)$$

in a reduced basis $S_{0\alpha}, S_{\alpha\beta}, S_{i\alpha}, S_{ij}$ where 0 represents the zero section, indices α correspond to base divisors, and i correspond to Cartan elements of the gauge group; the matrix elements denoted by “*” are undetermined and the non-zero matrix elements are given by intersection products of divisors D_{α} in the base B , where K is the canonical class of the base. A rational change of basis removes all the * elements except the bottom right block, which becomes a matrix M_{phys} relating chiral multiplicities to the subset of flux parameters ϕ^{IJ} that correspond to symmetry-preserving F-theory fluxes (note that all other flux parameters are forced to vanish in order to satisfy the constraints $\Theta_{I\alpha} = 0$, which are necessary to preserve 4D Poincaré and gauge symmetry). This simple schematic structure becomes more complicated for models with additional abelian U(1) factors, as described in [39]. In particular, the presence of additional sections complicates the form of the reduced matrix (2.3), and makes it harder to describe the general solution of the constraints as easily. This is described in some detail for a simpler model with gauge group $(\text{SU}(2) \times \text{U}(1))/\mathbb{Z}_2$ in [39]; working through the details of this for the more complicated universal $(\text{SU}(3) \times \text{SU}(2) \times \text{U}(1))/\mathbb{Z}_6$ model is a central part of the work in this paper. The matrix M_{red} representing the integral pairing for the resolved $(\text{SU}(3) \times \text{SU}(2) \times \text{U}(1))/\mathbb{Z}_6$ model is displayed in Table 5 and Table 6 in two particular homologically independent bases for S_{IJ} , which are useful in complementary aspects of the analysis. This reduced matrix is used in Section 7 to describe the chiral matter content of the model with fluxes.

An interesting question one can ask related to the landscape of F-theory compactifications is whether or not all linearly independent anomaly-free combinations of chiral matter can be realized in F-theory, i.e., whether F-theory imposes further linear constraints on the available chiral spectrum beyond those associated with anomalies. (Note that we expect that all F-theory models will satisfy anomaly constraints; the geometric manifestation of these constraints has been studied in, e.g., [46, 50–52]). We address this question by geometrically computing the possible combinations of chiral matter multiplicities that can be realized in the $(\text{SU}(3) \times \text{SU}(2) \times \text{U}(1))/\mathbb{Z}_6$ model and comparing them to the full list of possible chiral matter combinations compatible with 4D anomaly cancellation, namely the set of all integer values for the chiral indices χ_r (where r is one of the eight complex representations appearing

in the left-most column of the right hand table in [Table 1](#)) subject to the constraints

$$\begin{aligned}
\chi(\mathbf{3},\mathbf{1})_{\frac{2}{3}} &= -\chi(\mathbf{1},\mathbf{1})_1 + 2\chi(\mathbf{1},\mathbf{2})_{\frac{3}{2}} - \chi(\mathbf{3},\mathbf{1})_{-\frac{4}{3}} \\
\chi(\mathbf{3},\mathbf{1})_{-\frac{1}{3}} &= -\chi(\mathbf{1},\mathbf{1})_1 + 2\chi(\mathbf{1},\mathbf{2})_{\frac{3}{2}} - 4\chi(\mathbf{3},\mathbf{1})_{-\frac{4}{3}} \\
\chi(\mathbf{1},\mathbf{2})_{\frac{1}{2}} &= -\chi(\mathbf{1},\mathbf{1})_1 - \chi(\mathbf{1},\mathbf{2})_{\frac{3}{2}} - 2\chi(\mathbf{3},\mathbf{1})_{-\frac{4}{3}} \\
\chi(\mathbf{3},\mathbf{2})_{\frac{1}{6}} &= \chi(\mathbf{1},\mathbf{1})_1 - 2\chi(\mathbf{1},\mathbf{2})_{\frac{3}{2}} + 2\chi(\mathbf{3},\mathbf{1})_{-\frac{4}{3}} \\
\chi(\mathbf{1},\mathbf{1})_2 &= -\chi(\mathbf{1},\mathbf{2})_{\frac{3}{2}} + \chi(\mathbf{3},\mathbf{1})_{-\frac{4}{3}}.
\end{aligned}
\tag{2.4}$$

Since there are eight possible chiral matter representations and five constraint equations (above), this leaves behind a three-dimensional linear space of anomaly-free chiral matter multiplicities. One basis for the three linearly-independent families of anomaly-free matter is displayed in [Table 3](#). Note that setting the chiral multiplicities of the exotic⁴ representations $(\mathbf{1}, \mathbf{2})_{\frac{3}{2}}$ and $(\mathbf{3}, \mathbf{1})_{-\frac{4}{3}}$ equal to zero reduces this three-dimensional family of anomaly-free chiral multiplicities to a one-dimensional family corresponding to a single generation of the MSSM chiral matter spectrum.⁵

We compare the anomaly-free chiral matter spectra satisfying [Eq. \(2.4\)](#) to the chiral indices of the resolved $(\text{SU}(3) \times \text{SU}(2) \times \text{U}(1))/\mathbb{Z}_6$ model induced by a non-trivial vertical flux background; see [Eq. \(7.47\)](#). Consistent with the findings of [\[39\]](#), namely that all anomaly-free linear combinations of matter can be realized in F-theory (without considering multiplicities) for the models considered there, we indeed find that the full set of three independent linear families of possible chiral matter multiplicities are realized in the $(\text{SU}(3) \times \text{SU}(2) \times \text{U}(1))/\mathbb{Z}_6$ model in the presence of a non-trivial vertical flux background for a generic choice of base. We comment on the precise quantization of the chiral indices imposed by the geometry of specific F-theory vacua (i.e., a specific choice of base and associated topological data) in [Section 9](#). In addition to the quantization constraints, tadpole constraints, which we do not consider here, will also limit the range of chiral matter multiplicities available in any given model.

3 Basic setup and resolution

The universal tuned $(\text{SU}(3) \times \text{SU}(2) \times \text{U}(1))/\mathbb{Z}_6$ model was identified in [\[2\]](#) by un-Higgsing a $\text{U}(1)$ model with charge $q = 4$ matter introduced in [\[53\]](#). The charge $q = 4$ $\text{U}(1)$ model of [\[53\]](#) was constructed as a singular hypersurface of an ambient projective bundle Y_0 whose fibers are isomorphic to \mathbb{P}^2 with homogeneous coordinates $[u : v : w]$. The hypersurface equation is

⁴We refer to charged matter transforming in representations that do not belong to the MSSM as “exotic” matter, although these are still generic features of the class of universal tuned $(\text{SU}(3) \times \text{SU}(2) \times \text{U}(1))/\mathbb{Z}_6$ F-theory models.

⁵Another specific linear combination of the anomaly-free families (with multiplicities of each family multiplied by 2, 0, 1 respectively), has no matter charged under the $\text{SU}(3)$ factor and indeed the resulting multiplicities correspond precisely to those of the $(\text{SU}(2) \times \text{U}(1))/\mathbb{Z}_2$ model [\[32\]](#) whose chiral spectrum is explored in [\[39\]](#).

	$(\mathbf{3}, \mathbf{2})_{\frac{1}{6}}$	$(\mathbf{3}, \mathbf{1})_{\frac{2}{3}}$	$(\mathbf{3}, \mathbf{1})_{-\frac{1}{3}}$	$(\mathbf{1}, \mathbf{2})_{\frac{1}{2}}$	$(\mathbf{1}, \mathbf{1})_1$	$(\mathbf{3}, \mathbf{1})_{-\frac{4}{3}}$	$(\mathbf{1}, \mathbf{2})_{\frac{3}{2}}$	$(\mathbf{1}, \mathbf{1})_2$
(MSSM)	1	-1	-1	-1	1	0	0	0
(exotic 1)	2	-1	-4	-2	0	1	0	1
(exotic 2)	-2	2	2	-1	0	0	1	-1

Table 3. Multiplicities of the three anomaly-free families of generic chiral matter in 4D models with $(\text{SU}(3) \times \text{SU}(2) \times \text{U}(1))/\mathbb{Z}_6$ gauge group

as follows:

$$p_0^{q=4} = (a_1 v + b_1 w)(d_0 v^2 + d_1 v w + d_2 w^2) + u(s_1 u^2 + s_2 u v + s_3 v^2 + s_5 u w + s_6 v w + s_8 w^2) = 0. \quad (3.1)$$

In terms of the above construction, the un-Higgsing $\text{U}(1) \rightarrow (\text{SU}(3) \times \text{SU}(2) \times \text{U}(1))/\mathbb{Z}_6$ is achieved by restricting to a special locus in complex structure moduli space on which the sections $a_1 = s_3$ vanish:

$$X_0 = \{p_0^{q=4} = a_1 = s_3 = 0\} =: \{p_0 = 0\} \subset Y_0, \quad (3.2)$$

so that

$$p_0 = b_1 w(d_0 v^2 + d_1 v w + d_2 w^2) + u(s_1 u^2 + s_2 u v + s_5 u w + s_6 v w + s_8 w^2) = 0. \quad (3.3)$$

We now discuss this construction in more detail. First, observe that the above elliptic fibration is equipped with two rational sections:

$$\begin{aligned} \text{zero section: } & \{s_1 u + s_2 v = w = 0\}, \\ \text{generating section: } & \{u = w = 0\}. \end{aligned} \quad (3.4)$$

The coefficients of the cubic (in u, v, w) monomials appearing in the homogeneous polynomial p_0 in [Eq. \(3.3\)](#) are (the pullbacks to Y_0 of) sections of various line bundles over B . We may equivalently express these line bundles in terms of their first Chern classes, each of which can in turn be expressed as a linear combination of the following divisor classes:

$$K, \quad \Sigma_2 = [d_0], \quad \Sigma_3 = [b_1], \quad Y = [s_2]. \quad (3.5)$$

We refer to the above four divisor classes as the characteristic data of the elliptic fibration $Y_0 \rightarrow B$. Let us describe these divisor classes in further detail:

- K is the canonical class of B ;
- Σ_2, Σ_3 are the $\mathfrak{su}(2), \mathfrak{su}(3)$ gauge divisors wrapped by 7-branes;
- and Y is the divisor class of the locus in B over which the zero section and the generating section associated with the $\mathfrak{u}(1)$ factor intersect.

The classes of the zero loci of the other sections appearing in p_0 besides d_0, b_1, s_2 are

$$\begin{aligned}
[s_1] &= -K + Y - \Sigma_3 - \Sigma_2, \\
[d_1] &= -2K - Y - \Sigma_3, \\
[d_2] &= -4K - 2Y - 2\Sigma_3 - \Sigma_2, \\
[s_5] &= -2Y - \Sigma_3 - \Sigma_2, \\
[s_6] &= -K, \\
[s_8] &= -3K - Y - \Sigma_3 - \Sigma_2.
\end{aligned} \tag{3.6}$$

The ambient space of the elliptic fibration, Y_0 , can be viewed as the projectivization of a rank-two vector bundle:

$$Y_0 = \mathbb{P}(\oplus_{i=1}^3 \mathcal{L}_i) \xrightarrow{\varpi} B, \quad \mathcal{L}_i \rightarrow B. \tag{3.7}$$

To ensure that the homogeneous polynomial p_0 is a well-defined section of the line bundle

$$\otimes_i \mathcal{L}_i \tag{3.8}$$

we assign the following choice (unique up to an overall additive constant) of divisor classes⁶ $L_i = c_1(\mathcal{L}_i)$ to the hyperplanes $u, v, w = 0$ in the Chow ring of Y_0

$$\begin{aligned}
[u] &= \mathbf{H} + L_1 = \mathbf{H} - \mathbf{Y} + \Sigma_3 \\
[v] &= \mathbf{H} + L_2 = \mathbf{H} - \mathbf{K} - \mathbf{Y} - \Sigma_2 \\
[w] &= \mathbf{H} + L_3 = \mathbf{H} - \mathbf{K} + \Sigma_3.
\end{aligned} \tag{3.9}$$

Although the hypersurface equation Eq. (3.3) differs from the standard Weierstrass form presented in [2] (with the two equations being related by Nagell's algorithm⁷), the singular locus of X_0 is nevertheless still given by the zero locus of the discriminant $\Delta = 4f^3 + 27g^2$. Explicit expressions for f, g can be found in [53, 2] (for related discussions, see also [54, 55]).

We resolve the singularities of X_0 through codimension two by means of the following sequence of blowups⁸

$$X_5 \xrightarrow{(w,t|e_5)} X_4 \xrightarrow{(u,w|e_4)} X_3 \xrightarrow{(e_2,w|e_3)} X_2 \xrightarrow{(b_1,u|e_2)} X_1 \xrightarrow{(d_0,u,w|e_1)} X_0. \tag{3.10}$$

⁶We use bold symbols \mathbf{D} to denote divisor classes in the Chow ring of the ambient projective bundle Y_0 ; in particular, \mathbf{D}_α denotes the pullback of a divisor $D_\alpha \in B$ (e.g., $\mathbf{K} = K^\alpha \mathbf{D}_\alpha$ is the pullback of K to the Chow ring of Y_0).

⁷See Appendix B of [54] for a discussion of Nagell's algorithm.

⁸The notation $f_{i+1} = (g_{i+1,1}, \dots, g_{i+1,n_{i+1}} | e_{i+1})$ is shorthand for the blowup $f_{i+1} : Y_{i+1} \rightarrow Y_i$ of the ambient space Y_i along the blowup center $\{g_{i+1,1} = \dots = g_{i+1,n_{i+1}} = 0\} \subset Y_i$ whose exceptional divisor is the zero locus $e_{i+1} = 0$. The corresponding blowup $X_{i+1} \rightarrow X_i$ is then given by the restriction of f_{i+1} to the complete intersection $X_i = \{p_{i,1} = \dots = p_{i,m_i} = 0\} \subset Y_i$. We abuse notation and implement the $i+1$ th blowup by making the substitution $g_{i+1,j} \rightarrow e_{i+1} g_{i+1,j}$ whenever $g_{i+1,j}$ is a local coordinate, and we denote the proper transform of $X_i \subset Y_i$ by $X_{i+1} \subset Y_{i+1}$.

In this sequence of blowups, the variable t appearing in the defining equation for X_4 is defined as follows:

$$t := s_2v + e_1e_2e_3e_4s_1u. \quad (3.11)$$

The first three blowups appearing in Eq. (3.10) (counting from the right) are conceptually straightforward, as they are restricted to codimension-one components of the discriminant locus in B . However, the fourth and fifth blowups appearing in Eq. (3.10), whose corresponding blowdown maps are (respectively) $X_4 \rightarrow X_3, X_5 \rightarrow X_4$, are somewhat unintuitive in that they appear to blow up the entire base B . However, it turns out that these choices of blowups produce new divisors with precisely the desired geometry: the proper transform of each blowup is topologically a small blowup of the base B at the points over which the elliptic fibers become singular, and hence is a smooth birational representative of a rational section (see Eq. (3.4)).⁹

The proper transform of X_0 under the above composition of blowups, X_5 , is the complete intersection

$$\begin{aligned} X_5 &= \{p_{5,1} = p_{5,2} = 0\} \subset Y_5 \\ p_{5,1} &= b_1d_1e_3e_4e_5vw^2 + b_1d_2e_1e_3^2e_4^2e_5^2w^3 + b_1d_0v^2w + e_2e_4tu^2 + e_1e_2e_3e_4^2s_5u^2w \\ &\quad + e_4s_6uvw + e_1e_3e_4^2e_5s_8uw^2 \\ p_{5,2} &= -te_5 + e_1e_2e_3e_4s_1u + s_2v \end{aligned} \quad (3.12)$$

and the ambient space Y_5 is equipped with homogeneous coordinates

$$\begin{aligned} [e_1e_2e_3e_4u : v : e_1e_3e_4e_5w] [e_2e_3e_4u : e_3e_4e_5w : d_0] \\ [e_4u : b_1] [e_2 : e_4e_5w] [u : e_5w] [w : t] \end{aligned} \quad (3.13)$$

The above homogeneous coordinates are identified under the rescalings

$$\begin{aligned} u \rightarrow \lambda_0\lambda_1\lambda_2\lambda_4u, \quad v \rightarrow \lambda_0v, \quad w \rightarrow \lambda_0\lambda_1\lambda_3\lambda_4\lambda_5w, \quad d_0 \rightarrow d_0\lambda_1, \quad b_1 \rightarrow b_1\lambda_2, \\ e_1 \rightarrow \frac{e_1}{\lambda_1}, \quad e_2 \rightarrow \frac{e_2\lambda_3}{\lambda_2}, \quad e_3 \rightarrow \frac{e_3}{\lambda_3}, \quad e_4 \rightarrow \frac{e_4}{\lambda_4}, \quad e_5 \rightarrow \frac{e_5}{\lambda_5}, \quad t \rightarrow \lambda_0\lambda_5t \end{aligned} \quad (3.14)$$

⁹To see why the fourth and fifth blowups in Eq. (3.10) have precisely the intended effect, let us study blowups of this form in the context of a toy model. Let Y_0 be the total space of a \mathbb{P}^2 fibration over a base B . Suppose that the fibers of Y_0 have homogeneous coordinates $[x : y : z]$ and let us restrict to a \mathbb{C}^2 open set of B with local affine coordinates (a, b) . Let $X_0 \subset Y_0$ be the hypersurface $ax + by = 0$. The hypersurface X_0 has a section $x = y = 0$. There is a conifold singularity at $a = b = x = y = 0$. Suppose we resolve this singularity by means of a blowup along $x = y = 0$, i.e. we make the substitution $x \rightarrow e_1x, y \rightarrow e_1y$ with $e_1 = 0$ a local equation for the exceptional divisor in the ambient space. The proper transform X_1 is the hypersurface $ax + by = 0$ in the new ambient space Y_1 with an affine open set described by the homogeneous coordinates $[x : y][e_1x : e_1y : z](a, b)$ (and some unspecified \mathbb{C}^* action). Having blown up the section, we can study its proper transform by restricting to the exceptional locus $e_1 = 0$. Away from the ‘‘discriminant locus’’ $a = b = 0$ in B , we find that the exceptional divisor is isomorphic to the original section, and corresponds to the set of points $[-b : a][0 : 0 : z](a, b)$. When restricted to the discriminant locus, we find that the point $[0 : 0 : z]$ of the fiber has been replaced with a \mathbb{P}^1 , i.e. the set of points $[x : y][0 : 0 : z](0, 0)$. Thus, we see that the proper transform of the section has the topology of a small blowup of the base B at the point $(0, 0)$. An analogous story holds for the proper transforms of the sections Eq. (3.4) under the fourth and fifth blowups in Eq. (3.10).

for $\lambda_i \in \mathbb{C}^*$. One can verify via explicit computation in the affine open sets of X_5 that the rank of the Jacobian $[[\partial_i p_{5,j}]]$ does not (in general) reduce over any codimension-two loci in B , indicating that X_5 is smooth through codimension-two in B without additional tunings of the parameters defining the $(\mathrm{SU}(3) \times \mathrm{SU}(2) \times \mathrm{U}(1))/\mathbb{Z}_6$ Weierstrass model.¹⁰ We abuse terminology and refer to X_5 as “smooth”, a “resolution”, etc., keeping in mind that X_5 may contain singular fibers over certain codimension-three loci; these codimension-three singularities do not affect the main results of this paper.

We next analyze the geometry of X_5 to identify the kinematics of the low-energy effective 4D $\mathcal{N} = 1$ supergravity theory describing the $(\mathrm{SU}(3) \times \mathrm{SU}(2) \times \mathrm{U}(1))/\mathbb{Z}_6$ model at long distances. Unless otherwise stated, throughout our analysis we work over an arbitrary smooth base B .

4 Codimension one: gauge symmetry

In this section, we analyze the geometry of the singular elliptic fibers of X_5 over codimension one loci of the discriminant locus in B , in order to verify that our resolution correctly exhibits the expected gauge algebra

$$\mathfrak{g} = \oplus_s \mathfrak{g}_s = \mathfrak{su}(3) \oplus \mathfrak{su}(2) \oplus \mathfrak{u}(1) \tag{4.1}$$

characterizing the 4D $\mathcal{N} = 1$ theory describing F-theory compactified on the singular fourfold X_0 .

4.1 $\mathfrak{u}(1)$

In F-theory compactifications pure $\mathfrak{u}(1)$ gauge symmetries are identified with the Mordell–Weil (MW) group of rational sections of the elliptic fibration [7, 56–58], where the zero section (i.e., a choice of zero element of the MW group, extended fiber-wise over B) corresponds to the Kaluza–Klein (KK) $\mathfrak{u}(1)$ and all other sections generating the free part of the MW group correspond to additional $\mathfrak{u}(1)$ factors.¹¹ Therefore, pure abelian gauge symmetries are not determined by codimension one singularities in B , although they are nonetheless associated to smooth divisors $\hat{D}_{\bar{a}}$ of X_5 ; see Eq. (7.2) for a description of the proper transforms of the zero and generating sections \hat{D}_0, \hat{D}_1 under the composition of blowups leading to X_5 .

Note that since \hat{D}_0 is rational, rather than holomorphic, the resolution X_5 describes a phase of M-theory in which some of the primitive BPS particles in the 3D spectrum carry non-trivial $\mathfrak{u}(1)_{\mathrm{KK}}$ charge; this point is explored further in Section 5.1.¹² Since 3D BPS particles

¹⁰Note that certain choices of base B can impose additional specializations on the Weierstrass model parameters that can in principle lead to additional singularities appearing over higher codimension components of the discriminant locus.

¹¹More precisely, in the dual M-theory picture, in the vicinity of a divisor of a smooth elliptic CY, it is possible to locally expand the M-theory 3-form in a basis of harmonic forms ω_i as $C_3 = A^I \wedge \omega_I + \dots$, where A^i are abelian gauge fields and the harmonic forms ω_i are Poincaré dual to the divisors \hat{D}_i . See Section 4.3 of [42] and references therein for further discussion.

¹²See, e.g., [40] for a discussion of the interplay between rational sections and KK charges in the context of 6D F-theory compactifications.

arise from M2-branes wrapping holomorphic curves C , these quantized $\mathfrak{u}(1)_{\text{KK}}$ charges can be computed in terms of the intersection pairing $\hat{D}_0 \cdot C$. Similarly, the additional $\mathfrak{u}(1)$ charges of BPS particles can be determined by computing the intersection pairings $\hat{D}_1 \cdot C$.

4.2 $\mathfrak{su}(3) \oplus \mathfrak{su}(2)$

In contrast to $\mathfrak{u}(1)$ gauge symmetries, simple nonabelian gauge symmetries \mathfrak{g}_s are associated to singularities of the elliptic fibers over codimension one components of the discriminant locus $\Delta = 0$ in B . Since the discriminant Δ of the *singular* Weierstrass model Eq. (3.3) exhibits the following behavior,

$$f = \mathcal{O}(\varepsilon^0), \quad g = \mathcal{O}(\varepsilon^0), \quad \Delta = \varepsilon^5 b_1^3 d_0^2 + \mathcal{O}(\varepsilon^6), \quad (4.2)$$

we can see there is an I_2 singularity over $d_0 = 0$ and an I_3 singularity over $b_1 = 0$ in X_0 (see, e.g., [59]). We use our explicit description of the resolution $X_5 \rightarrow X_0$ in Eqs. (3.12) and (3.13) to verify that both singular fibers are split in the sense of arithmetic geometry and indicate the presence of (resp.) $\mathfrak{su}(2)$ and $\mathfrak{su}(3)$ gauge symmetries. We describe the singular fibers in more detail below.

In the following discussion, for convenience, we study the singular fibers and their intersections in the affine open set $e_4 e_5 \neq 0$, away from possible points of intersection with the rational sections \hat{D}_0, \hat{D}_1 . The singular elliptic fibers F over the locus $d_0 e_1 = 0$ split into the following irreducible rational curves:

$$\mathfrak{su}(2) \quad : \quad F|_{d_0 e_1 = 0} = F_0 + F_1. \quad (4.3)$$

Setting $d_0 = 0$, we learn that the irreducible curve F_0 is the normalization of the singular cubic curve in \mathbb{P}^2 with coordinates $[u : v : w]$ (after appropriate coordinate redefinitions), where the singularity $u = w = 0$ has been replaced with the exceptional curve F_1 . Setting $e_1 = 0$, one can see that F_1 is a smooth conic in \mathbb{P}^2 with coordinates $[u : w : d_0]$. The intersection $F_0 \cap F_1$ consists of two distinct points, hence the generic fibers are type I_2 and we associate F_0, F_1 to, respectively, the affine and non-affine nodes of the affine $\mathfrak{su}(2)$ Dynkin diagram. In codimension one, \hat{D}_0 intersects F_0 in a point, whereas \hat{D}_1 intersects F_1 in a point.

Next we turn our attention to the fibers over the locus $b_1 e_2 e_3 = 0$:

$$\mathfrak{su}(3) \quad : \quad F|_{b_1 e_2 e_3 = 0} = F'_0 + F'_2 + F'_3. \quad (4.4)$$

Analogous to F_0 , we associate F'_0 to the affine node and F'_2, F'_3 to the other two nodes of the affine $\mathfrak{su}(3)$ Dynkin diagram. Making the redefinitions $w \rightarrow uw/(e_3 e_5), e_2 \rightarrow e_2/e_3, v \rightarrow e_1 e_4 u v$, we learn that F'_0 can be described locally as a smooth conic in a subspace birational to \mathbb{P}^2 with coordinates $[e_2 : v : w]$ with the points $[0 : 1 : 0]$ and $[s_2 v : s_1 e_2 : 0]$ removed. Next, we consider the curve F'_2 . Making coordinate redefinitions $u \rightarrow u/(e_1 e_4), e_3 \rightarrow e_3/(e_1 e_4 e_5 w)$, we find that F'_2 is the sum of a base and fiber curve in \mathbb{F}_1 with homogeneous coordinates $[v : e_3][u : b_1] \cong [\lambda_0 v : \lambda_0 e_3][\lambda_0 \lambda_2 u : \lambda_2 b_1]$. Finally, in the case of the curve F'_3 , after making the coordinate redefinitions $w \rightarrow v d_0 w/(e_4 e_5), u \rightarrow v d_0 u/e_4$ we learn that the class

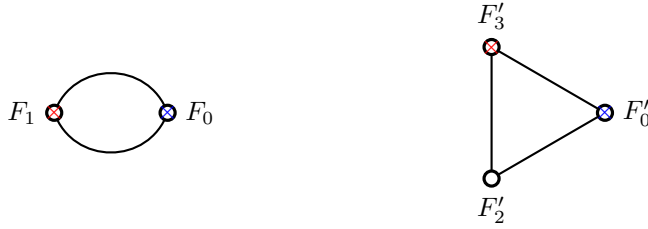


Figure 1. Schematic diagram of the singular elliptic fibers over the codimension-one $\mathfrak{su}(2)$ (left) and $\mathfrak{su}(3)$ (right) loci of the discriminant locus in B . Over the $\mathfrak{su}(2)$ locus $d_0 e_1 = 0$, the singular elliptic fiber F is Kodaira type I_2 , and admits the decomposition $F = F_0 + F_1$; over the $\mathfrak{su}(3)$ locus $b_1 e_2 e_3 = 0$, the singular elliptic fiber is Kodaira type I_3^{split} , and admits the decomposition $F = F'_0 + F'_2 + F'_3$. Note that all irreducible components F_a, F'_b are rational curves. The blue \times indicates that F_0, F'_0 intersect the zero section \hat{D}_0 in a point, whereas the red \times symbol indicates that F_1, F'_3 intersect the generating section \hat{D}_1 in a point.

of F'_3 is a sum of the base and fiber curve classes in \mathbb{F}_{-1} with homogeneous coordinates $[u : b_1][e_2 : w] \cong [\lambda_2 u : \lambda_2 b_1][\lambda_2^{-1} \lambda_3 e_2 : \lambda_3 w]$. It is straightforward to verify that the three pairwise intersections $F'_0 \cap F'_2, F'_0 \cap F'_3, F'_2 \cap F'_3$ are all points, and hence the fibers over $b_1 e_2 e_3 = 0$ are of Kodaira type I_3^{split} . In codimension one \hat{D}_0 intersects F'_0 in a point, whereas \hat{D}_1 intersects F_3 in a point.

See [Figure 1](#) for a schematic depiction of the codimension-one singular fibers.

5 Codimension two: local matter

In this section we study the geometry of the codimension-two singular fibers (i.e., collisions of codimension-one singular fibers including those described in [Section 4](#)) associated to local matter representations

$$(\mathbf{R}_3, \mathbf{R}_2)_{w_{\bar{1}}}, \quad (5.1)$$

where

$$\mathbf{R}_s := r_s \oplus r_s^* \quad (5.2)$$

is an irreducible quaternionic representation of the nonabelian gauge algebra \mathfrak{g}_s and $w_{\bar{1}} = q$ is the $\mathfrak{u}(1)$ charge. We show, in particular, that the codimension-two singularities are consistent with the matter spectrum discussed in [\[2\]](#).

5.1 Kaluza–Klein charges

As was mentioned briefly in [Section 4.1](#), a special feature of the resolution X_5 is that the zero section \hat{D}_0 is rational, rather than holomorphic, which is closely related to our realization of the F-theory vacuum X_0 as a hypersurface of a general \mathbb{P}^2 fibration as opposed to a Weierstrass model $y^2 z = x^3 + f x z^2 + g z^3$ (the Weierstrass model, by contrast, is naturally

equipped with a holomorphic zero section $x = z = 0$). It turns out that the zero section \hat{D}_0 is isomorphic to a small blowup of the base B at various points and is hence only birational to B . This can be seen by noting that the locus $s_2 = 0$, over which the zero and generating sections intersect (and hence over which our choice of zero section fails to be holomorphic), has non-trivial intersection with the discriminant locus. Thus, the singular elliptic fibers of X_0 over the codimension-two locus $\Delta = s_2 = 0$ have singular points that are blown up as part of the resolution $X_5 \rightarrow X_0$; the proper transforms of these points are irreducible \mathbb{P}^1 components of I_2 singular fibers over $\Delta = s_2 = 0$. Since these exceptional \mathbb{P}^1 's are by definition extremal generators of the Mori cone of X_5 , they necessarily have non-trivial intersection with $\hat{D}_0 \cong \text{Bl}_{\{\Delta=s_2=0\}}B$, and thus it follows that the central charges of the primitive 3D BPS particles corresponding to M2 branes wrapping these exceptional \mathbb{P}^1 's carry non-zero $u(1)_{\text{KK}}$ charge. These 3D BPS particles' KK central charges are in fact small in comparison to their Coulomb branch central charges (see Eq. (7.43)), so there is no mass hierarchy between BPS particles with zero KK charge and BPS particles with non-zero KK charge. While the presence of light particles with non-trivial KK charge clearly does not alter the 4D spectrum, this does imply that we cannot simply read off the 4D kinematics from the naive 3D BPS spectrum in the usual manner.¹³ Thus, we need to be able to use the geometry of X_5 to precisely specify the contribution of the KK charges to the 3D Coulomb branch dynamics, so that we can disentangle the KK spectrum from our analysis. We discuss how to do this below.

We first focus on the zero section. Rescaling the homogeneous coordinates appropriately and defining $w \rightarrow e_2uw, e_4 \rightarrow e_4/u$, we can describe the restriction of the zero section to the locus $s_2 = 0$ by the complete intersection

$$\hat{D}_0|_{s_2=0} : s_1e_1e_2e_3e_4 = e_4t + (s_6v + b_1d_0v^2)w + s_5e_1e_2e_3e_4^2w = 0. \quad (5.3)$$

In the above equation, the monomial $s_1e_1e_2e_3e_4$ vanishes on the union of three components of the discriminant locus restricted to $s_2 = 0$, namely the union of the loci $s_1 = 0$, $d_0e_1 = 0$, and $b_1e_2e_3 = 0$:

$$f|_{s_2=0} = \mathcal{O}(\varepsilon^0), \quad g|_{s_2=0} = \mathcal{O}(\varepsilon^0), \quad \Delta|_{s_2=0} = \varepsilon^9(b_1e_2e_3)^4(d_0e_1)^3s_1^2 + \mathcal{O}(\varepsilon^{10}). \quad (5.4)$$

We thus expect the intersection of $\hat{D}_0 \cap \hat{Y}$ with each of these codimension one loci to describe the following collection of exceptional \mathbb{P}^1 's:

Setting $e_1 = 0$ and working in the affine open set $s_1e_2e_3 \neq 0$, after appropriately rescaling and defining new variables $e_4 \rightarrow ve_4/(e_2e_3), t \rightarrow vt$ we find

$$\hat{D}_0|_{s_2=e_1=0} : e_4t + b_1d_0w + s_6e_4w = 0 \quad (5.5)$$

in a subspace birational to $\mathbb{P}^1 \times \mathbb{P}^1$ with homogeneous coordinates $[e_4 : d_0][w : t]$. Similarly, by setting $e_3 = 0$ and working in the open set $s_1e_1e_2 \neq 0$, after making some appropriate

¹³For example, in this situation the one-loop Chern–Simons couplings receive contributions from the KK central charges. Thus, it is not possible to determine the form of the Chern–Simons couplings from purely 3D field-theoretic considerations, as the KK tower now participates in the light spectrum [60, 40].

coordinate redefinitions we find an identical local description in a subspace birational to $\mathbb{P}^1 \times \mathbb{P}^1$ with homogeneous coordinates $[e_4 : b_1][w : t]$. Finally, by setting $s_1 = 0$ and working in the open set $e_1 e_2 e_3 = 0$, and making the coordinate redefinitions $d_0 \rightarrow d_0/e_1, b_1 \rightarrow b_1/(e_2 e_3), e_4 \rightarrow e_4/(e_1 e_2 e_3)$, we may write

$$\hat{D}_0|_{s_2=s_1=0} : e_4 t + s_5 w e_4^2 + s_6 w e_4 v + d_0 b_1 v^2 w = 0 \quad (5.6)$$

in a subspace birational to a Hirzebruch surface¹⁴ \mathbb{F}_1 with coordinates $[e_4 : v][w : t] \cong [\lambda_0 e_4 : \lambda_0 v][\lambda_5 w : \lambda_0 \lambda_5 t]$. In all three cases, we see that the zero section wraps a full rational curve, i.e., the elliptic fiber splits as $F \rightarrow F' + F''$, with $F', F'' \cong \mathbb{P}^1$. As discussed, since these exceptional curves F' lie in \hat{D}_0 , the primitive BPS particles corresponding to M2 branes wrapping F' carry non-trivial KK charge given by $\hat{D}_0 \cdot F' \neq 0$.

Having specified the geometric origin of the light BPS particles in the 3D spectrum with non-trivial $\mathfrak{u}(1)_{\text{KK}}$ charges, we next turn our attention to local matter charged under $\mathfrak{su}(3) \oplus \mathfrak{su}(2) \oplus \mathfrak{u}(1)$.

5.2 $(\mathbf{1}, \mathbf{1})_{w_{\bar{1}}}$

The pure $\mathfrak{u}(1)$ charged matter loci were found in [2] to correspond to singular fibers of X_0 over the following components of the discriminant locus $\Delta = 0$:

$$\begin{aligned} (\mathbf{1}, \mathbf{1})_1 & : V_{q=1} = 0 \\ (\mathbf{1}, \mathbf{1})_2 & : s_1 = s_2 = 0. \end{aligned} \quad (5.7)$$

In the above equation

$$\begin{aligned} V_{q=1} & = V \setminus (\{s_1 = s_2 = 0\} \cup \{b_1 = s_2 = 0\} \cup \{d_0 = s_2 = 0\}) \\ V & = \left\{ \begin{aligned} & -d_0 b_1 s_1^2 s_2 (d_1 s_2^2 - 2d_0 s_2 s_5 + 2d_0 s_1 s_6) + d_0^3 b_1^2 s_1^4 \\ & + d_2 s_2^6 - s_2^2 (s_2 s_5 - s_1 s_6) (d_1 s_2^2 - d_0 s_2 s_5 + d_0 s_1 s_6) \\ & = -b_1 d_1 s_1 s_2^3 + 2d_0 b_1 s_1 s_5 s_2^2 - 3d_0 b_1 s_1^2 s_2 s_6 \\ & + 2b_1^2 d_0^2 s_1^3 + s_2^4 s_8 - s_2^3 s_5 s_6 + s_1 s_2^2 s_6^2 \end{aligned} \right\}. \end{aligned} \quad (5.8)$$

To see that the fibers in the resolution X_5 degenerate as expected over the total transforms of both loci described above, we work in the open set $d_0 e_1 b_1 e_2 e_3 \neq 0$. For the charge $q = 1$ locus, we further restrict to the open set $s_2 \neq 0$ and solve for d_2, s_8 in the equation $V_{q=1} = 0$. Doing so, we find that

$$F|_{V_{q=1}=0} = F_{q=1}^+ + F_{q=1}^- \quad (5.9)$$

We learn also that the zero section intersects $F_{q=1}^+$ in a point, while the generating section intersects $F_{q=1}^-$ in a point. Moreover, it is straightforward to verify that the intersection $F_{q=1}^+ \cap F_{q=1}^-$ consists of two distinct points, hence we see the fibers over $V_{q=1} = 0$ are type

¹⁴ \mathbb{F}_n denotes the Hirzebruch surface $\mathbb{P}(\mathcal{O} \oplus \mathcal{O}(n)) \rightarrow c$, with divisor classes f, c satisfying $f^2 = 0, f \cdot c = 1, c^2 = -n$.

I_2 , as anticipated, where $F_{q=1}^+$ as the affine component of the affine $\mathfrak{su}(2)$ Dynkin diagram describing the intersection structure of the enhancement. The enhancement of the elliptic fiber to an I_2 Kodaira fiber indicates the presence of charged matter and since this enhancement occurs away from the components of the discriminant locus associated to nonabelian gauge symmetry, we conclude this matter can only be charged under the $\mathfrak{u}(1)$ of the 4D gauge algebra. The $\mathfrak{u}(1)$ charges can be checked by computing intersection products $\hat{D}_{\bar{1}} \cdot F_{q=1}^\pm$.

We treat the charge $q = 2$ locus in a similar manner. Setting $s_1 = s_2 = 0$, Eq. (3.12) splits into two components, $p_{5,2}(s_1 = s_2 = 0) = e_5 t = 0$. It follows that the fibers over this locus degenerate:

$$F|_{s_1=s_2=0} = F_{q=2}^+ + F_{q=2}^-, \quad F_{q=2}^+ = F|_{s_1=s_2=t=0}, \quad F_{q=2}^- = F|_{s_1=s_2=e_5=0}. \quad (5.10)$$

Notice that the above definitions imply that the zero section wraps the exceptional curve $F_{q=2}^-$. To study the geometry of the degenerated fibers more explicitly, we use local descriptions of the fibers in affine open sets, as we now describe.

For $F_{q=2}^+$, Making the redefinitions $u \rightarrow u/(e_1 e_2 e_4)$, $w \rightarrow w/(e_1 e_3 e_4)$, we can describe $F_{q=2}^+$ locally as a smooth conic in \mathbb{P}^2 with homogeneous coordinates $[u : v : we_5]$ with the point $[0 : 1 : 0]$ removed. For $F_{q=2}^-$, we make the redefinitions $w \rightarrow e_2 e_4 u w / e_3$, $e_4 \rightarrow e_4 / (e_1 e_2 u)$ so that $F_{q=2}^-$ can be described locally as a sum of base and fiber curves in \mathbb{F}_1 with homogeneous coordinates $[e_4 : v][w : t] \cong [\lambda_0 e_4 : \lambda_0 v][\lambda_5 w : \lambda_0 \lambda_5 t]$.

The generating section \hat{D}_1 intersects $F_{q=2}^-$ in a point, but does not intersect $F_{q=2}^+$. Moreover, the intersection $F_{q=2}^+ \cap F_{q=2}^-$ consists of two distinct points, hence the fibers over the charge $q = 2$ locus are type I_2 . Once again, the charges can be determined explicitly by computing the intersection products $\hat{D}_{\bar{1}} \cdot F_{q=2}^\pm$.

5.3 $(\mathbf{1}, \mathbf{2})_{w_{\bar{1}}}$

The residual discriminant locus intersecting the codimension-one I_2 locus $d_0 = 0$ is

$$\begin{aligned} f &= (4b_1 d_1 s_2 - s_6^2)^2 + \mathcal{O}(d_0) \\ g &= (4b_1 d_1 s_2 - s_6^2)^3 + \mathcal{O}(d_0) \\ \Delta &= -\frac{1}{16} d_0^2 b_1^3 s_2 \Delta_{(a)} (4b_1 d_1 s_2 - s_6^2)^2 + \mathcal{O}(d_0^3), \end{aligned} \quad (5.11)$$

where

$$\begin{aligned} \Delta_{(a)} &= b_1^2 d_1^3 s_1^2 + b_1 d_1^2 s_2 s_5^2 - b_1 d_1^2 s_1 s_5 s_6 - 2b_1 d_1^2 s_1 s_2 s_8 \\ &\quad - 2b_1 d_2 d_1 s_2^2 s_5 + 3b_1 d_2 d_1 s_1 s_2 s_6 + b_1 d_2^2 s_2^3 + d_1 s_2^2 s_8^2 \\ &\quad + d_1 s_1 s_6^2 s_8 - d_1 s_2 s_5 s_6 s_8 - d_2 s_1 s_6^3 + d_2 s_2 s_5 s_6^2 - d_2 s_2^2 s_6 s_8. \end{aligned} \quad (5.12)$$

thus according to Tate's algorithm [59] we can anticipate the presence of localized matter charged under $\mathfrak{su}(2)$ for all codimension-two loci except for $d_0 = 4b_1 d_1 s_2 - s_6^2 = 0$. According to the analysis of [2], we anticipate the following representations

$$\begin{aligned} (\mathbf{1}, \mathbf{2})_{\frac{1}{2}} &: d_0 = \Delta_{(a)} = 0, \\ (\mathbf{1}, \mathbf{2})_{\frac{3}{2}} &: d_0 = s_2 = 0. \end{aligned} \quad (5.13)$$

In this subsection we focus on the local matter away from the collision of I_2 and I_3^{split} fibers; see [Figure 2](#). Bifundamental matter, which is localized at the collision of the I_2 and I_3^{split} fibers, is discussed in [Section 5.5](#).

Judging from [Eq. \(5.11\)](#), we expect the I_2 fiber to enhance to I_3^{split} over $\Delta_{(a)} = 0$. Unfortunately, an explicit algebraic description of the degeneration of the elliptic fibers over $\Delta_{(a)} = 0$ is difficult to obtain so we simply verify that the discriminant Δ_{F_0} of the cubic polynomial defining F_0 in [Eq. \(4.3\)](#) vanishes on this locus. In particular, we find

$$\Delta_{F_0} = (\cdots)\Delta_{(a)}. \quad (5.14)$$

In the above equation, (\cdots) denotes factors of b_1, e_2, e_3 responsible for the degeneration leading to bifundamental matter; we analyze this degeneration in detail in [Section 5.5](#). Schematically, we write

$$F_0|_{\Delta_{(a)}=0} = F_0^+ + F_0^-. \quad (5.15)$$

Unfortunately, without an explicit algebraic description, it is not precisely clear how \hat{D}_0, \hat{D}_1 intersect the irreducible components F_0^\pm of the elliptic fiber over this locus. However, given that the BPS particles corresponding to M2 branes wrapping F_0^\pm have much larger KK central charges than Coulomb branch central charges, we can further anticipate that \hat{D}_0 only intersects either F_0^+ or F_0^- in a point, rather wrapping the entire curve.

Turning next to $s_2 = 0$ and keeping in mind $p_{5,2}(e_1 = s_2 = 0) = te_5 = 0$, we find

$$F_1|_{s_2=0} = F_1^t + F_1^{e_5}. \quad (5.16)$$

The above equation describes a pair of curves intersecting transversally. A local algebraic description of F_1^t can be obtained by restricting the description of F_1 (see [Eq. \(4.3\)](#)) to the locus $s_2 = 0$. Making appropriate coordinate redefinitions, $F_1^{e_5}$ can be described locally as a sum of a base and fiber curve in subspace birational to \mathbb{F}_1 with coordinates $[u : d_0][w : t] \cong [\lambda_1 u : \lambda_1 d_0][\lambda_1 \lambda_5 w : \lambda_5 t]$. A straightforward computation shows that the pairwise intersections $F_0 \cap F_1^t, F_0 \cap F_1^{e_5}, F_1^t \cap F_1^{e_5}$ are distinct points and hence the degeneration over $s_2 = 0$ enhances the I_2 fiber to an I_3^{split} fiber, indicating matter transforming in the $\mathbf{2}$ of $\mathfrak{su}(2)$.

Note that \hat{D}_0 wraps the entire curve $F_1^{e_5}$, and both \hat{D}_0, \hat{D}_1 intersect F_1^t in distinct points.

5.4 $(\mathbf{3}, \mathbf{1})_{w_1}$

The residual discriminant intersecting the I_3^{split} locus $b_1 = 0$ is

$$\begin{aligned} f &= -\frac{s_6^4}{48} + \mathcal{O}(b_1^2), \\ g &= \frac{s_6^6}{864} + \mathcal{O}(b_1^4), \\ \Delta &= -\frac{1}{16}b_1^3 d_0^2 s_2 s_6^3 (s_8 s_2^2 + s_1 s_6^2 - s_2 s_5 s_6)(d_0 e_1 s_8^2 + d_2 s_6^2 - d_1 s_8 s_6) \\ &\quad + \mathcal{O}(b_1^4). \end{aligned} \quad (5.17)$$

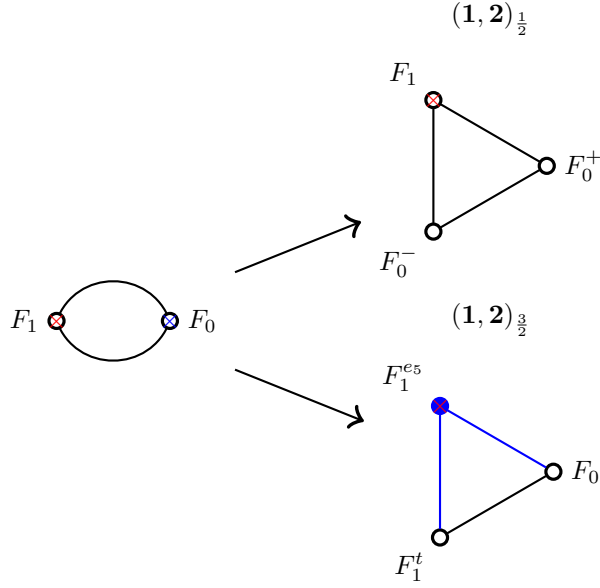


Figure 2. Schematic depiction of the degeneration of the I_2 Kodaira fibers over the codimension-two loci corresponding to local matter transforming in the representations $(\mathbf{1}, \mathbf{2})_{1/2}$ (over $d_0 e_1 = \Delta_{(a)} = 0$) and $(\mathbf{1}, \mathbf{2})_{3/2}$ (over $d_0 e_1 = s_2 = 0$). Note that a blue (respectively, red) \times in the center of a node corresponding to an irreducible \mathbb{P}^1 component of the singular elliptic fiber indicates that \hat{D}_0 (respectively, \hat{D}_1) intersects the said \mathbb{P}^1 in a point. The blue node is wrapped entirely by \hat{D}_0 .

Following Tate's algorithm, we expect to see localized matter charged under $\mathfrak{su}(3)$ at all codimension-two components of the discriminant locus except for $b_1 = s_6 = 0$.¹⁵ The analysis of [2] anticipates the following $\mathfrak{su}(3)$ charged matter representations (see Figure 3):

$$\begin{aligned}
(\mathbf{3}, \mathbf{1})_{\frac{2}{3}} &: b_1 = s_8 s_2^2 - s_5 s_2 s_6 + s_1 s_6^2 = 0 \\
(\mathbf{3}, \mathbf{1})_{-\frac{1}{3}} &: b_1 = d_2 s_6^2 - d_1 s_6 s_8 + d_0 e_1 s_8^2 = 0 \\
(\mathbf{3}, \mathbf{1})_{-\frac{4}{3}} &: b_1 = s_2 = 0.
\end{aligned} \tag{5.18}$$

Over the locus $s_8 s_2^2 - s_5 s_2 s_6 + s_1 s_6^2 = 0$, we find that the fibers in the resolution X_5 behave as follows:

$$F'_0|_{s_8 s_2^2 + s_1 s_6^2 - s_2 s_5 s_6 = 0} = F_0'^+ + F_0'^-. \tag{5.19}$$

Substituting $w \rightarrow w/(e_4 e_5)$, $e_2 \rightarrow e_2/(e_4 u)$ we find in the open set $s_2 \neq 0$ that $F_0'^{\pm}$ can be given a local algebraic description as a pair of lines in \mathbb{P}^2 with coordinates $[e_1 e_3 e_2 : v : e_1 e_3 w]$ and the point $[1 : 0 : 0]$ removed. Given this description, it is straightforward to verify that the pairwise intersections $F_0'^- \cap F_2'$, $F_0'^+ \cap F_3'$, $F_0'^+ \cap F_0'^-$ are distinct points, hence the fiber

¹⁵The locus $b_1 = s_6 = 0$ is an IV locus, and does not support any charged matter [2].

enhances to I_4^{split} indicating matter in the **3**. Note that \hat{D}_0 intersects $F_0'^-$ in a point along $w = 0$, whereas \hat{D}_0 does not intersect $F_0'^+$.

Similarly, over the locus $d_0e_1s_8^2 + d_2s_6^2 - d_1s_8s_6 = 0$ the curve F_2' degenerates as follows:

$$F_2'|_{d_0e_1s_8^2+d_2s_6^2-d_1s_8s_6=0} = F_2'^+ + F_2'^-. \quad (5.20)$$

Making the coordinate substitutions $e_3 \rightarrow e_3/(e_4e_5w), u \rightarrow u/e_4$ we find that in the open set $s_6s_8 \neq 0$ that $F_2'^{\pm}$ can be described locally as a pair of lines in \mathbb{F}_1 (the homogeneous coordinates for this \mathbb{F}_1 are described in [Section 4.2](#)). The pairwise intersections $F_2'^+ \cap F_0', F_2'^- \cap F_0', F_2'^+ \cap F_2'^-$ are distinct points, and thus we find an enhancement to an I_4^{split} fiber again indicating matter in the **3** of $SU(3)$.

Finally we come to the locus $s_2 = 0$. The component F_3' degenerates as follows:

$$F_3'|_{s_2=0} = F_3'^t + F_3'^{e_5}. \quad (5.21)$$

Making coordinate redefinitions $t \rightarrow vt, u \rightarrow d_0vu, w \rightarrow d_0vw$, we find that the irreducible components of the above degeneration can be described by

$$\begin{aligned} F_3'^t &= \{t = b_1w + e_2e_4tu^2 + e_4s_6uw = 0\} \subset \mathbb{P}_{[e_4u:b_1]}^1 \times \mathbb{P}_{[w:t]}^1 \\ F_3'^{e_5} &= \{e_5 = b_1w + e_2e_4tu^2 + e_4s_6uw = 0\} \subset \mathbb{F}_{1[e_4u:b_1][e_2:e_4e_5w]} \end{aligned} \quad (5.22)$$

where $[e_4u : b_1][e_2 : e_4e_5w] \cong [\lambda_2e_4u : \lambda_2b_1][\lambda_3\lambda_2^{-1}e_2 : \lambda_3e_4e_5w]$. The pairwise intersections $F_3'^t \cap F_2', F_3'^{e_5} \cap F_0', F_3'^t \cap F_3'^{e_5}, F_0' \cap F_2'$ are all distinct points, hence we again find an enhancement of type I_4^{split} .

Note that \hat{D}_0 wraps $F_3'^{e_5}$ and \hat{D}_1 intersects $F_3'^{e_5}$ in a point $\hat{D}_0 \cap \hat{D}_1$ away from the intersection $F_3'^t \cap F_3'^{e_5}$.

5.5 $(\mathbf{3}, \mathbf{2})_{w\bar{1}}$

In this section we describe the collision of I_2, I_3^{split} fibers over the codimension-two locus $b_1 = d_0 = 0$:

$$F|_{b_1e_2e_3=d_0e_1=0} = F_{00} + F_{02} + F_{10} + F_{12} + F_{13}, \quad (5.23)$$

where F_{ab} denotes the curve obtained by setting $e_a = e_b = 0$ for $a, b \neq 0$, or $d_0, b_1 = 0$ for (resp.) $a, b = 0$.

The analysis of [\[2\]](#) indicates that $\mathfrak{su}(3) \oplus \mathfrak{su}(2)$ charged matter is localized at the collision of the I_2, I_3^{split} singularities (see [Figure 4](#)):

$$(\mathbf{3}, \mathbf{2})_{\frac{1}{6}} : d_0 = b_1 = 0. \quad (5.24)$$

Working in the affine open set $\lambda_5 = e_5 \neq 0$, we can give the above irreducible components local descriptions as follows. For F_{00} , making the redefinitions $w \rightarrow w/(e_3e_4e_5), e_2 \rightarrow e_2/(e_4u)$ leads to the local description of F_{00} as a smooth conic in \mathbb{P}^2 with coordinates $[e_1e_2 : v : e_1w]$ with the point $[0 : 1 : 0]$ removed. For F_{02} , redefining $u \rightarrow e_3e_5wu, e_2 \rightarrow e_2/e_3$ leads to

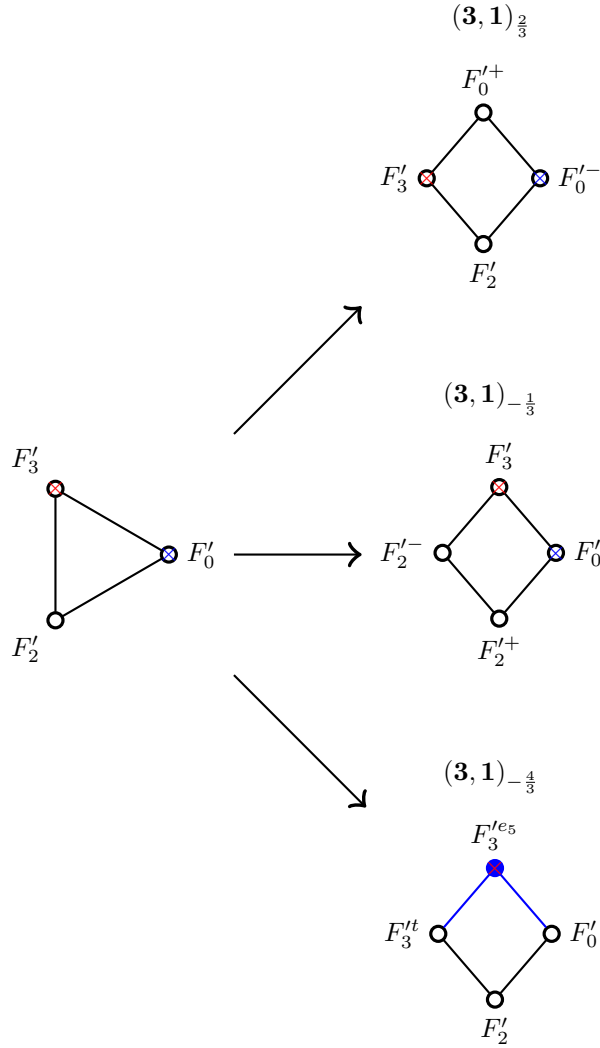


Figure 3. Schematic depiction of the degeneration of the I_3^{split} Kodaira fibers over the codimension-two loci corresponding to local matter transforming in the representations $(\mathbf{3}, \mathbf{1})_{2/3}$ (over $b_1 e_2 e_3 = s_8 s_2^2 - s_5 s_2 s_6 + s_1 s_6^2 = 0$), $(\mathbf{3}, \mathbf{1})_{-1/3}$ (over $b_1 e_2 e_3 = d_2 s_6^2 - d_1 s_6 s_8 + d_0 e_1 s_8^2 = 0$), and $(\mathbf{3}, \mathbf{1})_{-4/3}$ (over $b_1 e_2 e_3 = s_2 = 0$). Note that a blue (respectively, red) \times in the center of a node corresponding to an irreducible \mathbb{P}^1 component of the singular elliptic fiber indicates that \hat{D}_0 (respectively, \hat{D}_1) intersects the said \mathbb{P}^1 in a point. The blue node in the bottom-most graph is wrapped entirely by \hat{D}_0 .

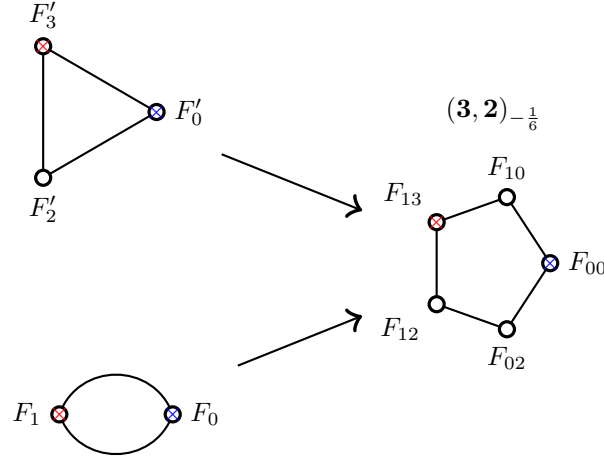


Figure 4. Schematic depiction of the collision of I_2 and I_3^{split} Kodaira fibers over the codimension-two locus corresponding to local matter transforming in the representation $(\mathbf{3}, \mathbf{2})_{-1/6}$ (over $d_0 e_1 = b_1 e_2 e_3 = 0$). Note that a blue (respectively, red) \times in the center of a node corresponding to an irreducible \mathbb{P}^1 component of the singular elliptic fiber indicates that \hat{D}_0 (respectively, \hat{D}_1) intersects the said \mathbb{P}^1 in a point.

a description as curve of bi-degree $(1, 1)$ in $\mathbb{P}^1 \times \mathbb{P}^1$ with coordinates $[v : e_1 w][u : b_1]$. For F_{10} , redefining $w \rightarrow vw/(e_4 e_5)$, $e_2 \rightarrow ve_2/e_4 u$ allows us to describe F_{10} locally as a line in \mathbb{P}^2 with homogeneous coordinates $[e_3 e_2 : e_3 w : d_0]$. For F_{12} , making the redefinitions $u \rightarrow vu/e_4$, $e_3 \rightarrow ve_3/(e_4 e_5 w)$, we find that F_{12} can be described as a curve of bi-degree $(1, 1)$ in \mathbb{F}_1 with homogeneous coordinates $[e_3 : d_0][u : b_1]$. Finally, for F_{13} , making the redefinitions $e_4 \rightarrow d_0 v e_4/u$, $w \rightarrow uw/e_5$ and rescaling the coordinates appropriately, we find that F_{13} can be described by the equation

$$F_{13} = \{s_2 e_2 e_4 + b_1 w + s_6 e_4 w = 0\} \subset \mathbb{F}_1 \quad (5.25)$$

where the \mathbb{F}_1 in the above equation has homogeneous coordinates $[e_4 : b_1][e_2 : e_4 w] \cong [\lambda_2 e_4 : \lambda_2 b_1][\lambda_2^{-1} \lambda_3 e_2 : \lambda_3 e_4 w]$. It is straightforward to verify that the only intersections $F_{00} \cap F_{02}$, $F_{00} \cap F_{10}$, $F_{02} \cap F_{12}$, $F_{10} \cap F_{13}$, $F_{12} \cap F_{13}$ are distinct points, hence we find that the elliptic fiber is type I_5^{split} .

Note that \hat{D}_0 intersects F_{00} in a point, while \hat{D}_1 intersects F_{13} in a point.

6 Codimension three: Yukawa interactions

In this section, we study the degenerations of the elliptic fibers over codimension-three loci in B that are characterized by triple intersections of matter curves,

$$C_{R_1} \cap C_{R_2} \cap C_{R_3} \subset B. \quad (6.1)$$

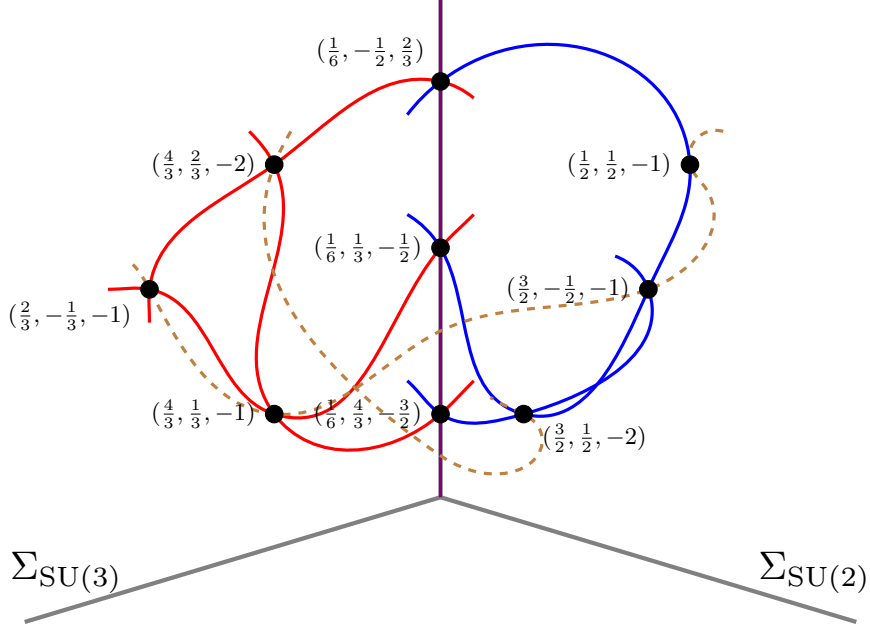


Figure 5. Cartoon depiction of the various junctions of triples of matter curves $C_R, C_{R'}, C_{R''} \in B$ associated to candidate Yukawa interactions appearing in the low-energy 4D $\mathcal{N} = 1$ action. Each codimension-three point in B in the above figure (represented by a black dot) is labeled by the triple of $\mathfrak{u}(1)$ charges $w_{\bar{1}}, w'_{\bar{1}}, w''_{\bar{1}}$ of the three representations r, r', r'' (see Eq. (6.4)) contracted into a gauge singlet term in the low-energy Lagrangian; note that each triple labels one of a pair of possible complex conjugate interaction terms. The red, blue, and purple curves correspond to matter curves associated to non-trivial $\mathfrak{su}(3), \mathfrak{su}(2)$, and $\mathfrak{su}(3) \oplus \mathfrak{su}(2)$ representations, respectively. By contrast, the dashed lines denote matter curves corresponding to pure $\mathfrak{u}(1)$ charges. Note also that the $(\mathbf{1}, \mathbf{1})_{-1}$ matter curve intersects the $(\mathbf{1}, \mathbf{2})_{1/2}$ in a tangent point.

Since the orders of vanishing of the sections f, g, Δ can further increase at these codimension-three loci, the singularity type of the elliptic fibers can enhance; we refer to this behavior as a degeneration of the elliptic fibers because analogous to the degenerations of the elliptic fibers over codimension-one or codimension-two components of the discriminant locus, these singularity enhancements also manifest themselves in the resolved geometry as the splitting of one or more of the components of the elliptic fibers into multiple irreducible \mathbb{P}^1 components. However, there is an important distinction to be made here, in that the elliptic fiber degenerations over loci of the form Eq. (6.1) do not produce additional generators of the cone of effective curves. This is because the degenerations are of the schematic form

$$F_{R_1} = F'_{R_2} + F''_{R_3} \quad (6.2)$$

at a given point in the locus Eq. (6.1). In the above equation, F_{R_i} is an irreducible component of the elliptic fibers (and hence a generator of the cone of effective curves) over a *generic* point the codimension-two locus C_{R_i} , and thus we see that the classes of any apparently “new”

curves that appear as a result of these degenerations turn out to be linear combinations of existing curve classes.

Eq. (6.2) implies that at each degeneration point in the resolved geometry, there resides a localized interaction in the M-theory effective action that mediates the splitting of a BPS state corresponding to an M2-brane wrapping F_{R_1} into a pair of BPS states corresponding to M2-branes wrapping F'_{R_2} and F''_{R_3} [43]. The representation-theoretic version of this statement that characterizes the F-theory limit is that degenerations of the form Eq. (6.2) indicate the existence of maps

$$R_1 \times R_2 \times R_3 \rightarrow 1, \quad (6.3)$$

which produce gauge singlets from the weights of the matter representations in the low-energy effective action. In other words, these codimension-three singularities correspond to Yukawa interactions appearing in the low-energy effective 4D action [12–14] (see also Section 6 of [42] and references therein). An important check that such interactions indeed can appear in the low-energy effective action is to identify an explicit elliptic fiber degeneration in the resolution of the singular F-theory background.¹⁶

In the case of the $(\mathrm{SU}(3) \times \mathrm{SU}(2) \times \mathrm{U}(1))/\mathbb{Z}_6$ model, we anticipate the existence of Yukawa interactions corresponding to the following gauge singlets:

$$(r_3, r_2)_{w_{\bar{1}}} \times (r'_3, r'_2)_{w'_1} \times (r''_3, r''_2)_{w''_1}. \quad (6.4)$$

To ensure that the couplings are gauge singlets separately for each gauge factor $\mathfrak{su}(3)$, $\mathfrak{su}(2)$, $\mathfrak{u}(1)$ we require that the nonabelian irreps are either singlets or pairwise complex conjugates and that the $\mathfrak{u}(1)$ charges sum to zero.¹⁷ In more detail, we compute the full list of possible Yukawa interactions by identifying all solutions to the equation $w_{\bar{1}} + w'_1 + w''_1 = 0$, where $w_{\bar{1}}, w'_1, w''_1$ are a subset of $\mathfrak{u}(1)$ charges in the low-energy (anti-)chiral spectrum, and then excluding all candidate solutions for which the nonabelian factors cannot be combined into a gauge singlet. With the exception of the possible gauge singlet described in Footnote 17, it turns out that all possible Yukawa interactions consistent with the matter representations of the $(\mathrm{SU}(3) \times \mathrm{SU}(2) \times \mathrm{U}(1))/\mathbb{Z}_6$ model arise as elliptic fiber singularity enhancements over codimension-three loci in B , assuming generic characteristic data. In the following, we discuss one of a pair of complex conjugate Yukawa interactions associated to each codimension-three singularity.

¹⁶Note that while there are also Yukawa type couplings that include (non-chiral) adjoint representations of the nonabelian factors, associated with non-localized matter fields in the bulk of the 7-branes, we focus here on localized Yukawa couplings associated with nonabelian fundamental fields and the charge combinations of local matter described in the previous section.

¹⁷As the one possible exception to this characterization of the Yukawa interactions in the $(\mathrm{SU}(3) \times \mathrm{SU}(2) \times \mathrm{U}(1))/\mathbb{Z}_6$ model, we point out that there could also exist a Yukawa interaction of the form $(\mathbf{3}, \mathbf{1})_{\frac{2}{3}} \times (\mathbf{3}, \mathbf{1})_{\frac{2}{3}} \times (\mathbf{3}, \mathbf{1})_{-\frac{4}{3}}$ (along with its conjugate). This interaction would have to be localized at the double intersection of the $(\mathbf{3}, \mathbf{1})_{-\frac{4}{3}}$ locus $b_1 e_2 e_3 = s_2 = 0$ with the $(\mathbf{3}, \mathbf{1})_{\frac{2}{3}}$ locus $b_1 e_2 e_3 = s_8 s_2^2 - s_5 s_2 s_6 + s_1 s_6^2 = 0$. However, the only possible double intersection would occur at tangent point $s_6^2 = 0$, which lies along the IV locus $b_1 e_2 e_3 = s_6 = 0$, which does not support any charged matter, hence there is no additional Yukawa interaction.

6.1 $(\mathbf{3}^*, \mathbf{2})_{w_{\bar{1}}} \times (\mathbf{3}, \mathbf{1})_{w'_1} \times (\mathbf{1}, \mathbf{2})_{w''_1}$

First we consider the case $(w_{\bar{1}}, w'_1, w''_1) = (-\frac{1}{6}, -\frac{4}{3}, \frac{3}{2})$. Using the description of the fiber degeneration Eq. (5.23) associated with local matter transforming in $(\mathbf{3}, \mathbf{2})_{\frac{1}{6}}$, over the locus $s_2 = 0$ we observe an additional degeneration $F'_{13} \rightarrow F''_{13} + F'^{e_5}_{13}$ inherited from the $(\mathbf{3}, \mathbf{1})_{-\frac{4}{3}}$ degeneration $F'_3 \rightarrow F''_3 + F'^{e_5}_3$ described in Eq. (5.21), so that

$$F|_{b_1 e_2 e_3 = d_0 e_1 = s_2 = 0} = F_{00} + F_{10}^{e_5} + F_{13}^{e_5} + F_{13}^t + F_{12}^t + F_{02}^t. \quad (6.5)$$

The nontrivial intersections are the distinct points $F_{00} \cap F_{10}^{e_5}, F_{10}^{e_5} \cap F_{13}^{e_5}, F_{13}^{e_5} \cap F_{13}^t, F_{13}^t \cap F_{12}^t, F_{12}^t \cap F_{02}^t, F_{02}^t \cap F_{00}$, thus we observe an enhancement $I_5^{\text{split}} \rightarrow I_6^{\text{split}}$. Note that \hat{D}_0 wraps $F_{10}^{e_5}$ and $F_{13}^{e_5}$, while \hat{D}_1 intersects $F_{13}^{e_5}$ in a point.

The second case is $(w_{\bar{1}}, w'_1, w''_1) = (-\frac{1}{6}, \frac{2}{3}, -\frac{1}{2})$. In the open set $e_5 \neq 0$ we observe the further degeneration $F_{00} \rightarrow F_{00}^+ + F_{00}^-$, that is

$$F|_{b_1 e_2 e_3 = d_0 e_1 = s_8 s_2^2 - s_2 s_5 s_6 + s_1 s_6^2 = 0} = F_{00}^+ + F_{00}^- + F_{02} + F_{10} + F_{12} + F_{13}. \quad (6.6)$$

Setting $s_8 = (s_2 s_5 s_6 - s_1 s_6^2)/s_2^2$, and making the coordinate redefinitions $w \rightarrow w/(e_3 e_4 e_5)$, the new rational curves can be described as

$$\begin{aligned} F_{00}^+ &= \{s_2 e_2 + s_6 w = 0\}, \\ F_{00}^- &= \{s_1 s_2 e_1 e_2 + s_2^2 v + s_2 s_5 e_1 w - s_1 s_6 e_1 w = 0\}. \end{aligned} \quad (6.7)$$

The new intersection points are $F_{00}^+ \cap F_{00}^-, F_{00}^- \cap F_{02}, F_{00}^+ \cap F_{10}$, with all other intersection points unchanged and thus we find another I_6^{split} enhancement. Here, \hat{D}_0 intersects F_{00}^- in a point.

The final case is $(w_{\bar{1}}, w'_1, w''_1) = (-\frac{1}{6}, -\frac{1}{3}, \frac{1}{2})$. We observe the further degeneration $F_{02} \rightarrow F_{02}^+ + F_{02}^-$, i.e.,

$$F|_{b_1 e_2 e_3 = d_0 e_1 = d_2 s_6^2 - d_1 s_6 s_8 + d_0 e_1 s_8^2 = 0} = F_{00} + F_{02}^+ + F_{02}^- + F_{10} + F_{12} + F_{13}, \quad (6.8)$$

where setting $d_2 = d_1 s_8/s_6$ and making the coordinate redefinitions $u \rightarrow e_3 e_5 w u, w \rightarrow w/(e_1 e_3 e_4 e_5)$, we may write

$$\begin{aligned} F_{02}^+ &= \{d_1 b_1 + s_6 u = 0\}, \\ F_{02}^- &= \{s_6 v + s_8 w = 0\}. \end{aligned} \quad (6.9)$$

The new intersection points are $F_{02}^+ \cap F_{02}^-, F_{02}^+ \cap F_{12}, F_{02}^- \cap F_{00}$ with all other intersection points remaining the same, hence we again find an I_6^{split} enhancement.

See Figure 6 for a schematic depiction of the singular fibers over these special points in B .

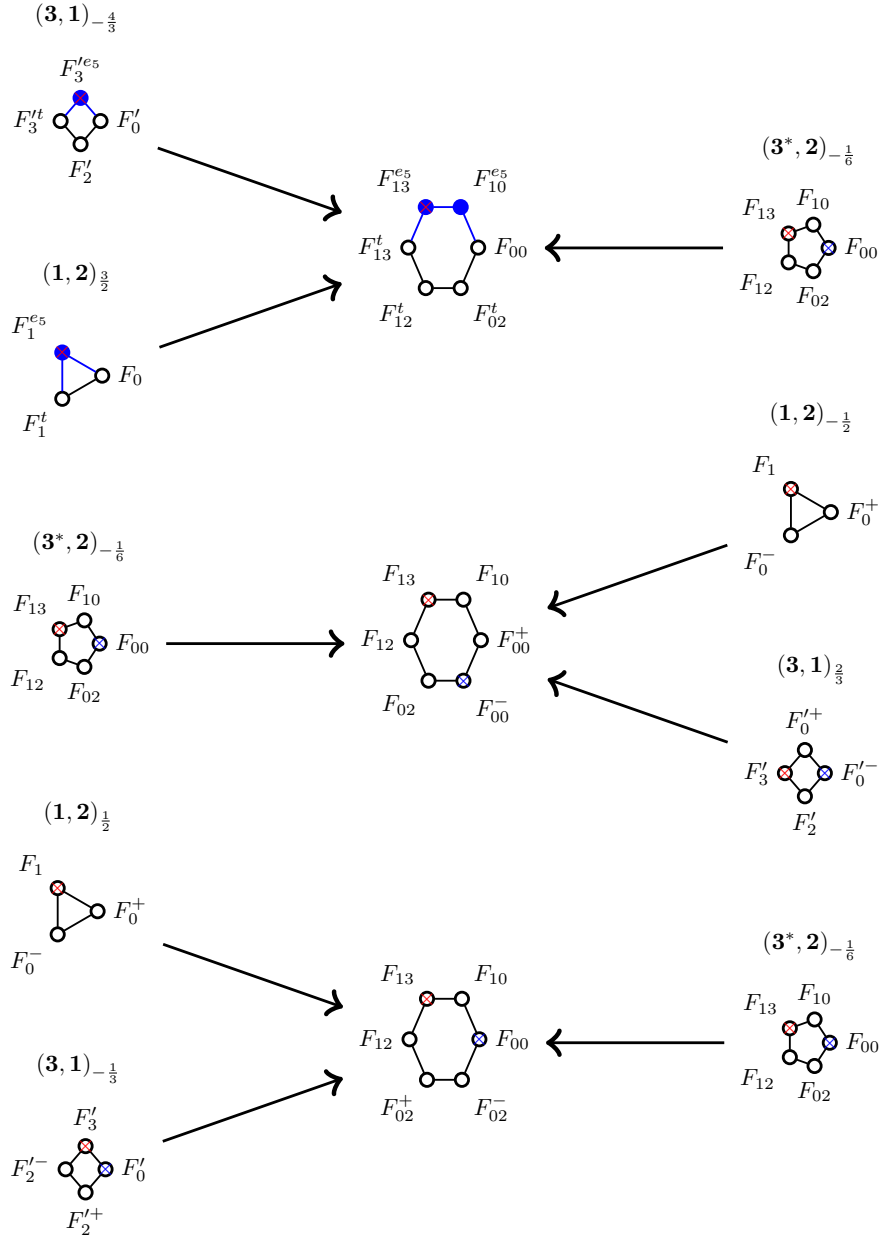


Figure 6. Singular fibers associated to Yukawa interactions of the form $(\mathbf{3}^*, \mathbf{2})_{w_{\bar{1}}} \times (\mathbf{3}, \mathbf{1})_{w'_{\bar{1}}} \times (\mathbf{1}, \mathbf{2})_{w''_{\bar{1}}}$.

6.2 $(\mathbf{3}^*, \mathbf{1})_{w_{\bar{1}}} \times (\mathbf{3}, \mathbf{1})_{w'_{\bar{1}}} \times (\mathbf{1}, \mathbf{1})_{w''_{\bar{1}}}$

First, consider the case $(w_{\bar{1}}, w'_{\bar{1}}, w''_{\bar{1}}) = (\frac{4}{3}, \frac{2}{3}, -2)$. We use the description of the $(\mathbf{3}, \mathbf{1})_{-\frac{4}{3}}$ degeneration given in Eq. (5.21), in which we already see the degeneration $F'_3 \rightarrow F_3'^{tt} + F_3'^{e_5}$. Over the locus $s_1 = 0$ an additional exceptional curve $F_0'^{e_5}$ appears due to the intersection of the zero section \hat{D}_0 with the affine component F'_0 of the singular elliptic fiber, leading to the degeneration

$$F|_{b_1 e_2 e_3 = s_2 = s_1 = 0} = F_0'^{tt} + F_0'^{e_5} + F_2' + F_3'^{tt} + F_3'^{e_5}. \quad (6.10)$$

The new intersection points are $F_0'^{e_5} \cap F_0'^{tt}$, $F_0'^{e_5} \cap F_3'^{e_5}$, $F_0'^{tt} \cap F_2'$, hence we find an enhancement $\mathbb{I}_4^{\text{split}} \rightarrow \mathbb{I}_5^{\text{split}}$. Notice that \hat{D}_0 now wraps both $F_3'^{e_5}$, $F_0'^{e_5}$, while \hat{D}_1 still intersects $F_3'^{e_5}$ in a point.

Next, consider the case $(w_{\bar{1}}, w'_{\bar{1}}, w''_{\bar{1}}) = (-\frac{2}{3}, -\frac{1}{3}, 1)$. We work with the description of the $(\mathbf{3}, \mathbf{1})_{\frac{2}{3}}$ degeneration in Eq. (5.19), in which $F'_0 \rightarrow F_0'^{++} + F_0'^{-}$. Here, consistent with the local matter representation $(\mathbf{3}, \mathbf{1})_{-\frac{1}{3}}$, for which we see the degeneration $F_2' \rightarrow F_2'^{++} + F_2'^{-}$, we find that the elliptic fiber decomposes as

$$F|_{b_1 e_2 e_3 = d_2 s_6^2 - d_1 s_6 s_8 + d_0 e_1 s_8^2 = s_8 s_2^2 - s_2 s_5 s_6 + s_1 s_6^2 = 0} = F_0'^{++} + F_0'^{-} + F_2'^{++} + F_2'^{-} + F_3'. \quad (6.11)$$

Solving simultaneously for s_8, d_1 and making the coordinate redefinitions $w \rightarrow w/(e_1 e_3 e_4 e_5)$, $t \rightarrow s_2 t/e_5$, and $u \rightarrow u/e_4$, we may write

$$\begin{aligned} F_2'^{++} &= \{s_6 t + s_8 w = 0\}, \\ F_2'^{-} &= \{b_1 d_0 e_1 s_6 t + e_1 s_6^2 u + b_1 d_1 s_6 w - b_1 d_0 e_1 s_8 w = 0\}. \end{aligned} \quad (6.12)$$

The new intersections points are $F_2'^{++} \cap F_2'^{-}$, $F_2'^{++} \cap F_0'^{-}$, $F_2'^{-} \cap F_3'$, hence we find another enhancement of the form $\mathbb{I}_4^{\text{split}} \rightarrow \mathbb{I}_5^{\text{split}}$.

Finally, consider the case $(w_{\bar{1}}, w'_{\bar{1}}, w''_{\bar{1}}) = (\frac{4}{3}, -\frac{1}{3}, -1)$. In this case we again work with the $(\mathbf{3}, \mathbf{1})_{-\frac{4}{3}}$ description given in Eq. (5.21). Consistent with the $(\mathbf{3}, \mathbf{1})_{\frac{1}{3}}$ degeneration $F_2' \rightarrow F_2'^{++} + F_2'^{-}$, we find

$$F|_{b_1 e_2 e_3 = s_2 = d_2 s_6^2 - d_1 s_6 s_8 + d_0 e_1 s_8^2 = 0} = F_0' + F_2'^{++} + F_2'^{-} + F_3'^{tt} + F_3'^{e_5}. \quad (6.13)$$

Using the projective scaling symmetry of the ambient space and making the coordinate redefinitions $u \rightarrow u/(e_1 e_4)$, $e_3 \rightarrow e_3/(e_1 e_4 e_5 w)$, $d_0 \rightarrow d_0/e_1$, the new irreducible curves can be expressed as

$$\begin{aligned} F_2'^{++} &= \{s_6 v + s_8 e_3 = 0\} \\ F_2'^{-} &= \{s_6^2 u + s_6 d_0 b_1 v + s_6 d_1 b_1 e_3 - s_8 b_1 d_0 e_3 = 0\} \end{aligned} \quad (6.14)$$

The new points of intersection are $F_2'^{++} \cap F_2'^{-}$, $F_2'^{++} \cap F_0'$, $F_2'^{-} \cap F_3'^{tt}$ and therefore we see an enhancement of the form $\mathbb{I}_4^{\text{split}} \rightarrow \mathbb{I}_5^{\text{split}}$.

See Figure 7 for a schematic depiction of the singular fibers over these special points in B .

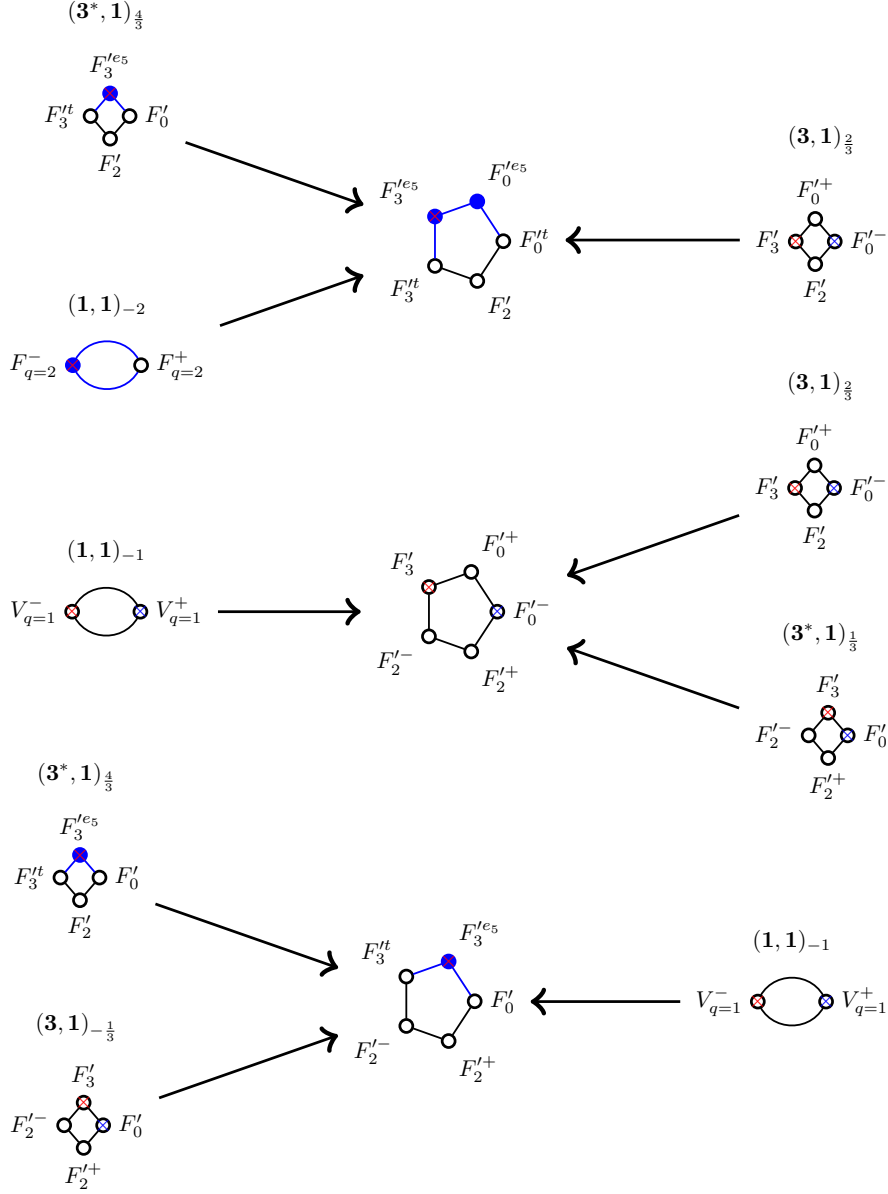


Figure 7. Singular fibers associated to Yukawa interactions of the form $(\mathbf{3}^*, \mathbf{1})_{w_{\bar{1}}} \times (\mathbf{3}, \mathbf{1})_{w'_{\bar{1}}} \times (\mathbf{1}, \mathbf{1})_{w''_{\bar{1}}}$.

6.3 $(\mathbf{1}, \mathbf{2})_{w_{\bar{1}}} \times (\mathbf{1}, \mathbf{2})_{w'_{\bar{1}}} \times (\mathbf{1}, \mathbf{1})_{w''_{\bar{1}}}$

The first case is $(w_{\bar{1}}, w'_{\bar{1}}, w''_{\bar{1}}) = (\frac{1}{2}, -\frac{3}{2}, 1)$. In this case, we borrow the description of the fiber degeneration $F_1 \rightarrow F_1^t + F_1^{e5}$ that occurs over the codimension-two locus associated to local matter transforming in the representation $(\mathbf{1}, \mathbf{2})_{\frac{3}{2}}$. In codimension three, we see the degeneration

$$F|_{d_0 e_1 = s_2 = \Delta_{(a)}/s_1 = 0} = F_0^+ + F_0^- + F_1^t + F_1^{e5} \quad (6.15)$$

where now, in contrast to the discussion in Section 5.3, the polynomial $\Delta_{(a)}$ factors over the locus $s_2 = 0$:

$$\frac{\Delta_{(a)}}{s_1} = s_1 d_1^3 b_1^2 e_2^2 e_3^2 - s_6 s_5 d_1^2 b_1 e_2 e_3 - s_6^3 d_2 + s_6^2 s_8 d_1 + \mathcal{O}(s_2). \quad (6.16)$$

The above factorization permits us to straightforwardly solve for an explicit algebraic description of the curves F_0^\pm . Solving $\Delta_{(a)}/s_1 = s_2 = 0$ for s_8 and eliminating the unit e_2 in the affine open set $s_1 e_1 e_3 e_4 u \neq 0$, we may use the following local descriptions

$$\begin{aligned} F_0^+ &= \{b_1 d_1 e_3 e_5 w + s_6 u = 0\}, \\ F_0^- &= \{-b_1 d_1^2 e_3 e_5^2 t^2 w + d_1 e_5 s_6 t^2 u + d_1 e_1 e_3 e_4 e_5 s_5 s_6 t u w \\ &\quad + d_1 e_1 e_3 e_4 s_1 s_6^2 u v w + d_2 e_1^2 e_3^2 e_4^2 e_5 s_1 s_6^2 u w^2 = 0\}. \end{aligned} \quad (6.17)$$

The new points of intersection are $F_0^+ \cap F_0^-$, $F_0^+ \cap F_1^t$, $F_0^- \cap F_1^{e5}$, hence we see an enhancement $\mathbb{I}_3^{\text{split}} \rightarrow \mathbb{I}_4^{\text{split}}$.

The next case is $(w_{\bar{1}}, w'_{\bar{1}}, w''_{\bar{1}}) = (\frac{1}{2}, \frac{3}{2}, -2)$. This Yukawa interaction can be analyzed in a manner analogous to that of the previous case, with the key distinction being that we now solve $\Delta_{(a)}|_{s_2=0} = 0$ by setting $s_1 = 0$. Here, it is illuminating to denote both degenerations by $F_0 \rightarrow F_0^t + F_0^{e5}$, $F_1 \rightarrow F_1^t + F_1^{e5}$:

$$F|_{d_0 e_1 = s_2 = s_1 = 0} = F_0^t + F_0^{e5} + F_1^t + F_1^{e5}, \quad (6.18)$$

where the points of intersection are $F_0^t \cap F_0^{e5}$, $F_1^t \cap F_1^{e5}$, $F_0^t \cap F_1^t$, $F_0^{e5} \cap F_1^{e5}$. We thus see an enhancement of the form $\mathbb{I}_3^{\text{split}} \rightarrow \mathbb{I}_4^{\text{split}}$. Notice that \hat{D}_0 now wraps both F_0^{e5} and F_1^{e5} , while \hat{D}_1 continues to intersect F_1^t in a point.

The final case is $(w_{\bar{1}}, w'_{\bar{1}}, w''_{\bar{1}}) = (\frac{1}{2}, \frac{1}{2}, -1)$. The restriction of the locus $\Delta_{(a)} = V_{q=1} = 0$ to $d_0 e_1 = 0$ can be expressed as

$$\{\Delta_{(a)} = V_{q=1} = 0\}|_{d_0 e_1 = 0} = \{d_2 s_2^2 - d_1 s_5 s_2 + d_1 s_1 s_6 = b_1 d_1 e_2 e_3 s_1 s_2 - s_8 s_2^2 + s_5 s_6 s_2 - s_1 s_6^2 = 0\}. \quad (6.19)$$

Note that the intersection of $V_{q=1} = 0$ and $\Delta_{(a)} = 0$ occurs at a tangent point as depicted in Figure 5, i.e., if we write $V_{q=1} := \{V_{q=1,1} = V_{q=1,2} = 0\}$ then

$$\Delta_{(a)}|_{V_{q=1,1}=0} = V_{q=1,2}^2, \quad \Delta_{(a)}|_{V_{q=1,2}=0} = V_{q=1,1}^2. \quad (6.20)$$

We solve the above equations by eliminating d_2, s_8 . Over this codimension-three locus, using the degeneration $F_0 \rightarrow F_0^+ + F_0^-$ inherited from the codimension-two enhancement associated

with local matter in the representation $(\mathbf{1}, \mathbf{2})_{\frac{1}{2}}$ described in Eq. (5.15), we see the further degeneration $F_0^+ + F_0^- \rightarrow F_0^{++} + F_0^{--} + F_0$:

$$F|_{d_0 e_1 = \Delta_{(a)} = V_{q=1} = 0} = F_0^{++} + F_0^{--} + F_0^0 + F_1, \quad (6.21)$$

where the points of intersection of the irreducible components are $F_0^{++} \cap F_0^0, F_0^{--} \cap F_0^0$, signaling an enhancement $I_3^{\text{split}} \rightarrow I_4^{\text{split}}$.

See Figure 8 for a schematic depiction of the singular fibers over these special points in B .

7 Intersection theory, 3D Chern–Simons couplings, and chiral matter multiplicities

In the preceding sections, we have studied the geometry of the resolution X_5 . This analysis confirms that the singularities of X_0 are consistent with the expected kinematics of the low-energy 4D theory [2], and provides a geometric grounding for further investigation of the structure of the matter spectrum and Yukawa interactions in the theory. In this section, we shift our attention to computing the chiral excesses introduced to the 4D matter spectrum by switching on a non-trivial flux background. Since we closely follow the approach described in [39], we omit here many technical details of the methodology involved and mostly focus on describing the results of using these methods to analyze the $(\text{SU}(3) \times \text{SU}(2) \times \text{U}(1))/\mathbb{Z}_6$ model; the interested reader should refer to [39] for details of the approach that are not spelled out here explicitly, and to [42] and further references in these two papers for further background and the earlier literature on chiral matter analyses in F-theory.

7.1 Quadruple intersection numbers and the reduced intersection matrix

The analysis of [39] provides a framework for understanding chiral multiplicities from fluxes in terms of a reduced intersection pairing matrix on the vertical part of the middle cohomology of the resolution $X_5 \rightarrow X_0$. This reduced intersection matrix can be computed from the quadruple intersection numbers of divisors in X_5 . One of the central results of [39] was the observation that the intersection pairing matrix appears to be independent of resolution, despite the fact that the quadruple intersection numbers are resolution-dependent. If this result indeed always holds, it suggests that the reduced intersection pairing matrix is the underlying resolution-independent mathematical structure that encodes information about the chiral matter spectrum in 4D F-theory compactifications. In the following discussion, we adopt this viewpoint and turn our attention towards computing the reduced intersection matrix associated to X_5 as a means to recover the chiral spectrum of the $(\text{SU}(3) \times \text{SU}(2) \times \text{U}(1))/\mathbb{Z}_6$ model.

The resolution X_5 has a basis of divisors

$$\hat{D}_{I=0,1,\alpha,i_2,i_3}, \quad (7.1)$$

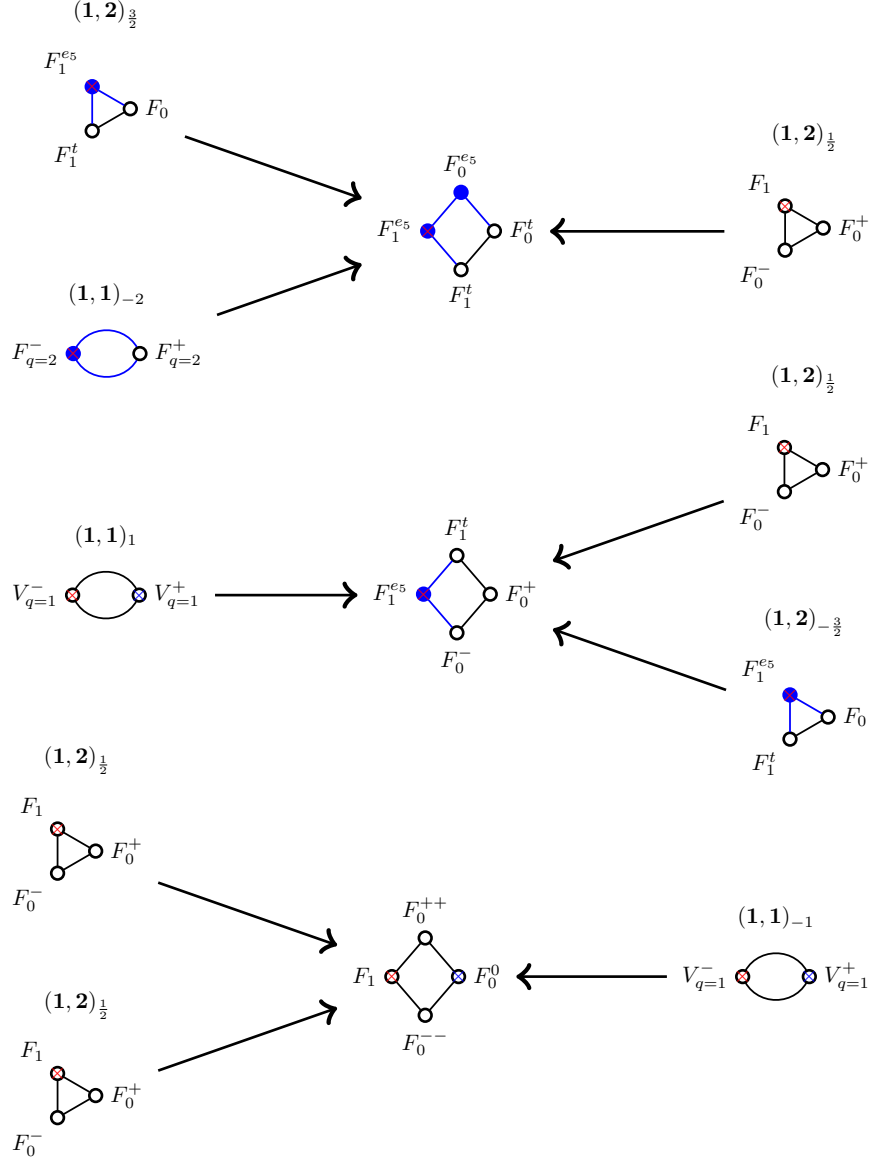


Figure 8. Singular fibers associated to Yukawa interactions of the form $(\mathbf{1}, \mathbf{2})_{w_1} \times (\mathbf{1}, \mathbf{2})_{w'_1} \times (\mathbf{1}, \mathbf{1})_{w''_1}$.

which includes a rational zero section \hat{D}_0 and rational generating section \hat{D}_1 associated to the $\mathfrak{u}(1)$ gauge factor,

$$\hat{D}_0 = \{e_5 = 0\} \cap X_5, \quad \hat{D}_1 = \{e_4 = 0\} \cap X_5, \quad (7.2)$$

as well as an $\mathfrak{su}(2)$ Cartan divisor $\hat{D}_{i_2} = \hat{D}_3$, and $\mathfrak{su}(3)$ Cartan divisors $\hat{D}_{i_3} = \hat{D}_4, \hat{D}_5$ appearing as irreducible components in the pullback of the gauge divisors Σ_s from B to X_5 :

$$\begin{aligned} \hat{\Sigma}_2 &= \Sigma_2^\alpha \hat{D}_\alpha = (\hat{\Sigma}_2 - \hat{D}_3) + \hat{D}_3 = \{d_0 e_1 = 0\} \cap X_5, \\ \hat{\Sigma}_3 &= \Sigma_3^\alpha \hat{D}_\alpha = (\hat{\Sigma}_3 - \hat{D}_4 - \hat{D}_5) + \hat{D}_4 + \hat{D}_5 = \{b_1 e_2 e_3 = 0\} \cap X_5. \end{aligned} \quad (7.3)$$

The $\mathfrak{u}(1)_{\text{KK}}$ and $\mathfrak{u}(1)$ divisors (i.e., the images of \hat{D}_0, \hat{D}_1 under the Shioda map [61]) are given by

$$\hat{D}_{\bar{0}} = \sigma_0^I \hat{D}_I = \hat{D}_0 - \frac{1}{2} \hat{K}, \quad (7.4)$$

$$\hat{D}_{\bar{1}} = \sigma_1^I \hat{D}_I = \hat{D}_1 - \hat{D}_0 + \hat{K} - \hat{Y} + \frac{1}{2} \hat{D}_3 + \frac{1}{3} (\hat{D}_4 + 2\hat{D}_5), \quad (7.5)$$

where $\hat{K} = K^\alpha \hat{D}_\alpha, \hat{Y} = Y^\alpha \hat{D}_\alpha$. Note that our convention for ordering the indices i_s of the Cartan divisors \hat{D}_{i_s} matches the following presentation of the $\mathfrak{su}(2) \oplus \mathfrak{su}(3)$ Cartan matrix:

$$[[\kappa_{i_s j_t}]] = \begin{pmatrix} 2 & 0 & 0 \\ 0 & 2 & -1 \\ 0 & -1 & 2 \end{pmatrix}. \quad (7.6)$$

Now that we have identified a suitable basis of divisors, our next task is to compute their quadruple intersection numbers. We use the adaptation of the pushforward technology of [62] to compute the pushforwards W_{IJKL} of the quadruple intersection numbers

$$\hat{D}_I \cdot \hat{D}_J \cdot \hat{D}_K \cdot \hat{D}_L \quad (7.7)$$

(here, \cdot denotes the intersection product in the Chow ring of X_5) to the Chow ring of B . In more detail, we first represent the pullbacks of the divisor classes \hat{D}_I as linear combinations of the divisors $\mathbf{D}_\alpha, \mathbf{H}, \mathbf{E}_i = [e_i]$ restricted to the class \mathbf{X}_5 of the hypersurface $X_5 \in Y_5$:

$$\hat{D}_I \cdot \mathbf{X}_5. \quad (7.8)$$

In the above equation, the class \mathbf{X}_5 is given by

$$\mathbf{X}_5 := [p_{5,i}] = 3\mathbf{H} - \mathbf{K} - \Sigma_2 + 2\Sigma_3 - 2\mathbf{Y} - 2\mathbf{E}_1 - \mathbf{E}_2 - \mathbf{E}_3 - \mathbf{E}_4 - \mathbf{E}_5 \quad (7.9)$$

and

$$\hat{D}_0 = \mathbf{E}_5, \quad \hat{D}_1 = \mathbf{E}_4, \quad \hat{D}_3 = \mathbf{E}_1, \quad \hat{D}_4 = \mathbf{E}_2 - \mathbf{E}_3, \quad \hat{D}_5 = \mathbf{E}_3 \quad (7.10)$$

so that in terms of the projection

$$\pi: Y_5 \rightarrow B, \quad (7.11)$$

the pushforwards of the quadruple intersection numbers can be expressed as

$$W_{IJKL} = \pi_*(\hat{D}_I \cdot \hat{D}_J \cdot \hat{D}_K \cdot \hat{D}_L \cdot \mathbf{X}_5). \quad (7.12)$$

The above formulas allow us to represent all intersection products as products of divisor classes in the Chow ring of Y_5 . We then use the fact that the projection map π can be represented as a composition of maps,

$$\pi = \varpi \circ f_1 \circ \cdots \circ f_5, \quad (7.13)$$

where f_i are the blowups appearing in Eq. (3.10) and the ϖ is the canonical projection $Y_0 \rightarrow B$ in Eq. (3.7), to represent the pushforward map π_* acting on elements of the Chow ring of Y_5 as the composition

$$\pi_* = \varpi_* \circ f_{1*} \circ \cdots \circ f_{5*}. \quad (7.14)$$

Since the action of ϖ_* , f_{i*} on any formal power series in the appropriate Chow ring is known explicitly, this decomposition enables us to compute the pushforward of any quadruple intersection number—see Appendix E of [39] for more details.

For convenience, we follow the approach of [63] and arrange the intersection numbers into the generating function

$$e^{\hat{J}} = \exp(\varphi^I \hat{D}_I) \cdot \mathbf{X}_5. \quad (7.15)$$

The real parameters φ^I in the above expression, which may be regarded as real numbers parametrizing a choice of Kähler form

$$\hat{J} = \varphi^I \hat{D}_I, \quad (7.16)$$

provide a useful parameterization for the generating function. The pushforward of Eq. (7.15) is

$$Z_\varphi = \pi_*(e^{\hat{J}}). \quad (7.17)$$

The intersection numbers can be extracted from Z_φ by computing derivatives:

$$W_{IJKL} = \frac{\partial^4}{\partial \varphi^I \partial \varphi^J \partial \varphi^K \partial \varphi^L} Z_\varphi \Big|_{\varphi=0}. \quad (7.18)$$

The pushforward of the generating function $e^{\hat{J}}$ under the map π_* encodes all of the intersection numbers of X_5 :

$$\begin{aligned} Z_\varphi = \exp(\varphi^\alpha D_\alpha) \cdot & \left(\frac{\mathcal{Z}_1}{K} + \frac{\mathcal{Z}_4 + \mathcal{Z}_6}{(K + Y) \cdot (K + \Sigma_3 + Y) \cdot (2K + \Sigma_3 + Y) \cdot (2K + \Sigma_2 + \Sigma_3 + Y)} \right. \\ & - \frac{\mathcal{Z}_2 + \mathcal{Z}_3}{(K + \Sigma_3) \cdot (K + \Sigma_2 + \Sigma_3) \cdot (K + Y)} + \frac{\mathcal{Z}_5}{(K + \Sigma_3 + Y) \cdot (2K + \Sigma_2 + \Sigma_3 + Y)} \\ & \left. + \frac{\mathcal{Z}_7}{K \cdot (K + \Sigma_3) \cdot (K + Y) \cdot (2K + \Sigma_3 + Y)} \right) \end{aligned} \quad (7.19)$$

where the functions $\mathcal{Z}_1, \dots, \mathcal{Z}_7$ are given by

$$\begin{aligned}
\mathcal{Z}_1 &= e^{\varphi^1 K + \varphi^3 \Sigma_2 + \varphi^5 \Sigma_3 + \varphi^0 Y}, \\
\mathcal{Z}_2 &= \Sigma_2 \cdot Y \cdot e^{\varphi^3(K + \Sigma_2 + \Sigma_3) + \varphi^0(K + Y)}, \\
\mathcal{Z}_3 &= (-K - \Sigma_2 - \Sigma_3 + Y) \cdot (K + \Sigma_3) \cdot e^{\varphi^0(K + Y)}, \\
\mathcal{Z}_4 &= -(3K + \Sigma_2 + \Sigma_3 + Y) \cdot (2K + Y + \Sigma_3) \cdot \Sigma_3 \cdot e^{\varphi^4(-K - Y)}, \\
\mathcal{Z}_5 &= -(4K + \Sigma_2 + 2\Sigma_3 + 2Y) \cdot e^{\varphi^4 \Sigma_3}, \\
\mathcal{Z}_6 &= -\left(K \cdot \Sigma_3 \cdot e^{\varphi^4(-K - Y)} \right. \\
&\quad \left. + (2K + \Sigma_3 + Y) \cdot (K + Y) \cdot e^{\varphi^4 \Sigma_3} \right) \cdot \Sigma_2 \cdot e^{\varphi^3(2K + \Sigma_2 + \Sigma_3 + Y)}, \\
\mathcal{Z}_7 &= -\left(Y \cdot (2K + \Sigma_3 + Y) \cdot e^{(\varphi^4 - \varphi^5)(-K - \Sigma_3) + \varphi^0(K + Y)} \right. \\
&\quad \left. + (K + \Sigma_3) \cdot K \cdot e^{(\varphi^5 - \varphi^4)(2K + \Sigma_3 + Y)} \right) \cdot \Sigma_3 \cdot e^{\varphi^4(K + \Sigma_3) + \varphi^3 \Sigma_2}.
\end{aligned} \tag{7.20}$$

Following the analysis of [39], we organize the pushforwards of the quadruple intersection numbers into a matrix of intersection pairings:

$$M_{(IJ)(KL)} = W_{IJKL} = S_{IJ} \cdot S_{KL}, \quad S_{IJ} := \hat{D}_I \cdot \hat{D}_J \in \Lambda_S, \tag{7.21}$$

where we view the matrix $M_{(IJ)(KL)}$ as acting on an integer lattice Λ_S spanned by the elements S_{IJ} . The components of $M_{(IJ)(KL)}$ are displayed in Table 4. Although the matrix $M_{(IJ)(KL)}$ may appear at face value to simply be a trivial repackaging of the intersection numbers, as discussed in [39] we expect the nondegenerate part of this matrix to be independent of resolution (up to a choice of basis), despite the fact that complete set of intersection numbers does not share this feature. The matrix $M_{(IJ)(KL)}$ has a non-trivial null space

$$\{\nu^{IJ} \in \Lambda_S \mid M_{(KL)(IJ)} \nu^{IJ} = 0 \text{ for all } (KL)\}, \tag{7.22}$$

which is spanned by (at least) the following vectors:

$$\left\{ \begin{array}{c}
Y^\alpha S_{1\alpha} - S_{01} \\
S_{04} \\
S_{14} \\
\Sigma_2^\alpha S_{1\alpha} - S_{13} \\
K^\alpha S_{1\alpha} - S_{11} \\
\Sigma_3^\alpha S_{1\alpha} - S_{15} \\
(K + Y)^\alpha S_{0\alpha} - Y^\alpha S_{1\alpha} - S_{00} \\
(K \Sigma_3 + \Sigma_3 Y)^\alpha S_{2\alpha} + (-K + \Sigma_3 - Y)^\alpha S_{\alpha 4} - \Sigma_3^\alpha S_{0\alpha} - \Sigma_3^\alpha S_{1\alpha} - S_{44} \\
(2K + \Sigma_2 + \Sigma_3 + Y)^\alpha S_{\alpha 3} - 2\Sigma_2^\alpha S_{1\alpha} - S_{03} - S_{33} - S_{35} \\
(2K + \Sigma_2 + \Sigma_3 + Y)^\alpha S_{\alpha 3} - 2\Sigma_2^\alpha S_{1\alpha} - \Sigma_2^\alpha S_{\alpha 5} - S_{03} - S_{33} \\
(-K - Y)^\alpha S_{\alpha 5} + \Sigma_3^\alpha S_{1\alpha} + S_{05} - S_{45} \\
(2K + \Sigma_3 + Y)^\alpha S_{\alpha 5} - 2\Sigma_3^\alpha S_{1\alpha} - S_{05} - S_{55}
\end{array} \right\}. \tag{7.23}$$

The quotient of the lattice Λ_S by the complete set of null vectors is isomorphic to the non-degenerate lattice $H_{2,2}^{\text{vert}}(X_5, \mathbb{Z})$ defined by the pairing M_{red} . While in simple cases (such as the base \mathbb{P}^3), the set Eq. (7.23) is a complete basis of the nullspace of M , there may be further null vectors, associated, for example, with fluxes $\phi^{\alpha 3} D_\alpha = D$, with $D \cdot \Sigma_2 = 0$. We write a general abstract form of M_{red} in Table 5 and Table 6, in two different choices of bases, with the understanding that some further null vectors may need to be removed to define the reduced basis for some bases, as discussed above. While we have computed this from a particular resolution, as in the cases studied in [39] we expect this form of M_{red} to be resolution-independent. We discuss the relationship between M-theory flux backgrounds and the middle cohomology subgroup $H_{2,2}^{\text{vert}}(X_5, \mathbb{Z})$ in more detail in the following subsection.

7.2 Fluxes preserving 4D $(\text{SU}(3) \times \text{SU}(2) \times \text{U}(1))/\mathbb{Z}_6$ gauge symmetry

7.2.1 Fluxes through vertical surfaces

As described in Section 7.1, our primary purpose in computing the quadruple intersection numbers is to determine an explicit parametrization for the lattice of M-theory fluxes through vertical surfaces

$$\Theta_{IJ} = \int_{S_{IJ}} G_4. \quad (7.24)$$

In the above equation, $G_4 = dC_3$ is the field strength of the M-theory 3-form C_3 and is expected to satisfy the shifted quantization condition $G_4 - c_2/2 \in H^4(X_5, \mathbb{Z})$ in consistent M-theory vacua [64], and $S_{IJ} := \hat{D}_I \cdot \hat{D}_J$ (see Eq. (7.21)) are so-called ‘‘vertical’’ 4-cycles whose homology classes generate the subgroup $H_{2,2}^{\text{vert}}(X_5)$.

While G_4 could in principle be any element of $H^4(X_5, \mathbb{Z})$, because the middle cohomology of smooth elliptic CY fourfolds X admits an orthogonal decomposition [65, 66]

$$H^4(X) = H_{\text{vert}}^{2,2}(X) \oplus H_{\text{hor}}^4(X) \oplus H_{\text{rem}}^4(X), \quad (7.25)$$

for the purpose of computing Eq. (7.24) we can restrict our attention to vertical flux backgrounds, i.e., $G_4 \in H_{\text{vert}}^{2,2}(X_5, \mathbb{Z}/2)$, possibly at the expense of being able to determine the precise quantization of the chiral indices (further discussion of the quantization issue appears in Section 9). We follow this approach, and for convenience we parametrize the vertical part of G_4 by its Poincaré dual,

$$\text{PD}(G_4^{\text{vert}}) =: \phi = \phi^{IJ} S_{IJ}, \quad (7.26)$$

where we view $\phi^{KL} \in \Lambda_S$ as an integer¹⁸ vector living in the integral lattice Λ_S of vertical flux backgrounds spanned by the 4-cycles S_{IJ} . This convenient choice of parametrization leads to the following simple linear algebraic expression for the space of vertical fluxes:

$$\Theta_{IJ} = S_{IJ} \cdot S_{KL} \phi^{KL} = M_{(IJ)(KL)} \phi^{KL}. \quad (7.27)$$

¹⁸The flux background ϕ could also be a half-integer vector. This is required, for example, when c_2 is not an even class as a consequence of the shifted quantization $G_4 - c_2/2 \in H^4(X_5, \mathbb{Z})$ as first pointed out in [64]; see Section 7.2.3 for further discussion.

7.2.2 Symmetry constraints

We are specifically interested in M-theory fluxes that lift to 4D F-theory fluxes preserving local Lorentz and $(\text{SU}(3) \times \text{SU}(2) \times \text{U}(1))/\mathbb{Z}_6$ gauge symmetry. In the above equation (7.27), these symmetry constraints can be imposed by restricting ϕ^{KL} to live in the sublattice $\Lambda_C \subset \Lambda_S$ of vertical flux backgrounds that preserve 4D Poincaré and $(\text{SU}(3) \times \text{SU}(2) \times \text{U}(1))/\mathbb{Z}_6$ symmetry, i.e., flux backgrounds whose corresponding fluxes satisfy [67, 12]

$$\Theta_{I\alpha} = 0. \quad (7.28)$$

We defer explicitly solving the constraints $\Theta_{I\alpha} = 0$ to Sections 7.5 and 7.6, where we give two complementary approaches to analyzing the lattice of constrained fluxes. For now, we focus on computing the constraints imposed on the vertical fluxes Θ_{IJ} by the geometry of the $(\text{SU}(3) \times \text{SU}(2) \times \text{U}(1))/\mathbb{Z}_6$ model defined over an arbitrary base, when these symmetry conditions are imposed. These constraints on the vertical fluxes will reveal whether or not the full set of chiral matter combinations compatible with 4D anomaly cancellation can be realized in a generic F-theory compactification. In [39], it was observed that the homology relations associated with the nullspace of the matrix $M_{(IJ)(KL)}$ correspond to linear constraints on the vertical fluxes Θ_{IJ} , due to the symmetry of M . Thus, an arbitrary null vector $\nu = \nu^{IJ} S_{IJ}$ in the span of the vectors described in Eq. (7.23) implies the existence of a null relation among fluxes,

$$\nu^{IJ} \Theta_{IJ} = \nu^{IJ} M_{(IJ)(KL)} \phi^{KL} = 0. \quad (7.29)$$

This implies that there exists a set of equivalences among vertical fluxes given by Eq. (7.23), in which the basis elements S_{IJ} are replaced by fluxes Θ_{IJ} . For example, $\Theta_{04} = 0$ and $Y^\alpha \Theta_{1\alpha} - \Theta_{01} = 0$. Restricting attention to fluxes obeying the symmetry constraints $\Theta_{I\alpha} = 0$, this leads to the following relations among vertical F-theory fluxes:

$$\begin{aligned} 0 &= \Theta_{01} = \Theta_{04} = \Theta_{14} = \Theta_{13} = \Theta_{11} = \Theta_{15} = \Theta_{00} \\ 0 &= \Theta_{44} \\ 0 &= \Theta_{03} + \Theta_{33} + \Theta_{35} \\ 0 &= \Theta_{03} + \Theta_{33} \\ 0 &= \Theta_{05} - \Theta_{45} \\ 0 &= \Theta_{05} + \Theta_{55}. \end{aligned} \quad (7.30)$$

In Section 7.4, after equating the F-theory fluxes Θ_{IJ} to 3D Chern–Simons couplings, we translate the above linear relations into relations among chiral indices and compare the resulting relations to the 4D anomaly cancellation constraints to see whether or not F-theory geometry is more restrictive than the physical anomaly cancellation conditions.

7.2.3 Integrality of the second Chern class

The shifted quantization condition $G_4 - c_2/2 \in H^4(X_5, \mathbb{Z})$ implies that when $c_2/2$ is not an integer class, G_4 must also be a half-integer class. This in turn implies that $\phi = \text{PD}(G_4)$

cannot take integer values. Note, however, that ϕ can be fractionally quantized in some cases even when $c_2/2$ is an integer class, as discussed further in [Section 9](#), although in such situations integer values of ϕ are still possible.

To clarify some of the issues involved here, let us define¹⁹ two sublattices of $H_4(X_5, \mathbb{Z})$:

$$\Lambda_{\text{vert}} = \text{span}_{\mathbb{Z}}(S_{IJ}) / \sim \tag{7.31}$$

$$\bar{\Lambda}_{\text{vert}} = H_4(X_5, \mathbb{Z}) \cap H_{2,2}^{\text{vert}}(X_5, \mathbb{C}). \tag{7.32}$$

The quotient in the first line of the above equation is by the nullspace of M , i.e., by the equivalence relation

$$\phi \sim \phi' \Leftrightarrow M_{(IJ)(KL)}(\phi - \phi')^{KL} = 0 \text{ for all } (IJ). \tag{7.33}$$

In general, $\bar{\Lambda}_{\text{vert}}$ is an overlattice of Λ_{vert} . While Λ_{vert} is easily computed from the set of integral divisors, as far as we know there is not yet any systematic way of determining $\bar{\Lambda}_{\text{vert}}$ for an arbitrary CY fourfold. When c_2 is even, but $c_2/2$ is not contained in Λ_{vert} , then integer values of ϕ are still allowed. When c_2 lies in Λ_{vert} but is not even in $H_4(X_5, \mathbb{Z})$, however, then ϕ must have some half-integer components. Half-integer elements of ϕ can modify certain important aspects of the theory, such as the precise quantization of the chiral indices or even the enforcement of the symmetry constraints [\(7.28\)](#), although as discussed in more detail below we do not encounter the latter issue for the constructions here. For this reason, it is important to determine for what choices of characteristic data $c_2/2$ fails to be an integer class.

One way to check if $c_2/2$ is not an integer class is to compute $\chi/24$ where χ is the Euler characteristic of the smooth CY fourfold X_5 . If $\chi/24$ fails to be an integer, this indicates that $c_2/2$ is not an integer class. In fact, from a physical standpoint, in such situations it is important that $c_2/2$ is not an integer class in order to maintain the integrality of the M2-brane tadpole,

$$N_{\text{M2}} = \frac{1}{24}\chi(X_5) - \frac{1}{2} \int_{X_5} G_4 \wedge G_4 \in \mathbb{Z}_{\geq 0}. \tag{7.34}$$

When $\chi/24$ fails to be an integer, the fractional part of $\chi/24$ is precisely canceled by contributions to the integral $\int_{X_5} G_4 \wedge G_4$ coming from the fractional part of G_4 (i.e., $c_2/2$), see, e.g., [\[68\]](#).

We can use the pushforward technology described in the previous subsection to evaluate

¹⁹The expression $H_{2,2}^{\text{vert}}(X_5, \mathbb{Z})$ is defined in [\[39\]](#) as the first of these objects, but may in other places in the literature be defined as the latter; we define these distinct symbols to avoid confusion and ambiguity.

the pushforward of the Euler characteristic to B :²⁰

$$\begin{aligned}
\chi(X_5) &= \int_{X_5} c_4 \\
&= -12c_2(B) \cdot K - 144K^3 - 96K^2 \cdot \Sigma_2 - 168K^2 \cdot \Sigma_3 \\
&\quad - 24K \cdot \Sigma_2^2 - 66K \cdot \Sigma_3^2 - 75K \cdot \Sigma_2 \cdot \Sigma_3 - 6\Sigma_3^3 - 15\Sigma_2 \cdot \Sigma_3^2 - 9\Sigma_2^2 \cdot \Sigma_3 \\
&\quad + (-144K^2 - 51K \cdot \Sigma_2 - 111K \cdot \Sigma_3 - 3\Sigma_2^2 - 21\Sigma_3^2 - 18\Sigma_2 \cdot \Sigma_3) \cdot Y \\
&\quad + (-66K - 15\Sigma_2 - 27\Sigma_3) \cdot Y^2 - 6Y^3.
\end{aligned} \tag{7.35}$$

This expression for the Euler characteristic may be useful in various aspects of further analysis of these constructions, for instance aspects involving the tadpole constraint (Eq. (7.34)). It is also useful to have an explicit expression for c_2 . For example, using the fact that the hyperplane class is

$$\mathbf{H} \cdot \mathbf{X}_5 = -\hat{K} - \hat{\Sigma}_3 + \hat{D}_0 + 2\hat{D}_1 + \hat{D}_3 + \hat{D}_5 \tag{7.36}$$

we can represent the image of c_2 of in the lattice $H_{2,2}^{\text{vert}}(X_5, \mathbb{Z})$ as

$$\begin{aligned}
c_2(X_5) &= (-6K - 2\Sigma_2 - \Sigma_3 - Y)^\alpha S_{0\alpha} + (-6K + 2\Sigma_2 + \Sigma_3 + Y)^\alpha S_{1\alpha} \\
&\quad + (c_2(B) + 5K^2 + 2K \cdot \Sigma_2 + K \cdot \Sigma_3 + 5K \cdot Y + Y^2 + \Sigma_2 \cdot Y)^{\alpha\beta} S_{\alpha\beta} \\
&\quad + (-4K - \Sigma_3 - 2Y)^\alpha S_{\alpha 3} + (4K + \Sigma_2 + \Sigma_3 + 2Y)^\alpha S_{\alpha 4} + (\Sigma_2 - 2K)^\alpha S_{\alpha 5} \\
&\quad + 3S_{03} + S_{05} - S_{34}.
\end{aligned} \tag{7.37}$$

Notice that the above expression for c_2 is expanded in the reduced basis $S_{I\alpha}, S_{03}, S_{05}, S_{34}$ of $H_{2,2}^{\text{vert}}(X_5, \mathbb{Z})$. From this expression we can immediately see that for all our constructions, $c_2/2$ cannot be an element of Λ_{vert} , since it contains the components $(3S_{03} + S_{05} - S_{34})/2$. As discussed above, however, this does not definitively indicate that $c_2/2$ cannot be an integral element of $H_4(X_5, \mathbb{Z})$, as it may live in $\bar{\Lambda}_{\text{vert}}$.

Another way to check if $c_2/2$ is *not* an integer element of cohomology is to compute $c_2^2/4$. If this is not integer-valued, then $c_2/2$ cannot be an integer class, since the intersection product on integer cohomology takes integer values. The matrix M_{red} , of intersection pairings of any two elements belonging to $H_{2,2}^{\text{vert}}(X_5, \mathbb{Z})$ is presented in Table 6 using the basis relevant for Eq. (7.37). Using the explicit expression given there for M_{red} , we find that one-fourth of the square of the second Chern class is given by

$$\begin{aligned}
\frac{1}{4}c_2(X_5)^2 &= -6c_2 \cdot K - 8K^2 \cdot \Sigma_2 - 14K^2 \cdot \Sigma_3 - 12K^2 \cdot Y - 12K^3 - \frac{17}{4}K \cdot \Sigma_2 \cdot Y \\
&\quad - \frac{37}{4}K \cdot \Sigma_3 \cdot Y - 2K \cdot \Sigma_2^2 - \frac{11}{2}K \cdot \Sigma_3^2 - \frac{25}{4}K \cdot \Sigma_2 \cdot \Sigma_3 - \frac{11}{2}K \cdot Y^2 \\
&\quad - \frac{5}{4}\Sigma_2 \cdot Y^2 - \frac{9}{4}\Sigma_3 \cdot Y^2 - \frac{1}{4}\Sigma_2^2 \cdot Y - \frac{7}{4}\Sigma_3^2 \cdot Y - \frac{3}{2}\Sigma_2 \cdot \Sigma_3 \cdot Y - \frac{5}{4}\Sigma_2 \cdot \Sigma_3^2 \\
&\quad - \frac{3}{4}\Sigma_2^2 \cdot \Sigma_3 - \frac{1}{2}\Sigma_3^3 - \frac{1}{2}Y^3.
\end{aligned} \tag{7.38}$$

²⁰Note that the total Chern class $c(X_5)$ can be expressed as a formal power series in $D_\alpha, \mathbf{H}, \mathbf{E}_i$ —see Appendix E of [39]).

Whenever the characteristic data K, Σ_2, Σ_3, Y are such that the above expression is non-integer valued, c_2 cannot be an even class. In [Section 8.1](#) we show explicitly that there are many cases where this occurs, so that integer flux parameters ϕ^{IJ} are not possible in those cases.

7.3 3D Chern–Simons couplings

As described in [Section 5](#) of [\[39\]](#), and following [\[69, 70, 60, 45\]](#), the final step in our strategy for computing the chiral indices $\chi_r = n_r - n_{r^*}$ of the $(\text{SU}(3) \times \text{SU}(2) \times \text{U}(1))/\mathbb{Z}_6$ model is to match the vertical F-theory fluxes $\Theta_{\bar{I}\bar{J}}$ (satisfying the symmetry constraints [Eq. \(7.28\)](#)) with the one-loop Chern–Simons (CS) couplings $\Theta_{\bar{I}\bar{J}}^{\text{3D}}$ characterizing the low-energy 3D $\mathcal{N} = 2$ action describing M-theory compactified on X_5 .²¹ We then use the fact that the 3D CS couplings can be expressed as linear combinations of the chiral indices,

$$\Theta_{\bar{I}\bar{J}}^{\text{3D}} = -x_{\bar{I}\bar{J}}^r \chi_r, \quad (7.39)$$

leading to the invertible²² system

$$\Theta_{\bar{I}\bar{J}} = -x_{\bar{I}\bar{J}}^r \chi_r. \quad (7.40)$$

Inverting the matrix of coefficients $x_{\bar{I}\bar{J}}^r$ allows us to write the chiral indices as linear combinations of $\Theta_{\bar{I}\bar{J}}$.

Since we have already computed the F-theory fluxes through surfaces, what remains is to compute the coefficients $x_{\bar{I}\bar{K}}^r$. This can be accomplished with the help of 3D $\mathcal{N} = 2$ supersymmetry. From the point of view of the 3D effective field theory, the one-loop 3D CS couplings can be expressed as²³

$$\begin{aligned} \Theta_{ij}^{\text{3D}} &= \sum_w \left(\frac{1}{2} + \lfloor |r_{\text{KK}} \varphi \cdot w| \rfloor \right) \text{sign}(\varphi \cdot w) w_i w_j, \\ \Theta_{0i}^{\text{3D}} &= \sum_w \left(\frac{1}{12} + \frac{1}{2} \lfloor |r_{\text{KK}} \varphi \cdot w| \rfloor (\lfloor |r_{\text{KK}} \varphi \cdot w| \rfloor + 1) \right) w_i, \\ \Theta_{00}^{\text{3D}} &= \sum_w \frac{1}{6} \lfloor |r_{\text{KK}} \varphi \cdot w| \rfloor (\lfloor |r_{\text{KK}} \varphi \cdot w| \rfloor + 1) (2 \lfloor |r_{\text{KK}} \varphi \cdot w| \rfloor + 1). \end{aligned} \quad (7.41)$$

In order to match the above expressions with our M-theory vacuum, we must supply as input the signs of the central charges of 3D BPS particles in the specific phase of the vector multiplet

²¹The “gauge” basis indices \bar{I} take the values $\bar{I} = \bar{0}, \bar{1}, \alpha, 3, 4, 5$, where $\hat{D}_{\bar{0}}, \hat{D}_{\bar{1}}$ are defined in [Eq. \(7.4\)](#). See also [Appendix A](#).

²²It is not entirely clear that every crepant resolution corresponds to a 3D phase in which the system [Eq. \(7.40\)](#) is invertible—see [Appendix G](#) of [\[39\]](#).

²³Our conventions are as follows. Let \mathfrak{g} be a semisimple Lie algebra. We may view a collection of real Coulomb branch moduli φ^i as the components of a real 3D vector multiplet scalar expanded in a basis of simple coroots, $\varphi = \varphi^i \alpha_i^\vee$ where $i = 1, \dots, \text{rank}(\mathfrak{g})$. Similarly, a weight w transforming in a representation \mathbf{r} of \mathfrak{g} may be expanded in a basis of fundamental weights, $w = w_i \omega^i$. The fundamental weights are canonically dual to the simple coroots and we denote their inner product by $\alpha_i^\vee \cdot \omega^j = \delta_i^j$, hence $\varphi \cdot w = \varphi^i w_i$. We define $\varphi^0 = 1/r_{\text{KK}}$.

	00	01	11	00	10	00	03	13	03	33	04	14	04	34	44	05	15	05	35	45	55
00	$K^2 + 2KY - 2Y^2$	Y^2	KY^2	$K^2 D_0 + KY D_0 - Y^2 D_0$	$Y^2 D_0$	$K D_0^2$	$-KY D_2 - 2Y^2 D_2$	$Y^2 D_2$	$-Y D_0 D_2$	$-KY D_2 - Y^2 D_2$	0	0	0	0	0	$-KY D_3 - 2Y^2 D_3$	$Y^2 D_3$	$-Y D_0 D_3$	$-Y D_2 D_3$	0	$-KY D_3 - Y^2 D_3 - Y D_2 D_3$
01	Y^2	KY^2	$K^2 Y$	$Y^2 D_0$	$KY D_0$	$Y D_0^2$	$Y^2 D_2$	$KY D_2$	$Y D_0 D_2$	$Y D_2^2$	0	0	0	0	0	$Y^2 D_3$	$KY D_3$	$Y D_0 D_3$	$Y D_2 D_3$	0	$Y D_2 D_3$
11	$-KY^2 - 2Y^2 D_2$	$K^2 Y$	$K^2 Y$	$KY D_0$	$K^2 D_0$	$K D_0^2$	$KY D_2$	$K^2 D_2$	$-K D_0 D_2$	$K D_2^2$	0	0	0	0	0	$-KY D_3$	$K^2 D_3$	$K D_0 D_3$	$K D_2 D_3$	0	$K D_2 D_3$
00	$K^2 D_0 + KY D_0 - Y^2 D_0$	$Y^2 D_0$	$KY D_0$	$K D_0^2$	$Y D_0^2$	D_0^3	$-Y D_0 D_2$	$Y D_0 D_2$	0	$-Y D_0 D_2$	0	0	0	0	0	$-Y D_0 D_3$	$Y D_0 D_3$	0	0	0	$-Y D_0 D_3$
10	$Y^2 D_0$	$KY D_0$	$K^2 D_0$	$Y D_0^2$	$K D_0^2$	D_0^3	$Y D_0 D_2$	$K D_0 D_2$	$D_0^2 D_2$	$D_0 D_2^2$	0	0	0	0	0	$Y D_0 D_3$	$K D_0 D_3$	$D_0^2 D_3$	$D_0 D_2 D_3$	0	$D_0 D_2 D_3$
00	$K D_0^2$	$Y D_0^2$	$K D_0^2$	D_0^3	0	0	0	$D_0^2 D_2$	0	$-2 D_0^2 D_2$	0	0	0	0	$-2 D_0^2 D_2$	0	$D_0^2 D_3$	0	0	$D_0^2 D_3$	$-2 D_0^2 D_3$
03	$-KY D_2 - 2Y^2 D_2$	$Y^2 D_2$	$KY D_2$	$-Y D_0 D_2$	$Y D_0 D_2$	0	$-KY D_2 - Y^2 D_2 - Y D_2^2$	$Y D_2^2$	$-Y D_0 D_2$	$-KY D_2 - 2Y D_2^2 - Y D_2 D_2^2$	0	0	0	0	0	$-Y D_2 D_3$	$Y D_2 D_3$	0	0	0	$-Y D_2 D_3$
13	$Y^2 D_2$	$KY D_2$	$K^2 D_2$	$Y D_0 D_2$	$K D_0 D_2$	$D_0^2 D_2$	$Y D_2^2$	$K D_2^2$	$D_0 D_2^2$	$D_0 D_2^2$	0	0	0	0	0	$Y D_2 D_3$	$K D_2 D_3$	$D_0 D_2 D_3$	$D_2^2 D_3$	0	$D_2^2 D_3$
03	$-Y D_0 D_2$	$Y D_0 D_2$	$K D_0 D_2$	0	$D_0^2 D_2$	0	$-Y D_0 D_2$	$D_0 D_2^2$	$-2 D_0^2 D_2$	$-4 K D_0 D_2 - Y D_0 D_2 - 4 D_0 D_2^2 - 2 D_0 D_2 D_2^2$	0	0	0	$-D_0 D_2 D_3$	$-D_0 D_2 D_3$	0	$D_0 D_2 D_3$	0	0	$D_0 D_2 D_3$	$-2 D_0 D_2 D_3$
33	$-KY D_2 - Y^2 D_2 - Y D_2^2$	$Y D_2^2$	$K D_2^2$	$-Y D_0 D_2$	$D_0 D_2^2$	$-2 D_0^2 D_2$	$-KY D_2 - 2Y D_2^2 - Y D_2 D_2^2$	D_2^3	$-4 K D_0 D_2 - Y D_0 D_2 - 4 D_0 D_2^2 - 2 D_0 D_2 D_2^2$	$-8 K^2 D_2 - 5 K Y D_2 - 4 D_0 D_2^2 - 12 K D_2^2 - 3 Y D_2^2 - 6 D_2^2 - 8 K D_2 D_2 - 2 Y D_2 D_2 - 6 D_2^2 D_2 - 2 D_2^2 D_2^2$	0	0	0	$-D_0 D_2 D_3$	$-2 K D_2 D_3 - Y D_2 D_3 - 2 D_2^2 D_3 - D_2 D_2^2$	0	$D_2^2 D_3$	0	0	$D_2^2 D_3$	$-2 D_2^2 D_3$
04	0	0	0	0	0	0	0	0	0	0	0	0	0	0	0	0	0	0	0	0	0
14	0	0	0	0	0	0	0	0	0	0	0	0	0	0	0	0	0	0	0	0	0
04	0	0	0	0	0	0	0	0	0	0	0	0	$-2 D_0^2 D_2$	$-D_0 D_2 D_3$	$2 K D_0 D_2 + 2 Y D_0 D_2 + D_0 D_2^2$	0	0	$D_0^2 D_3$	$D_0 D_2 D_3$	$-K D_0 D_3 + Y D_0 D_3$	$2 K D_0 D_3 + Y D_0 D_3 + D_0 D_2^2$
34	0	0	0	0	0	0	0	0	$-D_0 D_2 D_3$	$-2 K D_2 D_3 - Y D_2 D_3 - 2 D_2^2 D_3 - D_2 D_2^2$	0	0	$-D_0 D_2 D_3$	$-K D_2 D_3 - Y D_2 D_3 - D_2^2 D_3 - D_2 D_2^2$	0	0	$D_0 D_2 D_3$	$D_2^2 D_3$	$-K D_2 D_3 + Y D_2 D_3$	$2 K D_2 D_3 + Y D_2 D_3 + D_2^2 D_3$	
44	0	0	0	0	0	$-2 D_0^2 D_2$	0	0	$-D_0 D_2 D_3$	$-K D_2 D_3 - D_2^2 D_3$	0	0	$2 K D_0 D_2 + 2 Y D_0 D_2 + 2 D_0 D_2^2$	$K D_2 D_3 + Y D_2 D_3 + 2 K Y D_2 + 2 K D_2^2 + 2 Y D_2^2 - 2 D_2^2$	0	$-K D_0 D_3 - Y D_0 D_3$	$-K D_2 D_3 - Y D_2 D_3$	$K^2 D_3 + 2 K Y D_3 + Y^2 D_3 - K D_2^2 - Y D_2^2$	$-2 K^2 D_3 - 2 K Y D_3 - Y^2 D_3 - K D_2^2 - Y D_2^2$		
05	$-KY D_3 - 2Y^2 D_3$	$Y^2 D_3$	$KY D_3$	$-Y D_0 D_3$	$Y D_0 D_3$	0	$-Y D_2 D_3$	$Y D_2 D_3$	0	0	0	0	0	0	0	$-KY D_3 - Y D_2^2 D_3 - Y^2 D_3 - Y D_2^2$	$Y^2 D_3$	$-Y D_0 D_3$	$-Y D_2 D_3$	0	$-KY D_3 - 2Y^2 D_3 - Y D_2^2 D_3$
15	$Y^2 D_3$	$KY D_3$	$K^2 D_3$	$Y D_0 D_3$	$K D_0 D_3$	$D_0^2 D_3$	$Y D_2 D_3$	$K D_2 D_3$	$D_0 D_2 D_3$	$D_2^2 D_3$	0	0	0	0	0	$Y D_2 D_3$	$K D_2 D_3$	$D_0 D_2 D_3$	$D_2^2 D_3$	0	$D_2^2 D_3$
05	$-Y D_0 D_3$	$Y D_0 D_3$	$K D_0 D_3$	0	$D_0^2 D_3$	0	0	$D_0 D_2 D_3$	0	0	0	0	0	0	0	$-K D_0 D_3 - Y D_0 D_3$	$-Y D_0 D_3$	$-2 D_0^2 D_3$	$-2 D_0 D_2 D_3$	$2 K D_0 D_3 + Y D_0 D_3 + D_0 D_2^2$	$-4 K D_0 D_3 - Y D_0 D_3 + Y D_2 D_3 + 4 D_0 D_2^2$
35	$-Y D_2 D_3$	$Y D_2 D_3$	$K D_2 D_3$	0	$D_0 D_2 D_3$	0	0	$D_2^2 D_3$	0	0	0	0	0	$D_0 D_2 D_3$	$-K D_2 D_3 - Y D_2 D_3$	$-Y D_2 D_3$	$-2 D_0 D_2 D_3$	$-2 D_0 D_2 D_3$	$2 K D_2 D_3 + Y D_2 D_3 + D_2^2 D_3$	$-4 K D_2 D_3 - Y D_2 D_3 + 4 D_2 D_2^2$	
45	0	0	0	0	0	$D_0^2 D_2$	0	0	$D_0 D_2 D_3$	$D_2^2 D_3$	0	0	$K D_0 D_3 + Y D_0 D_3$	$-K D_2 D_3 - Y D_2 D_3$	$K^2 D_3 + 2 K Y D_3 + Y^2 D_3$	0	0	$2 K D_0 D_3 + Y D_0 D_3 + D_0 D_2^2$	$2 K D_2 D_3 + Y D_2 D_3 + D_2^2 D_3$	$-2 K^2 D_3 - 2 K Y D_3 - Y^2 D_3 - 4 K^2 D_3 + 3 K Y D_3 + 4 K Y D_3 + Y^2 D_3 + K D_2^2 - Y D_2^2 + 2 Y D_2^2 - D_2^2$	
55	$-KY D_3 - Y^2 D_3 - Y D_2^2$	$Y D_2^2$	$K D_2^2$	$-Y D_0 D_3$	$D_0 D_2^2$	$-2 D_0^2 D_2$	$-Y D_2 D_3$	$Y D_2 D_3$	$-2 D_0 D_2 D_3$	$-2 D_2^2 D_3$	0	0	$2 K D_0 D_2 + Y D_0 D_2 + D_0 D_2^2$	$2 K D_2 D_3 + Y D_2 D_3 + Y^2 D_3 - K D_2^2 - Y D_2^2$	$-2 K^2 D_3 - 3 K Y D_3 - 2 Y D_2^2$	$-4 K D_0 D_3 - Y D_0 D_3 + 4 D_0 D_2^2$	$-4 K D_2 D_3 + 4 D_2 D_2^2$	$4 K^2 D_3 + 4 K Y D_3 + 4 K Y D_3 + Y^2 D_3 + K D_2^2 - Y D_2^2 + 2 Y D_2^2 - D_2^2$	$4 K^2 D_3 + 4 K Y D_3 + 4 K Y D_3 + Y^2 D_3 + Y^2 D_3 + 12 K D_2^2 + 3 Y D_2^2 - 6 D_2^2$		

Table 4. Matrix of pushforwards of quadruple intersection numbers $M_{(IJ)(KL)} = S_{IJ} \cdot S_{KL}$ (recall that $S_{IJ} := \hat{D}_I \cdot \hat{D}_J$) associated to the resolution X_5 of the $(\text{SU}(3) \times \text{SU}(2) \times \text{U}(1))/\mathbb{Z}_6$ model. The entries of the uppermost (leftmost) row (column) are the indices IJ of the corresponding classes S_{IJ} . We work in the basis $\hat{D}_{I=0,1,\alpha,i_s}$ where \hat{D}_0, \hat{D}_1 are the rational sections, \hat{D}_α is the pullback of a divisor in B , and $\hat{D}_{i_2=3}, \hat{D}_{i_3=4,5}$ are (resp.) the $\mathfrak{su}(2), \mathfrak{su}(3)$ Cartan divisors. We omit the \cdot notation indicating the intersection product for brevity and use the shorthand $D_\alpha^2 = D_\alpha \cdot D_\beta, D_\alpha^3 = D_\alpha \cdot D_\beta \cdot D_\gamma$.

	0α	1α	$\alpha\beta$	$\alpha 3$	$\alpha 4$	$\alpha 5$	33	34	55
0α	$K D_\alpha^2$	$Y D_\alpha^2$	D_α^3	\emptyset	\emptyset	\emptyset	$-Y D_\alpha \Sigma_2$	\emptyset	$-Y D_\alpha \Sigma_3$
1α	$Y D_\alpha^2$	$K D_\alpha^2$	D_α^3	$D_\alpha^2 \Sigma_2$	\emptyset	$D_\alpha^2 \Sigma_3$	$D_\alpha \Sigma_3^2$	\emptyset	$D_\alpha \Sigma_3^2$
$\alpha\beta$	D_α^3	D_α^3	\emptyset	\emptyset	\emptyset	\emptyset	$-2 D_\alpha^2 \Sigma_2$	\emptyset	$-2 D_\alpha^2 \Sigma_3$
$\alpha 3$	\emptyset	$D_\alpha^2 \Sigma_2$	\emptyset	$-2 D_\alpha^2 \Sigma_2$	\emptyset	\emptyset	$-D_\alpha \Sigma_2$ $(4K + Y + 4\Sigma_2 + 2\Sigma_3)$	$-D_\alpha \Sigma_2 \Sigma_3$	$-2 D_\alpha \Sigma_2 \Sigma_3$
$\alpha 4$	\emptyset	\emptyset	\emptyset	\emptyset	$-2 D_\alpha^2 \Sigma_3$	$D_\alpha^2 \Sigma_3$	$-D_\alpha \Sigma_2 \Sigma_3$	$-D_\alpha \Sigma_2 \Sigma_3$	$D_\alpha \Sigma_3 (2K + Y + \Sigma_3)$
$\alpha 5$	\emptyset	$D_\alpha^2 \Sigma_3$	\emptyset	\emptyset	$D_\alpha^2 \Sigma_3$	$-2 D_\alpha^2 \Sigma_3$	\emptyset	$D_\alpha \Sigma_2 \Sigma_3$	$-D_\alpha \Sigma_3 (4K + Y + 4\Sigma_3)$
33	$-Y D_\alpha \Sigma_2$	$D_\alpha \Sigma_3^2$	$-2 D_\alpha^2 \Sigma_2$	$-D_\alpha \Sigma_2$ $(4K + Y + 4\Sigma_2 + 2\Sigma_3)$	$-D_\alpha \Sigma_2 \Sigma_3$	\emptyset	$-D_\alpha (8K^2 + 5KY + Y^2 + 12K\Sigma_2 + 3Y\Sigma_2 + 6\Sigma_2^2 + 8K\Sigma_3 + 2Y\Sigma_3 + 6\Sigma_2\Sigma_3 + 2\Sigma_3^2)$	$-D_\alpha \Sigma_3 (2K + Y + 2\Sigma_2 + \Sigma_3)$	$-2 \Sigma_2^2 \Sigma_3$
34	\emptyset	\emptyset	\emptyset	$-D_\alpha \Sigma_2 \Sigma_3$	$-D_\alpha \Sigma_2 \Sigma_3$	$D_\alpha \Sigma_2 \Sigma_3$	$-D_\alpha \Sigma_3$ $(2K + Y + 2\Sigma_2 + \Sigma_3)$	$-D_\alpha \Sigma_3 (K + \Sigma_2 + \Sigma_3)$	$D_\alpha \Sigma_3 (2K + Y + \Sigma_3)$
55	$-Y D_\alpha \Sigma_3$	$D_\alpha \Sigma_3^2$	$-2 D_\alpha^2 \Sigma_3$	$-2 D_\alpha \Sigma_2 \Sigma_3$	$D_\alpha \Sigma_3 (2K + Y + \Sigma_3)$	$-D_\alpha \Sigma_3 (4K + Y + 4\Sigma_3)$	$-2 \Sigma_2^2 \Sigma_3$	$D_\alpha \Sigma_3 (2K + Y + \Sigma_3)$	$-D_\alpha \Sigma_3 (8K^2 + 5KY + Y^2 + 12K\Sigma_2 + 3Y\Sigma_2 + 6\Sigma_2^2)$

Table 5. Matrix elements $M_{\text{red}(IJ)(KL)}$ for the reduced intersection pairing M_{red} of the lattice $H_{2,2}^{\text{vert}}(X_5, \mathbb{Z})$. We compute the matrix elements $M_{\text{red}(IJ)(KL)}$ by quotienting by the equivalence relation \sim , where $\phi \sim \phi'$ iff $M_{(IJ)(KL)}(\phi - \phi')^{KL} = 0$, assuming additional null vectors have been removed to get reduced bases for $S_{\alpha\beta}, S_{I\alpha}$, etc.. Note that the indices used in this reduced basis are $IJ = I\alpha, 33, 34, 55$. We use the same notation as in Table 4, namely we omit the \cdot notation indicating the intersection product for brevity and use the shorthand $D_\alpha^2 = D_\alpha \cdot D_\beta, D_\alpha^3 = D_\alpha \cdot D_\beta \cdot D_\gamma$.

	0α	1α	$\alpha\beta$	$\alpha 3$	$\alpha 4$	$\alpha 5$	03	05	34
$0\alpha'$	$K D_\alpha^2$	$Y D_\alpha^2$	D_α^3	0	0	0	$-\Sigma_2 Y D_\alpha$	$-\Sigma_3 Y D_\alpha$	0
$1\alpha'$	$Y D_\alpha^2$	$K D_\alpha^2$	D_α^3	$\Sigma_2 D_\alpha^2$	0	$\Sigma_3 D_\alpha^2$	$\Sigma_2 Y D_\alpha$	$\Sigma_3 Y D_\alpha$	0
$\alpha'\beta'$	D_α^3	D_α^3	0	0	0	0	0	0	0
$\alpha'3$	0	$\Sigma_2 D_\alpha^2$	0	$-2\Sigma_2 D_\alpha^2$	0	0	$-\Sigma_2 Y D_\alpha$	0	$-\Sigma_2 \Sigma_3 D_\alpha$
$\alpha'4$	0	0	0	0	$-2\Sigma_3 D_\alpha^2$	$\Sigma_3 D_\alpha^2$	0	0	$-\Sigma_2 \Sigma_3 D_\alpha$
$\alpha'5$	0	$\Sigma_3 D_\alpha^2$	0	0	$\Sigma_3 D_\alpha^2$	$-2\Sigma_3 D_\alpha^2$	0	$-\Sigma_3 Y D_\alpha$	$\Sigma_2 \Sigma_3 D_\alpha$
03	$-\Sigma_2 Y D_\alpha$	$\Sigma_2 Y D_\alpha$	0	$-\Sigma_2 Y D_\alpha$	0	0	$-\Sigma_2 Y (K + \Sigma_2 + Y)$	$-\Sigma_2 \Sigma_3 Y$	0
05	$-\Sigma_3 Y D_\alpha$	$\Sigma_3 Y D_\alpha$	0	0	0	$-\Sigma_3 Y D_\alpha$	$-\Sigma_2 \Sigma_3 Y$	$-\Sigma_3 Y (K + \Sigma_3 + Y)$	0
34	0	0	0	$-\Sigma_2 \Sigma_3 D_\alpha$	$-\Sigma_2 \Sigma_3 D_\alpha$	$\Sigma_2 \Sigma_3 D_\alpha$	0	0	$-\Sigma_2 \Sigma_3 (K + \Sigma_2 + \Sigma_3)$

Table 6. Matrix elements $M_{\text{red}(IJ)(KL)}$ in alternative basis. Compared to the basis used in Table 5, we find this basis to be more convenient in some approaches for computing the chiral indices—see Section 7.5.

moduli space described by the resolution X_5 . These signs can in principle be computed geometrically by using the Kähler class $\hat{J} = \varphi^{\bar{I}} \hat{D}_{\bar{I}}$ to compute the volumes $\text{vol}(C_w) = \hat{J} \cdot C_w = \varphi^{\bar{I}} w_{\bar{I}}$ of all primitive holomorphic and anti-holomorphic curves C_w in the Mori cone of X_5 (and its negative), as the 3D BPS particle spectrum descends from M2 branes wrapping these curves.²⁴ Since the volumes $\text{vol}(C_w)$ are equal to the BPS central charges, partitioning the Mori cone generators $\{C_w\}$ into holomorphic and anti-holomorphic (based on whether $\text{vol}(C_w)$ is positive or negative) determines the full set of signs associated to X_5 .

Rather than following the above approach, we use a shortcut. Namely, we identify the signs appearing in Eq. (7.41) by formally matching intersection numbers of the form $W_{\bar{I}\bar{J}\bar{K}}$

²⁴The coefficients $w_{\bar{I}}$ can either be interpreted as KK charges $w_{\bar{0}}$, or as Cartan charges/Dynkin labels w_i of weights transforming in some representation \mathbf{R} of \mathfrak{g} .

with 5D CS couplings $k_{\bar{I}\bar{J}\bar{K}}$ in which the coefficients have been appropriately “promoted” to the classes of matter curves $C_R \in B$; see Section 5 of [39] for a more detailed discussion of this procedure.

To simplify the task of computing the 5D CS couplings, we first focus on the KK charges. To this end, we use the fact that Y is the pushforward of the intersection of the zero section with the generating section to conclude that the only elementary BPS particles with nontrivial KK charge are those transforming in the representations $(\mathbf{1}, \mathbf{1})_2, (\mathbf{1}, \mathbf{2})_{\frac{3}{2}}, (\mathbf{3}, \mathbf{1})_{-\frac{4}{3}}$, as these are the only local matter representations whose associated matter curves in B have the schematic form

$$C_R = Y \cdot (\dots). \quad (7.42)$$

We then proceed to compute 5D Chern–Simons couplings according to the standard matching procedure detailed in Section 5.2 of [39]. Following this approach, we find that the resolution Eq. (3.10) that leads to X_5 corresponds to the signs in Table 7 and KK masses in the parametric regime

$$\llbracket r_{\text{KK}}\varphi \cdot w^{(\mathbf{1}, \mathbf{1})_2} \rrbracket = \llbracket r_{\text{KK}}\varphi \cdot w_+^{(\mathbf{1}, \mathbf{2})_{\frac{3}{2}}} \rrbracket = \llbracket r_{\text{KK}}\varphi \cdot w_-^{(\mathbf{3}, \mathbf{1})_{-\frac{4}{3}}} \rrbracket = 1, \quad (7.43)$$

with all other primitive BPS particles having vanishing KK charge. This data can in turn be used to evaluate the one-loop exact expressions for the 3D Chern–Simons couplings presented in Eq. (7.41).

In the following subsection, we describe the results of inverting the linear system Eq. (7.40).

7.4 Chiral indices

Our goal in this section is to match the geometric fluxes with the 3D Chern–Simons (CS) terms in order to determine the chiral indices of the $(\text{SU}(3) \times \text{SU}(2) \times \text{U}(1))/\mathbb{Z}_6$ model. For ease of comparison, we first convert the fluxes to the gauge basis $\bar{I} = \bar{0}, \bar{1}, \alpha, i_s$ using Eq. (A.5) (recall that the indices $\bar{0}, \bar{1}$ correspond, respectively, to the abelian gauge factors $\text{U}(1)_{\text{KK}}, \text{U}(1)$). In the gauge basis, we find that the linear relations Eq. (7.30) can be expressed as:

$$\begin{aligned} 0 &= \Theta_{\bar{0}\bar{0}} = \Theta_{\bar{0}4} = \Theta_{35} = \Theta_{44}, \\ 0 &= \Theta_{45} + \Theta_{55}, \\ 0 &= 3\Theta_{\bar{1}5} - 4\Theta_{55}, \\ 0 &= \Theta_{\bar{0}5} + \Theta_{55}, \\ 0 &= 6\Theta_{\bar{1}4} - 3\Theta_{34} + 4\Theta_{55}, \\ 0 &= 6\Theta_{\bar{1}3} - 9\Theta_{33} - 2\Theta_{34}, \\ 0 &= \Theta_{\bar{0}3} + \Theta_{33}, \\ 0 &= 12\Theta_{\bar{1}\bar{1}} - 15\Theta_{33} - 4\Theta_{34} - 16\Theta_{55}, \\ 0 &= 6\Theta_{\bar{0}\bar{1}} + 3\Theta_{33} + 4\Theta_{55}. \end{aligned} \quad (7.44)$$

$(\mathbf{1}, \mathbf{1})_{w_{\bar{1}}}$	$(\mathbf{1}, \mathbf{2})_{w_{\bar{1}}}$	$(\mathbf{3}, \mathbf{1})_{w_{\bar{1}}}$	$(\mathbf{3}, \mathbf{2})_{w_{\bar{1}}}$
$\left(\begin{array}{c cccc} \frac{\varphi \cdot w}{ \varphi \cdot w } & w_{\bar{1}} & w_3 & w_4 & w_5 \\ \hline + & 1 & 0 & 0 & 0 \\ + & 2 & 0 & 0 & 0 \end{array} \right)$	$\left(\begin{array}{c cccc} \frac{\varphi \cdot w}{ \varphi \cdot w } & w_{\bar{1}} & w_3 & w_4 & w_5 \\ \hline + & \frac{1}{2} & 1 & 0 & 0 \\ + & \frac{1}{2} & -1 & 0 & 0 \\ + & \frac{3}{2} & 1 & 0 & 0 \\ + & \frac{3}{2} & -1 & 0 & 0 \end{array} \right)$	$\left(\begin{array}{c cccc} \frac{\varphi \cdot w}{ \varphi \cdot w } & w_{\bar{1}} & w_3 & w_4 & w_5 \\ \hline + & \frac{1}{3} & 0 & 1 & 0 \\ - & \frac{1}{3} & 0 & -1 & 1 \\ - & \frac{1}{3} & 0 & 0 & -1 \\ - & -\frac{4}{3} & 0 & 1 & 0 \\ - & -\frac{4}{3} & 0 & -1 & 1 \\ - & -\frac{4}{3} & 0 & 0 & -1 \\ + & \frac{2}{3} & 0 & 1 & 0 \\ + & \frac{2}{3} & 0 & -1 & 1 \\ + & \frac{2}{3} & 0 & 0 & -1 \end{array} \right)$	$\left(\begin{array}{c cccc} \frac{\varphi \cdot w}{ \varphi \cdot w } & w_{\bar{1}} & w_3 & w_4 & w_5 \\ \hline + & \frac{1}{6} & 1 & 1 & 0 \\ + & \frac{1}{6} & 1 & -1 & 1 \\ + & \frac{1}{6} & 1 & 0 & -1 \\ + & \frac{1}{6} & -1 & 1 & 0 \\ - & \frac{1}{6} & -1 & -1 & 1 \\ - & \frac{1}{6} & -1 & 0 & -1 \end{array} \right)$

Table 7. Signs and Cartan charges associated to the BPS spectrum of the $(\text{SU}(3) \times \text{SU}(2) \times \text{U}(1))/\mathbb{Z}_6$ model resolution Eq. (3.10). The charges are the Dynkin coefficients w_i of the weights w transforming in various representations and the signs correspond to the signs of the BPS central charges $\varphi \cdot w$ for a given choice of Coulomb branch moduli φ^i . The indices i of the Dynkin coefficients are chosen to match the indices of the Cartan divisors \hat{D}_i in Eq. (7.10) associated to the simple coroots of the gauge group. We adopt the convention that the Coulomb branch modulus φ^1 dual to the $\mathfrak{u}(1)$ factor is non-positive in the Coulomb branch, in contrast to the Coulomb branch moduli $\varphi^{i_2=3}, \varphi^{i_3=4,5}$ associated to nonabelian Cartan $\mathfrak{u}(1)$ s, which are non-negative.

Moreover, the one-loop 3D Chern–Simons couplings $\Theta_{\bar{I}\bar{J}}^{3\text{D}}$ are given by

$$\begin{aligned}
\Theta_{0\bar{1}}^{3\text{D}} &= \frac{1}{12}\chi_{(\mathbf{1},\mathbf{1})_1} - \frac{11}{6}\chi_{(\mathbf{1},\mathbf{1})_2} - \frac{1}{12}\chi_{(\mathbf{1},\mathbf{1})_{\frac{1}{2}}} - \frac{7}{4}\chi_{(\mathbf{1},\mathbf{1})_{\frac{3}{2}}} \\
&\quad + \frac{1}{6}\chi_{(\mathbf{3},\mathbf{1})_{\frac{2}{3}}} - \frac{1}{12}\chi_{(\mathbf{3},\mathbf{1})_{-\frac{1}{3}}} + \chi_{(\mathbf{3},\mathbf{1})_{-\frac{4}{3}}} - \frac{1}{12}\chi_{(\mathbf{3},\mathbf{2})_{\frac{1}{6}}}, \\
\Theta_{\bar{1}\bar{1}}^{3\text{D}} &= \frac{1}{2}\chi_{(\mathbf{1},\mathbf{1})_1} + 6\chi_{(\mathbf{1},\mathbf{1})_2} + \frac{1}{4}\chi_{(\mathbf{1},\mathbf{2})_{\frac{1}{2}}} + \frac{9}{2}\chi_{(\mathbf{1},\mathbf{2})_{\frac{3}{2}}} \\
&\quad + \frac{2}{3}\chi_{(\mathbf{3},\mathbf{1})_{\frac{2}{3}}} - \frac{1}{18}\chi_{(\mathbf{3},\mathbf{1})_{-\frac{1}{3}}} - \frac{40}{9}\chi_{(\mathbf{3},\mathbf{1})_{-\frac{4}{3}}} + \frac{1}{36}\chi_{(\mathbf{3},\mathbf{2})_{\frac{1}{6}}}, \\
\Theta_{\bar{1}\bar{3}}^{3\text{D}} &= -\frac{3}{2}\chi_{(\mathbf{1},\mathbf{2})_{\frac{3}{2}}} - \frac{1}{3}\chi_{(\mathbf{3},\mathbf{2})_{\frac{1}{6}}}, \\
\Theta_{\bar{1}\bar{4}}^{3\text{D}} &= \frac{1}{3}\chi_{(\mathbf{3},\mathbf{1})_{-\frac{1}{3}}} - \frac{1}{6}\chi_{(\mathbf{3},\mathbf{2})_{\frac{1}{6}}}, \\
\Theta_{\bar{1}\bar{5}}^{3\text{D}} &= \frac{4}{3}\chi_{(\mathbf{3},\mathbf{1})_{-\frac{4}{3}}}, \\
\Theta_{\bar{3}\bar{3}}^{3\text{D}} &= \chi_{(\mathbf{1},\mathbf{2})_{\frac{1}{2}}} + 2\chi_{(\mathbf{1},\mathbf{2})_{\frac{3}{2}}} + \chi_{(\mathbf{3},\mathbf{2})_{\frac{1}{6}}}, \\
\Theta_{\bar{3}\bar{4}}^{3\text{D}} &= -\chi_{(\mathbf{3},\mathbf{2})_{\frac{1}{6}}}, \\
\Theta_{\bar{3}\bar{5}}^{3\text{D}} &= 0, \\
\Theta_{\bar{4}\bar{4}}^{3\text{D}} &= \chi_{(\mathbf{3},\mathbf{1})_{\frac{2}{3}}} - \chi_{(\mathbf{3},\mathbf{1})_{-\frac{4}{3}}} + \chi_{(\mathbf{3},\mathbf{2})_{\frac{1}{6}}}, \\
\Theta_{\bar{4}\bar{5}}^{3\text{D}} &= -\frac{1}{2}\chi_{(\mathbf{3},\mathbf{1})_{\frac{2}{3}}} + \frac{1}{2}\chi_{(\mathbf{3},\mathbf{1})_{-\frac{1}{3}}} + \frac{1}{2}\chi_{(\mathbf{3},\mathbf{1})_{-\frac{4}{3}}}, \\
\Theta_{\bar{5}\bar{5}}^{3\text{D}} &= \chi_{(\mathbf{3},\mathbf{1})_{\frac{2}{3}}} - \chi_{(\mathbf{3},\mathbf{1})_{-\frac{1}{3}}} - 2\chi_{(\mathbf{3},\mathbf{1})_{-\frac{4}{3}}}.
\end{aligned} \tag{7.45}$$

By identifying the 3D CS terms with the geometric fluxes in [Section 7.4](#) (see [Eq. \(7.24\)](#)), we learn that the following constraints are satisfied by the chiral multiplicities in the $(\text{SU}(3) \times \text{SU}(2) \times \text{U}(1))/\mathbb{Z}_6$ model:

$$\begin{aligned}
0 &= -\chi_{(\mathbf{1},\mathbf{1})_2} - \chi_{(\mathbf{1},\mathbf{2})_{\frac{3}{2}}} + \frac{1}{3}\chi_{(\mathbf{3},\mathbf{1})_{\frac{2}{3}}} - \frac{1}{3}\chi_{(\mathbf{3},\mathbf{1})_{-\frac{1}{3}}}, \\
0 &= -\chi_{(\mathbf{1},\mathbf{2})_{\frac{1}{2}}} - 3\chi_{(\mathbf{1},\mathbf{2})_{\frac{3}{2}}} + \frac{2}{3}\chi_{(\mathbf{3},\mathbf{1})_{\frac{2}{3}}} + \frac{1}{3}\chi_{(\mathbf{3},\mathbf{1})_{-\frac{1}{3}}}, \\
0 &= -\chi_{(\mathbf{3},\mathbf{1})_{-\frac{4}{3}}} + \frac{1}{3}\chi_{(\mathbf{3},\mathbf{1})_{\frac{2}{3}}} - \frac{1}{3}\chi_{(\mathbf{3},\mathbf{1})_{-\frac{1}{3}}}, \\
0 &= -\chi_{(\mathbf{1},\mathbf{1})_1} + 2\chi_{(\mathbf{1},\mathbf{2})_{\frac{3}{2}}} - \frac{4}{3}\chi_{(\mathbf{3},\mathbf{1})_{\frac{2}{3}}} + \frac{1}{3}\chi_{(\mathbf{3},\mathbf{1})_{-\frac{1}{3}}}, \\
0 &= -\chi_{(\mathbf{3},\mathbf{2})_{\frac{1}{6}}} - \frac{2}{3}\chi_{(\mathbf{3},\mathbf{1})_{\frac{2}{3}}} - \frac{1}{3}\chi_{(\mathbf{3},\mathbf{1})_{-\frac{1}{3}}}.
\end{aligned} \tag{7.46}$$

After rearrangement, these constraints exactly match those in [Eq. \(2.4\)](#). The constraints can also be used to write the chiral indices in terms of a minimal subset of the fluxes:

$$\begin{aligned}
\chi_{(\mathbf{1},\mathbf{1})_1} &= 2\Theta_{33} + \Theta_{34} + 2\Theta_{55}, \\
\chi_{(\mathbf{1},\mathbf{1})_2} &= -\Theta_{33} - \Theta_{55}, \\
\chi_{(\mathbf{1},\mathbf{2})_{\frac{1}{2}}} &= -3\Theta_{33} - \Theta_{34}, \\
\chi_{(\mathbf{1},\mathbf{2})_{\frac{3}{2}}} &= \Theta_{33}, \\
\chi_{(\mathbf{3},\mathbf{1})_{-\frac{4}{3}}} &= -\Theta_{55}, \\
\chi_{(\mathbf{3},\mathbf{1})_{-\frac{1}{3}}} &= 2\Theta_{55} - \Theta_{34}, \\
\chi_{(\mathbf{3},\mathbf{1})_{\frac{2}{3}}} &= -\Theta_{34} - \Theta_{55}, \\
\chi_{(\mathbf{3},\mathbf{2})_{\frac{1}{6}}} &= \Theta_{34}.
\end{aligned} \tag{7.47}$$

In terms of the parameterization in [Table 3](#), we see that the multiplicities of the first and second families are given by $-\Theta_{55}$ and Θ_{33} respectively, and the number of Standard Model generations is given by $\Theta_{34} + 2(\Theta_{33} + \Theta_{55})$. When there is no exotic matter, the number of generations of MSSM matter is then simply Θ_{34} .

Note that in the chiral multiplicity formulae of [Eq. \(7.47\)](#), we can freely replace the fluxes Θ_{33}, Θ_{55} with $-\Theta_{03}, -\Theta_{05}$, using [Eq. \(7.44\)](#) and the fact that $\Theta_{\bar{0}i} = \Theta_{0i}$ in the symmetry-constrained space where $\Theta_{\alpha I} = 0$. This allows us to easily move back and forth between the bases of [Table 5](#) and [Table 6](#).

7.5 Chiral spectrum

We now use the formulation of M_{red} in [Table 6](#) to solve the constraint equations $\Theta_{\alpha I} = 0$ and compute formulae for the chiral multiplicities, where $\Theta \sim M_{\text{red}}\phi$ is expressed in terms of flux parameters ϕ^{IJ} . This can be done in a systematic fashion even though, as mentioned above,

in some bases null vectors may remain for [Table 6](#). However, unlike F-theory models without U(1) factors, it is not straightforward to obtain a completely general solution by solving the constraint equations for all flux parameters $\phi^{\alpha I}$. As discussed in [\[39\]](#), the main obstruction to obtaining completely general solutions in models with U(1) factors is imposing the constraints

$$\Theta_{1\alpha} = 0. \tag{7.48}$$

Despite these apparent obstructions, in the case of the $(\text{SU}(3) \times \text{SU}(2) \times \text{U}(1))/\mathbb{Z}_6$ model we nevertheless find that we are able to circumvent the difficulties associated with solving the above constraints in full generality. The approach described in this subsection thus leads to a general solution to the constraints $\Theta_{I\alpha} = 0$, along with general expressions for the associated fluxes and chiral multiplicities, but at the cost of leaving the solution for the variable $\phi^{1\alpha}$ implicit. In [Section 7.6](#), we specialize to specific bases and follow an approach that more closely parallels the approach used in [\[39\]](#) for purely nonabelian theories.

To illustrate our systematic solution, we spell out the first constraints explicitly. We begin by solving the constraint $\Theta_{\alpha\beta} = 0$. Note that the space of homologically nontrivial $S_{\alpha\beta}$ has the same dimension $h^{1,1}(B)$ as the space of, e.g., $S_{0\alpha}$ by Poincaré duality. From [Table 6](#), we see that this set of constraints simply imply that

$$\phi^{1\alpha} = -\phi^{0\alpha}. \tag{7.49}$$

We next solve the equations $\Theta_{0\alpha} = 0$ for the flux parameters $\phi^{\alpha\beta}$, giving

$$\phi^{\alpha\beta} = \phi^{0\alpha}(Y - K)^\beta + \phi^{03}(\Sigma_2)^\alpha Y^\beta + \phi^{05}(\Sigma_3)^\alpha Y^\beta. \tag{7.50}$$

Next, consider the equation for $\Theta_{\alpha 4}$:

$$\phi^{\alpha 5}(\Sigma_3)^\beta = 2\phi^{\alpha 4}(\Sigma_3)^\beta + \phi^{34}(\Sigma_2)^\alpha(\Sigma_3)^\beta. \tag{7.51}$$

Since $\phi^{\alpha 5}D_\alpha$ is always combined with a factor of Σ_3 , we can use this equation to replace $\phi^{\alpha 5}$ everywhere it appears, and although not all the parameters $\phi^{\alpha 5}$ are fixed through this equation, those that are not are null vectors. Note that the constraint equations [\(7.49\)](#) to [\(7.51\)](#) are all consistent even when c_2 is not an even class, so that the associated symmetries can be preserved even in such cases. For example, from [Eq. \(7.37\)](#) we see that $\phi^{1\alpha}$ and $\phi^{0\alpha}$ each are half-integer flux parameters precisely when $(\Sigma_3 + Y)^\alpha$ is odd and c_2 is not even, so [Eq. \(7.49\)](#) is consistent even in these cases. Similar arguments hold for the other symmetry constraints, using in particular the fact that $c_2(B) + K^2$ is always even [\[68\]](#).

Continuing in this fashion, we can solve the $\Theta_{\alpha 3} = \Theta_{\alpha 5} = 0$ constraints, giving

$$\begin{aligned} \phi^{\alpha 3}(\Sigma_2)^\beta &= \frac{1}{2}(-\phi^{0\alpha} - \phi^{34}(\Sigma_3)^\alpha - \phi^{03}Y^\alpha)(\Sigma_2)^\beta, \\ \phi^{\alpha 4}(\Sigma_3)^\beta &= \frac{1}{3}(-\phi^{0\alpha} - \phi^{34}(\Sigma_2)^\alpha - \phi^{05}Y^\alpha)(\Sigma_2)^\beta. \end{aligned} \tag{7.52}$$

Note that this implies some extra nontrivial integral constraints on some of the flux parameters.

Putting this all together, the remaining constraint $\Theta_{1\alpha} = 0$ states that

$$A \cdot \bar{H} = \phi^{34} \Sigma_2 \cdot \Sigma_3 - 9\phi^{03} \Sigma_2 \cdot Y - 8\phi^{05} \Sigma_3 \cdot Y \quad (7.53)$$

where

$$A = \phi^{0\alpha} D_\alpha = -\phi^{1\alpha} D_\alpha \quad (7.54)$$

and

$$\bar{H} = -12K - 4\Sigma_3 - 3\Sigma_2 + 12Y \quad (7.55)$$

is the (scaled) height pairing divisor. Before imposing this set of constraints, the remaining fluxes are given by

$$\begin{aligned} \Theta_{03} &= \frac{1}{2} \Sigma_2 \cdot Y \cdot (-3A + \phi^{34} \Sigma_3 - 2\phi^{05} \Sigma_3 - \phi^{03} (2K + 2\Sigma_2 + Y)), \\ \Theta_{05} &= -\frac{1}{3} \Sigma_3 \cdot Y \cdot (4A + \phi^{34} \Sigma_2 + 3\phi^{03} \Sigma_2 + \phi^{03} (3K + 3\Sigma_2 + Y)), \\ \Theta_{34} &= \frac{1}{6} \Sigma_2 \cdot \Sigma_3 \cdot (A + (3\phi^{03} - 2\phi^{05})Y - \phi^{34} (6K + 2\Sigma_2 + 3\Sigma_3)). \end{aligned} \quad (7.56)$$

Note that this matches with the expectation that the exotic matter multiplicities $\chi_{(1,2)_{\frac{3}{2}}}, \chi_{(3,1)_{-\frac{4}{3}}}$ associated with Θ_{03}, Θ_{05} explicitly can only be nonzero when $\Sigma_2 \cdot Y, \Sigma_3 \cdot Y$ are non-vanishing as expected from [Table 1](#), while the possibility of matter charged under both the SU(3) and SU(2) factors controlled by Θ_{34} can only be non-vanishing if $\Sigma_2 \cdot \Sigma_3$ is a nontrivial curve in the base.

The constraints imposed by [Eq. \(7.53\)](#) reduce the number of independent fluxes $\phi^{1\alpha}, \phi^{03}, \phi^{05}, \phi^{34}$ to three independent parameters that give the fluxes [Eq. \(7.56\)](#) and some null vectors associated with parameters in A . One way to think about these constraints is as a geometric condition on curves. The curves $\Sigma_2 \cdot \Sigma_3, \Sigma_2 \cdot Y, \Sigma_3 \cdot Y$ span a space of dimension at most three in the linear space of curves on the base. We can think of \bar{H} as a linear map from the space of divisors on B to the dual space of curves on B . The set of possible flux configurations can be determined from the intersection of the image of this map \bar{H} with the space of curves spanned by the primary pair intersections listed above. These constraints can be thought of as constraints on the parameters in A or on the $\phi^{03}, \phi^{05}, \phi^{34}$. For example, if all three of the primary pair intersections are independent and the image of \bar{H} contains this full space (in which case, the curves are all contained in the divisor \bar{H}), then we can take as the basic set of three parameters any set of all or some of the parameters $\phi^{03}, \phi^{05}, \phi^{34}$, and a complementary set of parameters in A .

In some sense, [Eq. \(7.56\)](#) along with the constraint [Eq. \(7.53\)](#) give the simplest general formulation of the available fluxes for an arbitrary base geometry. We can proceed somewhat more explicitly, however, if we assume that the primary pair intersection products appearing in the fluxes are non-vanishing. In particular, if $\Sigma_2 \cdot \Sigma_3$ is a non-vanishing curve in the base,

then we can simply solve Eq. (7.53) for $\phi^{34}\Sigma_2 \cdot \Sigma_3$ and plug into Eq. (7.56). This gives a general formula for the chiral multiplicities

$$\begin{aligned}
\chi_{(\mathbf{1},\mathbf{2})_{\frac{3}{2}}} &= -\Theta_{03} = \Sigma_2 \cdot Y \cdot (K + \Sigma_2 - 4Y)\phi^{03} + \Sigma_3 \cdot Y \cdot (\Sigma_2 - 4Y)\phi^{05} \\
&\quad - \frac{1}{2}A \cdot Y \cdot (\bar{H} - 3\Sigma_2), \\
&= \Sigma_2 \cdot Y \cdot (K + \Sigma_2 - 4Y)\phi^{03} + \Sigma_3 \cdot Y \cdot (\Sigma_2 - 4Y)\phi^{05} \\
&\quad + A \cdot Y \cdot (6K + 2\Sigma_3 + 3\Sigma_2 - 6Y), \\
\chi_{(\mathbf{3},\mathbf{1})_{-\frac{4}{3}}} &= \Theta_{05} = -\Sigma_2 Y \cdot (\Sigma_3 + 3Y)\phi^{03} - \Sigma_3 Y \cdot (\Sigma_3 + 3Y + K)\phi^{05} \\
&\quad - \frac{1}{3}A \cdot Y \cdot (\bar{H} + 4\Sigma_3) \\
&= -\Sigma_2 Y \cdot (\Sigma_3 + 3Y)\phi^{03} - \Sigma_3 Y \cdot (\Sigma_3 + 3Y + K)\phi^{05} \\
&\quad + A \cdot Y \cdot (4K + \Sigma_2 + 4Y), \\
\chi_{(\mathbf{3},\mathbf{2})_{-\frac{1}{6}}} &= \Theta_{34} = -\Sigma_2 \cdot Y \cdot (9K + 3\Sigma_2 + 4\Sigma_3)\phi^{03} - \Sigma_3 \cdot Y \cdot (8K + 3\Sigma_2 + 4\Sigma_3)\phi^{05} \\
&\quad + \frac{1}{6}A \cdot (\Sigma_2 \cdot \Sigma_3 - \bar{H} \cdot (6K + 2\Sigma_2 + 3\Sigma_3)) \\
&= -\Sigma_2 \cdot Y \cdot (9K + 3\Sigma_2 + 4\Sigma_3)\phi^{03} - \Sigma_3 \cdot Y \cdot (8K + 3\Sigma_2 + 4\Sigma_3)\phi^{05} \\
&\quad - A \cdot Y \cdot (12K + 6\Sigma_3 + 4\Sigma_2) \\
&\quad + A \cdot K \cdot (12K + 10\Sigma_3 + 7\Sigma_2) \\
&\quad + A \cdot (\Sigma_2 \cdot \Sigma_2 + 3\Sigma_3 \cdot \Sigma_2 + 2\Sigma_3 \cdot \Sigma_3).
\end{aligned} \tag{7.57}$$

Note that there appear to be more than three independent flux parameters here since there are multiple parameters in A ; these linearly independent extra parameters, however, correspond to a combination of null vectors of the full matrix M_{red} and directions that are constrained by Eq. (7.53) as discussed above. For generic characteristic data, there are no further linear dependencies on these multiplicities, and we can realize all three linearly independent sets of chiral matter for many bases with arbitrary characteristic data. Note, however, that since the flux parameters on the LHS of Eq. (7.52) must be (half-)integer, and there must be an integer (or half-integer) parameter ϕ^{05} satisfying Eq. (7.53), there are nontrivial constraints on the choices of flux parameters appearing in Eq. (7.57). We illustrate these features explicitly with some examples in the following section.

The general formula for the multiplicities Eq. (7.57) holds whenever $\Sigma_3 \cdot \Sigma_2$ is a nontrivial curve, even if one of the other primary pair intersection products vanishes such as $\Sigma_2 \cdot Y = 0$, in which case $\Theta_{03} = 0$. In the cases where $\Sigma_3 \cdot \Sigma_2 = 0$, we cannot have jointly charged $\text{SU}(3) \times \text{SU}(2)$ matter, and the theory simplifies significantly, essentially to the combinations of anomaly-free matter expected for gauge groups $(\text{SU}(2) \times \text{U}(1))/\mathbb{Z}_2$ (as described in more detail in [39]) and $(\text{SU}(3) \times \text{U}(1))/\mathbb{Z}_3$. The multiplicities in such a case can be similarly computed assuming, e.g., that $\Sigma_2 \cdot Y$ is non-vanishing, in which case we can solve Eq. (7.53) for $\phi^{03}\Sigma_2 \cdot Y$ and compute the resulting multiplicities in a similar fashion to the above analysis.

7.6 Alternative treatment of the symmetry constraints

As an alternative approach, closer in spirit to the direct approach used for purely nonabelian theories in which the constraints are solved immediately for all $\phi^{I\alpha}$, one can solve the symmetry constraints $\Theta_{I\alpha} = 0$ before restricting to the sublattice $H_{2,2}^{\text{vert}}(X_5, \mathbb{Z})$. We accomplish this by leaving $\phi^{\hat{K}\hat{L}}$ free (note that the indices $\hat{I}\hat{J}$ are still restricted to an appropriate subset of the indices IJ) and instead replacing the intersection matrix $M_{(\hat{I}\hat{J})(\hat{K}\hat{L})}$ with the formal projection²⁵ (see Appendix C of [39] for further details in a more general context)

$$M_{C(\hat{I}\hat{J})(\hat{K}\hat{L})} = M_{C_{\text{na}}(\hat{I}\hat{J})(\hat{K}\hat{L})} - M_{C_{\text{na}}(\hat{I}\hat{J})(1\alpha)} M_{C_{\text{na}}}^{+(1\alpha)(1\beta)} M_{C_{\text{na}}(1\beta)(\hat{K}\hat{L})}. \quad (7.58)$$

In the above expression, $M_{C(IJ)(KL)}$ is the restriction of $M_{(IJ)(KL)}$ to Λ_C and similarly $M_{C_{\text{na}}(IJ)(KL)}$ is the restriction of $M_{(IJ)(KL)}$ to the sublattice $\Lambda_{C_{\text{na}}} \subset \Lambda_S$ (note $\Lambda_C \subset \Lambda_{C_{\text{na}}}$) of backgrounds preserving local Lorentz symmetry and at least the nonabelian (in this case, $\mathfrak{su}(3) \oplus \mathfrak{su}(2)$) gauge symmetry. The symmetric matrix $M_{C_{\text{na}}}$ can be obtained from M by acting on the right with a projection matrix P_{na} ²⁶

$$M_{C_{\text{na}}} = M P_{\text{na}} = P_{\text{na}}^t M \quad (7.59)$$

and has the following nontrivial matrix elements:

$$M_{C_{\text{na}}(IJ)(KL)} = W_{IJKL} - W_{IJ|i_s} \cdot W^{i_s|j_{s'}} W_{KLj_{s'}} - W_{0IJ} \cdot W_{KL} - W_{IJ} \cdot W_{0KL} + W_{00} \cdot W_{IJ} \cdot W_{KL} \quad (7.60)$$

$$M_{C_{\text{na}}(1\alpha)(KL)} = D_\alpha \cdot W_{\bar{1}KL} = D_\alpha \cdot (-W_{1|k_{s''}} W^{k_{s''}|i_s} W_{i_s KL} + W_{1IJ} - W_{0KL} + (W_{00} - W_{01}) \cdot W_{KL}) \quad (7.61)$$

$$M_{C_{\text{na}}(1\alpha)(1\beta)} = D_\alpha \cdot D_\beta \cdot W_{\bar{1}\bar{1}} = D_\alpha \cdot D_\beta \cdot (-W_{1|k_{s''}} W^{k_{s''}|i_s} W_{1i_s} + 2(W_{00} - W_{01})). \quad (7.62)$$

Note that in contrast to $M_{C_{\text{na}}}$, whose components can be expressed solely in terms of the triple intersections of the characteristic data K, Σ_2, Σ_3, Y , the components of the matrix $M_{C_{\text{na}}}^+$ (which is the inverse of $M_{C_{\text{na}}(1\alpha)(1\beta)}$, assuming it exists) generically depend on more intersection numbers of B as they are determined by the intersections of the height pairing

²⁵In generic situations, we may solve the symmetry constraints $\Theta_{I\alpha} = 0$ by eliminating only independent flux parameters of the form $\phi^{I\alpha}$ (in fact, this can always be done for resolutions of F-theory models that exhibit strictly nonabelian gauge symmetry and admit a holomorphic zero section). In such situations, pairs of hatted indices $\hat{I}\hat{J}$, for which $\hat{I}, \hat{J} = 0, 1, i_s$, are used to label the remaining unconstrained flux parameters. However, when the F-theory gauge algebra \mathfrak{g} includes $\mathfrak{u}(1)$ factors, in some cases imposing the symmetry constraints $\Theta_{I\alpha} = 0$ cannot be accomplished without eliminating some independent parameters ϕ^{IJ} for which $I, J \neq \alpha$ (and consequently leaving a subset of parameters of the form $\phi^{I\alpha}$ unconstrained.) In these somewhat special cases, we abuse notation and use $\hat{I}\hat{J}$, more generally, to denote the parameters that remain unconstrained after solving $\Theta_{I\alpha} = 0$, keeping in mind that the definition $\hat{I} \neq \alpha$ does not apply.

²⁶The right-acting projection P_{na} always exists for the class of resolutions of F-theory models analyzed in [39].

divisor $W_{\bar{1}\bar{q}}$ with the vertical curves of B . Without a more general approach to the analysis, $M_{C_{\text{na}}}^+$ can only be computed explicitly for a specific choice of base, and thus has to be worked out on a case-by-case basis. We can plug in the values of W_{IJKL} presented in [Table 4](#) into the above expressions in order to explicitly evaluate the fluxes $\Theta_{\hat{I}\hat{J}} = M_{C(\hat{I}\hat{J})(\hat{K}\hat{L})}\phi^{\hat{K}\hat{L}}$. We perform this analysis explicitly for the base \mathbb{P}^3 in the next section.

8 Examples

We next turn our attention to some examples with constrained choices of characteristic data and/or a specific choice of base B .

8.1 $B = \mathbb{P}^3$

We describe the specific case $B = \mathbb{P}^3$, $K = -4H$, $\Sigma_2 = n_2H$, $\Sigma_3 = n_3H$, $Y = yH$ to illustrate features of the general theory, which we analyze in several complementary ways.

8.1.1 $B = \mathbb{P}^3$ as a special case of the general formalism

The allowed values of the parameters n_2, n_3, y must satisfy the inequalities

$$n_2 > 0, \quad n_3 > 0, \quad [s_1] = 4 + y - n_2 - n_3 \geq 0, \quad [d_2] = 16 - 2y - n_2 - 2n_3 \geq 0, \quad (8.1)$$

or

$$y = 0, \quad n_2 > 0, \quad n_3 > 0, \quad [d_2] = 16 - n_2 - 2n_3 \geq 0, \quad (8.2)$$

for a good Weierstrass model to exist with the gauge group $(\text{SU}(3) \times \text{SU}(2) \times \text{U}(1))/\mathbb{Z}_6$ and no further enhancement of the group [\[2, 71\]](#). Note that in this example there is a single base index $\alpha = H$.

Note that for this class of examples, we have

$$\begin{aligned} \frac{1}{4}c_2^2 &= (17n_2 + 37n_3 - 192)y + 22n_2^2 + 8(n_2 - 16)n_2 + 25n_2n_3 - 224n_3 + 22y^2 + 912 \\ &\quad - \frac{1}{4}[(5n_2 + 9n_3)y^2 + (n_2^2 + 6n_3n_2 + 7n_3^2)y + n_3(n_2 + n_3)(3n_2 + 2n_3) + 2y^3]. \end{aligned} \quad (8.3)$$

In order for $c_2/2$ to be an integer class (and note that this is a necessary, but not sufficient condition), we at least require that the term in square brackets in the second line of the above expression is a multiple of 4. Even for the F_{11} model, there are many examples where this condition cannot be satisfied and hence the flux must be half-integer quantized. In the case of the F_{11} model over $B = \mathbb{P}^3$, we must set $y = 0$, so that the term in brackets reduces to

$$n_3(n_2 + n_3)(3n_2 + 2n_3). \quad (8.4)$$

By scanning over various small integer values of n_2, n_3 , one can verify that choices of characteristic data within this class of examples for which $c_2/2$ is not integer appear to be quite common (for example, $n_2 = 4, n_3 = 1$), and hence the subtleties surrounding half-integer quantization of the flux cannot generically be ignored when studying these models.

As mentioned earlier, a complication that appears to plague F-theory models with U(1) gauge factors such as the $(\text{SU}(3) \times \text{SU}(2) \times \text{U}(1))/\mathbb{Z}_6$ model is that, unlike in purely nonabelian theories, it is not straightforward to solve the constraints $\Theta_{I\alpha} = 0$ directly for the full set of variables $\phi^{I\alpha}$. The approach of [Section 7.5](#) gives a general, but somewhat more indirect solution of this problem, while the more direct approach taken in [Section 7.6](#) involves inversion of the matrix of intersections of height pairing divisor with other base divisors, typically giving a rational form of the solution. Fortunately, for the latter approach, in this specific example, the matrix of intersections of the height pairing divisor with other base divisors is rather simple, namely

$$M_{C(1H)(1H)} =: h/6, \quad (8.5)$$

where h is the (rescaled) height pairing divisor

$$h = 48 + 12y - 4n_3 - 3n_2 = 12[s_1] + 8n_3 + 9n_2. \quad (8.6)$$

From the constraints on the characteristic data described at the beginning of this subsection, we know that h is invertible (in fact, positive) in the region of allowed values for n_2, n_3, y . Thus, we can proceed by solving the constraint equations $\Theta_{IH} = 0$ for the corresponding ϕ^{IH} , leading to expressions with h in the denominator. Alternatively, we can solve for other variables to get polynomial expressions, following the lines of [Section 7.5](#). The following two subsections give the details of the solution using these two approaches. We recall that the three independent non-trivial fluxes can alternatively be taken to be $\Theta_{33}, \Theta_{34}, \Theta_{55}$ or $\Theta_{03}, \Theta_{05}, \Theta_{34}$. We use these two different basis sets in the two different analyses that follow, recalling that they can be related through [Eq. \(7.30\)](#).

8.1.2 Rational solution

Solving the constraint equations $\Theta_{IH} = 0$ for all ϕ^{IH} gives

$$\Theta_{\hat{i}\hat{j}} = M_{C(\hat{i}\hat{j})(33)}(-\phi^{03} + \phi^{33}) + M_{C(\hat{i}\hat{j})(34)}\phi^{34} + M_{C(\hat{i}\hat{j})(55)}(-\phi^{05} - \phi^{45} + \phi^{55}), \quad (8.7)$$

where the coefficients for Θ_{33} are

$$\begin{aligned} M_{C(33)(33)} &= -\frac{n_2y(-192 - 3n_2^2 - 4n_2n_3 - 3n_2y + 60n_2 - 2n_3y + 16n_3 + 6y^2 - 24y)}{h}, \\ M_{C(33)(34)} &= -\frac{n_2n_3y(24 - 3n_2 - 2n_3 + 6y)}{h}, \\ M_{C(33)(55)} &= -\frac{n_2n_3y(48 - 3n_2 - 4n_3)}{h}, \end{aligned} \quad (8.8)$$

the coefficients for Θ_{34} are

$$\begin{aligned} M_{C(34)(33)} &= -\frac{n_2n_3y(24 - 3n_2 - 2n_3 + 6y)}{h}, \\ M_{C(34)(34)} &= -\frac{n_2n_3(-192 - n_2^2 - 3n_2n_3 + 4n_2y + 28n_2 - 2n_3^2 + 6n_3y + 40n_3 - 48y)}{h}, \\ M_{C(34)(55)} &= \frac{n_2n_3y(16 - n_2 + 4y)}{h}, \end{aligned} \quad (8.9)$$

and the coefficients for Θ_{55} are

$$\begin{aligned}
M_{C(55)(33)} &= -\frac{n_2 n_3 y (48 - 3n_2 - 4n_3)}{h}, \\
M_{C(55)(34)} &= \frac{n_2 n_3 y (16 - n_2 + 4y)}{h}, \\
M_{C(55)(55)} &= \frac{n_3 y (-192 - 3n_2 n_3 - n_2 y + 12n_2 - 4n_3^2 + 64n_3 + 4y^2 - 32y)}{h}.
\end{aligned} \tag{8.10}$$

From these expressions it is clear that the chiral multiplicities are parameterized by the three independent linear combinations of fluxes appearing in Eq. (8.7). While these expressions all have a factor of h in the denominator, the fact that all flux backgrounds $\phi^{\hat{I}\hat{J}}$ must be (half-)integral guarantees that this factor will be cancelled properly for any set of allowed integer fluxes, such that corresponding fluxes $\Theta_{\hat{I}\hat{J}}$ are then integral.

8.1.3 Polynomial expressions and chiral multiplicities

In the base \mathbb{P}^3 , the triple intersection products in the base simply become products of numerical integer factors. Thus, from the general form of M_{red} , in a basis of fluxes (we use the index 2 here for the divisor H)

$$\phi^{02}, \quad \phi^{22}, \quad \phi^{23}, \quad \phi^{24}, \quad \phi^{25}, \quad \phi^{12}, \quad \phi^{03}, \quad \phi^{05}, \quad \phi^{34} \tag{8.11}$$

the reduced matrix of Table 6 is simply

$$M_{\text{red}} = \begin{pmatrix} -4 & 1 & 0 & 0 & 0 & y & -n_2 y & -n_3 y & 0 \\ 1 & 0 & 0 & 0 & 0 & 1 & 0 & 0 & 0 \\ 0 & 0 & -2n_2 & 0 & 0 & n_2 & -n_2 y & 0 & -n_2 n_3 \\ 0 & 0 & 0 & -2n_3 & n_3 & 0 & 0 & 0 & -n_2 n_3 \\ 0 & 0 & 0 & n_3 & -2n_3 & n_3 & 0 & -n_3 y & n_2 n_3 \\ y & 1 & n_2 & 0 & n_3 & -4 & n_2 y & n_3 y & 0 \\ -n_2 y & 0 & -n_2 y & 0 & 0 & n_2 y & (4 - y - n_2)n_2 y & -n_2 n_3 y & 0 \\ -n_3 y & 0 & 0 & 0 & -n_3 y & n_3 y & -n_2 n_3 y & (4 - y - n_3)n_3 y & 0 \\ 0 & 0 & -n_2 n_3 & -n_2 n_3 & n_2 n_3 & 0 & 0 & 0 & n_2 n_3 (4 - n_2 - n_3) \end{pmatrix}, \tag{8.12}$$

Note that with this ordering we see the characteristic structure of the upper left 5×5 block, which is resolution-independent and encodes the basic structure of the base geometry and the nonabelian gauge factors.

In this case the analysis of Section 7.5 applies, and the space of curves on B is one-dimensional (spanned by H^2), so all curves in Eq. (7.53) lie in the same one-dimensional space and we can solve the constraint for any of the parameters involved. For variety, we solve here explicitly for the ϕ^{2I} variables except ϕ^{12} and use ϕ^{05} instead to solve Eq. (7.53),

giving

$$\begin{aligned}
\Theta_{03} &= \frac{n_2}{8} [(n_2 + 32 - 4y)y\phi^{03} - (48 - 3n_2 - 4n_3)\phi^{12} + n_3(4y - n_2)\phi^{34}], \\
\Theta_{34} &= \frac{n_2}{8} [(3n_2 + 4n_3)y\phi^{03} + (n_2 - 16 - 4y)\phi^{12} + n_3(32 - 3n_2 - 4n_3)\phi^{34}], \\
\Theta_{05} &= -\frac{n_2}{8} [(36 - 3y - n_3)y\phi^{03} + n_3(n_3 + 3y - 4)\phi^{34} \\
&\quad - (192 + 32y - 4y^2 - (12 - y)n_2 - 64n_3 + 3n_2n_3 + 4n_3^2)\phi^{12}].
\end{aligned} \tag{8.13}$$

The requirement that all ϕ^{IJ} take integer (or, appropriately, half-integer) values provides additional constraints that guarantee that these expressions related to chiral multiplicities are all integers. These constraints all follow from the condition

$$8n_3y\phi^{05} = -9n_2y\phi^{03} + h\phi^{12} + n_2n_3\phi^{34}, \tag{8.14}$$

which is [Eq. \(7.53\)](#). Generally, the resulting chiral multiplicities are all nonzero, so that all three independent families of chiral matter are allowable, though the multiplicities only take certain combinations of integer values when the flux parameters ϕ^{IJ} are (half-)integral.

In order to make a direct comparison with the rational solutions described in [Section 8.1.2](#), we need to use the constraint [Eq. \(8.14\)](#) to eliminate the parameter ϕ^{12} in the expressions for $\Theta_{03}, \Theta_{34}, \Theta_{05}$ given in [Eq. \(8.13\)](#). For generic choices of characteristic data, the scaled height pairing divisor $h \neq 0$, so in any such case we impose the constraint

$$\phi^{12} = \frac{1}{h}(9n_2y\phi^{03} + 8n_3y\phi^{05} - n_2n_3\phi^{34}). \tag{8.15}$$

We also make use of the relations implied by the restriction of the null vectors [Eq. \(7.23\)](#) to the subspace Λ_C defined by the condition $\Theta_{1\alpha} = 0$. These relations enable us to account for the redundancy in the set of parameters $\phi^{03}, \phi^{33}, \phi^{34}, \phi^{05}, \phi^{45}, \phi^{55}$ used to parametrize the solutions of [Section 8.1.2](#). Specifically, we find that before eliminating the null directions, we may make the identification

$$\begin{aligned}
&\phi^{03}S_{03} + \phi^{33}S_{33} + \phi^{34}S_{34} + \phi^{05}S_{05} + \phi^{45}S_{45} + \phi^{55}S_{55} \\
&\cong (\phi^{03} - \phi^{33})S_{03} + \phi^{34}S_{34} + (\phi^{05} + \phi^{45} - \phi^{55})S_{05}.
\end{aligned} \tag{8.16}$$

The constrained null vectors also imply relations among the fluxes, in particular the last 3 relations of [Eq. \(7.30\)](#). This in turn implies that when comparing the solutions in [Section 8.1.2](#) to [Eq. \(8.13\)](#), we should identify, e.g., the coefficient of $(\phi^{03} - \phi^{33})$ in Θ_{33} in [Section 8.1.2](#) with the coefficient of ϕ^{03} in Θ_{03} of [Eq. \(8.13\)](#), and so on. As an explicit illustration of this method of comparison, we impose the condition [Eq. \(8.15\)](#) in the expression for Θ_{03} in [Eq. \(8.13\)](#) to obtain

$$\begin{aligned}
\Theta_{03} &= -\frac{n_2y\phi_{03}(3n_2y + 2n_3y + 3n_2^2 - 60n_2 + 4n_2n_3 - 16n_3 - 6y^2 + 24y + 192)}{3n_2 + 4n_3 - 12y - 48} \\
&\quad + \frac{n_2n_3y\phi_{34}(3n_2 + 2n_3 - 6y - 24)}{3n_2 + 4n_3 - 12y - 48} - \frac{n_2n_3(3n_2 + 4n_3 - 48)y\phi_{05}}{3n_2 + 4n_3 - 12y - 48},
\end{aligned} \tag{8.17}$$

which is precisely (minus) the expression for Θ_{33} whose coefficients are presented in Eq. (8.8).

As an example of applying these results, consider the case with $n_2 = n_3 = y = 1$. In this case Eq. (8.14) becomes $\phi^{34} = -53\phi^{12} + 9\phi^{03} + 8\phi^{34}$. While $\phi^{03}, \phi^{05}, \phi^{34}$ can be half-integer valued (from Eq. (7.37)), ϕ^{12} is integer-valued. This gives the fluxes

$$\Theta_{03} = -25\phi^{12} + 7\phi^{03} + 3\phi^{05}, \quad \Theta_{05} = 19\phi^{12} - 4\phi^{03}, \quad \Theta_{34} = -168\phi^{12} + 29\phi^{03} + 25\phi^{05}, \quad (8.18)$$

which are all clearly integer-valued, even when ϕ^{03}, ϕ^{05} are both half-integers.

As another class of examples, we can look at the chiral multiplicities that are possible without exotic matter representations. Setting $\Theta_{03} = \Theta_{05} = 0$ in Eq. (8.12), the expression for Θ_{34} simplifies to

$$\Theta_{34} = \frac{1}{2}(12 - n_2 - n_3 - y)(4 - m - n + y)\phi^{12}. \quad (8.19)$$

For example with $n_2 = n_3 = y = 1$, the number of generations of Standard Model matter is given by $-27\phi^{12}/2$. The condition from Eq. (8.18) that $\Theta_{05} = 0$ implies that ϕ^{12} is a multiple of 2 (whether ϕ^{03} is an integer or of the form $(2k+1)/2$), so the number of generations is a multiple of 27. Imposing also the condition $\Theta_{03} = 0$ gives the general solution

$$\phi^{03} = \frac{19}{2}\beta, \quad \phi^{05} = -\frac{11}{2}\beta, \quad \phi^{12} = 2\beta, \quad \Theta_{34} = -198\beta, \quad (8.20)$$

so in general the multiplicity can be any multiple of 198, when $c_2/2$ is an even homology class, and any odd multiple of 198 when $c_2/2$ is not even (in this case Eq. (8.3) is integral, which does not answer the question of evenness — for further discussion of this distinction see Section 9). Note, as a cross-check on the equivalence of the different methods of analysis used above, that plugging these values into Eq. (8.17), the numerators of the first and third terms add to $3225\beta/2$, while the numerator of the second term is 25, so indeed (half-)integer quantization of ϕ_{34} is compatible with the integrality of Θ_{34}

8.2 Special cases $Y = 0$ (F_{11} model)

8.2.1 General F_{11} models

In the special case $Y = 0$ for which the $(\text{SU}(3) \times \text{SU}(2) \times \text{U}(1))/\mathbb{Z}_6$ model reduces to the F_{11} model [32], the chiral indices of the exotic 4D matter must vanish and we are left with a one-dimensional family of non-trivial fluxes. Θ_{34} . In particular, in this particular class of models, the flux parameters ϕ^{03}, ϕ^{05} become null vectors of M_{red} , the multiplicity formulae Eq. (7.57) reduce to

$$\begin{aligned} \Theta_{03} &= 0, \\ \Theta_{05} &= 0, \\ \Theta_{34} &= \frac{1}{6}\Sigma_2 \cdot \Sigma_3 \cdot (A - \phi^{34}(6K + 2\Sigma_2 + 3\Sigma_3)), \end{aligned} \quad (8.21)$$

and the constraint Eq. (7.53) reduces to

$$A \cdot \bar{H} = \phi^{34} \Sigma_2 \cdot \Sigma_3. \quad (8.22)$$

Imposing the constraint we can alternatively write

$$\chi_{(\mathbf{3},2)_{-\frac{1}{6}}} = \Theta_{34} = -A(12K^2 + 2\Sigma_3^2 + 3\Sigma_3\Sigma_2 + \Sigma_2^2 + K(10\Sigma_3 + 7\Sigma_2)), \quad (8.23)$$

where the parameters in A are constrained such that Eq. (8.22) can be satisfied for (half-)integer ϕ^{34} ; in particular, parameters in A with a nonzero image under the map induced by \bar{H} from divisors to curves in any direction other than $\Sigma_2 \cdot \Sigma_3$ are fixed to vanish, while parameters in A associated with divisors such that $D \cdot \bar{H} = 0, D \cdot \Sigma_2 \cdot \Sigma_3 \neq 0$ can contribute.

8.2.2 Specialized “SU(5)” F_{11} models

Specializing further to the case $\Sigma_2 = \Sigma_3 = -K$, as studied in [34], which are associated with a hidden broken SU(5) unification group [2] as all the gauge branes lie on the same divisor, we have $\bar{H} = -5K, \Sigma_2 \cdot \Sigma_3 = K^2$, and

$$\Theta_{34} = -AK^2 = \frac{\phi^{34}}{5} K^3, \quad (8.24)$$

with the constraint $5AK = -\phi^{34}K^2$, in agreement with the results of [34]. For example, if $K = k\tilde{K}$ with $k \in \mathbb{Z}$ and \tilde{K}, \tilde{K}^2 a primitive divisor and primitive curve respectively, then we can parameterize $A = a\tilde{A}$ where \tilde{A} is the Poincaré dual divisor to \tilde{K}^2 , and we have $\Theta_{34} = -ak^2$, with the quantization condition $5a = -\phi^{34}k\tilde{K}^3$. Taking the special case of the base \mathbb{P}^3 (i.e., $n_2 = n_3 = k = 4, \tilde{K}^3 = 1$), we have, as in [34]:

$$\Theta_{34} = -16a = \frac{64}{5} \phi^{34}. \quad (8.25)$$

In this case, all parts of c_2 are manifestly even except for a shift by $S_{03} + S_{05} + S_{34}$, so if c_2 is an even class the flux parameter ϕ^{34} is integral, while if c_2 is an odd class, ϕ^{34} is of the form $(2k+1)/2$. The quantization constraint shows that $4|a$, and $5|\phi^{34}$ when ϕ^{34} is an integer, and $2|a, 5|2\phi^{34}$ when ϕ^{34} is a half-integer. We discuss the question of whether c_2 is even in the next section.

As another example, for the base $B = \mathbb{P}^2 \times \mathbb{P}^1$, we have $K = \tilde{K}, K^3 = 18$, and $\Theta_{34} = -a = 18\phi^{34}/5$, with similar quantization conditions.

9 Quantization of multiplicities

The question of precisely which chiral multiplicities are allowed for a given model is somewhat subtle. We give a few brief comments here that address some further aspects of which fluxes and corresponding chiral multiplicities may be possible in a broad class of flux compactifications. For convenience here, in parts of the discussion we take $G_{\mathbb{Z}} = G_4 + c_2(X_5)/2 \in$

$H^4(X_5, \mathbb{Z})$ to be an integer class, even when c_2 is not even; when c_2 is not even, fluxes must be suitably shifted by a half-integer class to G_4 . The analysis here expands in particular on related discussions in [34, 39]. Note that aside from the specific examples at the end of this section, most of the discussion of quantization here is relevant for general classes of F-theory models, independent of the specific gauge group and matter structure.

Recall from Eq. (7.31) and Eq. (7.32) the definitions of the lattices $\Lambda_{\text{vert}}, \bar{\Lambda}_{\text{vert}}$. The homology lattice $H_4(X_5, \mathbb{Z})$ has a unimodular intersection pairing. Thus, for any surface S that is a primitive²⁷ element of this lattice, in particular for any primitive surface in $\bar{\Lambda}_{\text{vert}}$, there exists some integer flux $G_{\mathbb{Z}} \in H^4(X_5, \mathbb{Z})$ such that $\int_S G_{\mathbb{Z}} = 1$. This would suggest that chiral multiplicities can always be quantized in arbitrary integer units, and that essentially any model would allow three generations of anomaly-free chiral matter (leaving aside the issue, for the moment, of non-even c_2). There are several reasons, however, why such a flux may not be possible or may not correspond to a physical vacuum of interest. First, it may be the case that a vertical surface $S_{IJ} = D_I \cap D_J \in \Lambda_{\text{vert}}$ is primitive in Λ_{vert} but is an integer multiple of an element of $\bar{\Lambda}_{\text{vert}}$ and $H_4(X_5, \mathbb{Z})$. In particular, a (vertical) matter surface S_r can be primitive in Λ_{vert} but not primitive in $\bar{\Lambda}_{\text{vert}}$; in such a situation, since $S_r = mS'$, with S' primitive in $\bar{\Lambda}_{\text{vert}}$, the associated chiral multiplicities $\chi_r = \int_{S_r} G_{\mathbb{Z}}$ will always be multiples of m , and unit multiplicity, for example, (or multiplicity 3 if $m \neq 3$) is not possible. Second, it is possible that the specific $G_{\mathbb{Z}}$ that is dual to a surface S that is primitive in $\bar{\Lambda}_{\text{vert}}$ and $H^4(X_5, \mathbb{Z})$ breaks Poincaré or gauge invariance by giving a nonzero $\int_{S_{I\alpha}} G_{\mathbb{Z}}$. If neither of the conditions just summarized are the case, then, recalling the decomposition Eq. (7.25), the flux $G_{\mathbb{Z}}$ that is dual to a primitive vertical matter surface S may have a fractional component in the vertical cohomology and a fractional part in the horizontal or remainder cohomology, and satisfy the desired properties. Completely determining which of these scenarios is realized depends on a full understanding of $H_4(X_5, \mathbb{Z})$ and its intersection form. Note also that while in many models the matter surfaces lie in Λ_{vert} , this need not be the case in general; in any specific model, a clear analysis of matter surfaces and/or the relationship between chiral multiplicities and integrated fluxes Θ_{IJ} is needed for precise statements regarding allowed multiplicities. Finally, we must incorporate the possibility of non-even values of c_2 into the preceding discussion. Note that when c_2 is not even, as in many examples discussed in the preceding section, the chiral multiplicities associated with integrating over matter curves are still integral, $\int_S c_2 \in \mathbb{Z}$, in which case the allowed multiplicities are odd multiples of some basic factor.

Because of the orthogonal decomposition (7.25), and the fact that the intersection product on $H_4(X_5, \mathbb{Z})$ is unimodular, the set of possible fluxes $\int_S G_{\mathbb{Z}}$ through vertical surfaces, and hence the set of chiral multiplicities, can be characterized by considering ϕ' in the projection of $H_4(X_5, \mathbb{Z})$ to $\bar{\Lambda}_{\text{vert}}$, which is the dual lattice $\text{dual}(\bar{\Lambda}_{\text{vert}})$ (i.e., the set of points in $H_{2,2}^{\text{vert}}(X_5, \mathbb{C})$ with integer inner product under M_{red} with all points in $\bar{\Lambda}_{\text{vert}}$). When $\bar{\Lambda}_{\text{vert}} = \Lambda_{\text{vert}}$, then

²⁷A lattice element $S \in H_4(X_5, \mathbb{Z})$ is primitive iff there does not exist a distinct non-zero element $S' \in H_4(X_5, \mathbb{Z})$ such that $S = mS'$ for $m \in \mathbb{Z}_{>1}$.

this dual space is characterized by the set of necessary conditions stated in [34], which are that $\int_S(G_4 + c_2(X_5)/2)$ must be integer-valued for any allowed flux G_4 and vertical surface $S \in \Lambda_{\text{vert}}$.²⁸ However, $\bar{\Lambda}_{\text{vert}}$ could contain extra integral points not realized in Λ_{vert} , in which case these necessary conditions would not be sufficient as there would be points in $\text{dual}(\Lambda_{\text{vert}})$ that are not in $\text{dual}(\bar{\Lambda}_{\text{vert}})$ and hence do not correspond to the set of physically-allowed fluxes. Furthermore, fluxes associated with some points in $\text{dual}(\bar{\Lambda}_{\text{vert}})$ may break gauge or Poincaré invariance. The information of Λ_{vert} and M_{red} is not generally sufficient to uniquely determine $\bar{\Lambda}_{\text{vert}}$. For example, the lattice defined by the inner product $\text{diag}(4, 4)$ can alternatively be embedded in a self-dual Euclidean 2D lattice by extending to an overlattice that includes one half of each generator, or can represent the complete integral 2D subspace of the unimodular lattice E_8 along a pair of orthogonal primitive vectors of length 4.

The upshot of this discussion is that to determine the possible chiral multiplicities for a given model, one must consider the possible integer overlattices $\bar{\Lambda}_{\text{vert}}$ of Λ_{vert} ; for each such overlattice the quantization condition is then determined by identifying all elements of the dual space $\text{dual}(\bar{\Lambda}_{\text{vert}})$ that leave Poincaré and gauge invariance unbroken. Determining which is the proper overlattice requires a complete determination of $H_4(X_5, \mathbb{Z})$, which is beyond the scope of this paper but will be addressed in future work. Note also that consistent chiral multiplicities associated with points ϕ_v in $\text{dual}(\bar{\Lambda}_{\text{vert}})$ that are not in $\bar{\Lambda}_{\text{vert}}$ can be allowed only if non-vertical components of flux are turned on. In such cases, the integrality of the D3-brane tadpole from ϕ_v can only be violated when the vertical component of flux is considered; thus, that condition (which was used in [34]) is not actually necessary for an allowed multiplicity, but rather amounts to the condition that the flux ϕ_v lies in an allowed overlattice $\bar{\Lambda}_{\text{vert}}$. Moreover, when flux is quantized properly with $G_{\mathbb{Z}} \in H^4(X_5, \mathbb{Z})$, the D3-brane quantization condition is automatically satisfied. The uncertainty of which overlattice is realized by $\bar{\Lambda}_{\text{vert}}$ also means that unless there is a clear signal such as non-integrality of Eq. (7.38) indicating that $c_2/2$ is not even, there may be some overlattices $\bar{\Lambda}_{\text{vert}}$ that contain $c_2/2$, in which case c_2 is even, and other overlattices that do not, in which case c_2 is not even—this further complicates the issue of precisely determining the flux quantization and associated chiral multiplicities.

As a specific example of the kinds of overlattice conditions that may arise, let us consider the quantization of chiral multiplicities in the simplest model considered above in Section 8.2.2, with base \mathbb{P}^3 , and $\Sigma_2 = \Sigma_3 = -K = 4H, Y = 0$. In this case, M_{red} from Eq. (8.12)

²⁸Note that when c_2 is not even, in principle it is possible that $\int_S(G_4 + c_2/2)$ may be half-integral for some vertical surfaces, although physical consistency dictates that it must be integral for any vertical matter surface, as in the examples studied in the previous section. In such situations, $G_{\mathbb{Z}}$, but not necessarily G , must project to $\text{dual}(\bar{\Lambda}_{\text{vert}})$.

simplifies to (dropping the null directions ϕ^{03}, ϕ^{05} , and moving ϕ^{12} to the second slot)

$$M_{\text{red}} = \begin{pmatrix} 4 & 0 & 1 & 0 & 0 & 0 & 0 \\ 0 & 4 & 1 & -4 & 0 & -4 & 0 \\ 1 & 1 & 0 & 0 & 0 & 0 & 0 \\ 0 & -4 & 0 & 8 & 0 & 0 & -16 \\ 0 & 0 & 0 & 0 & 8 & -4 & -16 \\ 0 & -4 & 0 & 0 & -4 & 8 & 16 \\ 0 & 0 & 0 & -16 & -16 & 16 & 64 \end{pmatrix}. \quad (9.1)$$

If we choose integer fluxes in Λ_{vert} , as discussed in [Section 8.2.2](#), the chiral multiplicity is an integer multiple of 64 through [Eq. \(8.25\)](#). The possible fluxes that preserve Poincaré and gauge invariance are of the form

$$\phi = p/16(1, -1, -4, -3, -2, 1, -5/4). \quad (9.2)$$

When such a flux is allowed, it gives a chiral multiplicity $\Theta_{34} = p$. The flux in [Eq. \(9.2\)](#) is in the dual lattice $\text{dual}(\bar{\Lambda}_{\text{vert}})$ whenever p is integral.

We now consider the issues of even/non-even c_2 and possible overlattices for $\bar{\Lambda}_{\text{vert}}$ in this specific case. First, note that

$$c_2/2 = c' + (0, 0, 0, 0, 0, 0, 1/2), \quad (9.3)$$

where $c' \in \Lambda_{\text{vert}}$. Thus, whether c_2 is even depends upon whether $S_{34}/2 \in \bar{\Lambda}_{\text{vert}}$. Note that [Eq. \(7.38\)](#) is integral in this case, so we cannot rule out the possibility that c_2 is even. Furthermore, there are several overlattices of Λ_{vert} that contain $c_2/2$. There is a maximal overlattice $\Lambda_{\text{over}}^{\text{max}}$ that includes the generators $(S_{01} - S_{12})/2, S_{23}/2, S_{24}/2, S_{25}/2, S_{34}/8$, and which is self-dual. If $\bar{\Lambda}_{\text{vert}} = \Lambda_{\text{over}}^{\text{max}}$ then c_2 is even, the minimum allowed p in [Eq. \(9.2\)](#) is $p = 16$, the quantization is controlled by integer values of a in [Eq. \(8.25\)](#) and the chiral multiplicity must be a multiple of 16. There is another overlattice of Λ_{vert} that contains only the additional vector $c_2/2$. The dual of this overlattice consists of all vectors of the form [Eq. \(9.2\)](#) with even p . If this overlattice is $\bar{\Lambda}_{\text{vert}}$, then the chiral multiplicity must be a multiple of 2, but non-vertical flux must be included for any multiplicity that is not a multiple of 32. Finally, if $\bar{\Lambda}_{\text{vert}} = \Lambda_{\text{vert}}$ then c_2 is odd, since $c_2/2$ is not in $\bar{\Lambda}_{\text{vert}}$. Because $c_2 \in \text{dual}(\Lambda_{\text{vert}})$ in this case, the flux associated with chiral multiplicity is quantized in units of 1, but non-vertical flux must be included for any chiral multiplicity that is not of the form $\chi = 32(2k + 1)$, and, e.g., a model with $\chi = 3$ will appear to violate the D3-brane tadpole integrality condition unless the non-vertical flux is properly included). There are a variety of other possible overlattices, such as other sublattices of $\Lambda_{\text{over}}^{\text{max}}$ that contain Λ_{vert} , some of which contain $c_2/2$ and others of which do not; we do not go through all the possibilities here. Thus, even in this simple case there are many possibilities for $\bar{\Lambda}_{\text{vert}}$, each of which gives distinct quantization conditions when restricted to vertical or more general integral fluxes. It would be interesting to gain further detailed information about $H_4(X_5, \mathbb{Z})$ to determine the precise form of $\bar{\Lambda}_{\text{vert}}$ and definitively determine the precise quantization condition on chiral multiplicities for these models.

10 Conclusions

In this paper we have performed a detailed analysis of the geometry and flux-induced chiral matter of the universal tuned $G_{\text{SM}} = (\text{SU}(3) \times \text{SU}(2) \times \text{U}(1))/\mathbb{Z}_6$ Weierstrass model identified in [2]. This model admits three linearly independent families of chiral matter transforming under the Standard Model gauge group G_{SM} . All three families can be produced by F-theory fluxes, so the observed Standard Model chiral matter structure is realized in a subset of models where one or two discrete parameters are tuned to vanish. Tuning the parameter $Y = 0$ gives the class of “ F_{11} ” models identified and studied in [32–34] and related works.

The analysis of this paper provides a framework for more detailed study of further phenomenological features of these tuned Standard Model-like models, including aspects of Yukawa interactions, chiral and non-chiral spectra, and moduli stabilization. This class of models complements other types of F-theory constructions such as the tuned $\text{SU}(5)$ GUT models [12–15] that have been studied for several decades, or the more recently constructed models that arise from flux breaking of a rigid E_6 or E_7 symmetry [27, 28]. Comparing how these different classes of F-theory Standard Model constructions differ in detailed phenomenology and in frequency in the landscape may provide insights into what features of beyond the Standard Model physics are correlated with the most typical or natural realizations of the Standard Model in F-theory.

While in this paper we have focused on the specific class of models with tuned gauge group G_{SM} , we have also developed here further the theoretical toolkit for analyzing the geometric structure and chiral matter content of broad classes of F-theory compactifications, extending the framework developed in [39]. In particular, we have extended the analysis of the middle intersection form on vertical cohomology to include theories with a $\text{U}(1)$ factor, which complicates the structure of the matrix M_{red} substantially, and we have given a more thorough analysis of quantization questions related to the multiplicity of chiral matter and allowed fluxes for large classes of F-theory models. One interesting aspect of this is that in the particular class of models studied here we were able to completely solve the flux constrained equations associated with Poincaré and gauge symmetries, although part of the solution was implicit. It would be interesting to investigate whether this kind of solution is possible for more general models with $\text{U}(1)$ gauge factors. Regarding the quantization of chiral multiplicities, the analysis here highlights the importance of attaining a full understanding of the structure of $H_4(X_5, \mathbb{Z})$ for F-theory models of interest.

Acknowledgments

We would like to thank Mboyo Esole, Manki Kim, Shing Yan Li, Nikhil Raghuram, and Timo Weigand for helpful discussions. This work was supported by DOE grant DE-SC00012567. AT is also supported by DOE (HEP) Award DE-SC001352 and the Tushar Shah and Sara Zion Fellowship. WT would like to thank the Aspen Center for Physics (ACP) for hospitality during part of this work. The authors would all like to thank the Witwatersrand (Wits) rural

facility and the MIT International Science and Technology Initiatives (MISTI) MIT–Africa–Imperial College seed fund program for hospitality and support during some stages of this project.

A Converting between the geometric and gauge bases

Let $X \rightarrow B$ denote a smooth CY manifold that is elliptically fibered over a smooth base B . There is a natural relationship between divisors $\hat{D}_{\bar{I}} \subset X$ and gauge fields appearing in the low-energy description of M-theory compactified on X . In particular, the divisors $\hat{D}_{\bar{I}}$ are Poincaré dual to harmonic $(1, 1)$ -forms $\omega_{\bar{I}}$ that appear in a local expansion of the M-theory 3-form C_3 in the vicinity of the 7-brane loci, i.e., $C_3 = A^{\bar{I}} \wedge \omega_{\bar{I}} + \dots$. Thus, to each gauge field $A^{\bar{I}}$, there corresponds a particular choice of divisor $\hat{D}_{\bar{I}}$, and the gauge charges $q_{\bar{I}}$ of BPS particles corresponding to M2 branes wrapping holomorphic curves $C \subset X$ can be computed in terms of their intersection product with $\hat{D}_{\bar{I}}$, i.e., $q_{\bar{I}} = \int_C \omega_{\bar{I}} = \hat{D}_{\bar{I}} \cdot C$. This suggests that the low-energy gauge-theoretic description of M-theory compactified on X defines a canonical basis of divisors $\hat{D}_{\bar{I}}$ —we refer to this basis as the “gauge” basis of divisors.

Despite the fact that the gauge basis is natural from the point of view of the low-energy effective theory, in practice, it tends to be simpler to expand divisors of X in terms of the “geometric” basis \hat{D}_I , where $I = 0$ corresponds to a (non-unique) choice of zero section and $I = a$ corresponds to a generator of the Mordell–Weil group of sections. As we describe below, the divisors \hat{D}_0, \hat{D}_a are linearly related to the divisors $\hat{D}_{\bar{0}}, \hat{D}_{\bar{a}}$, which correspond (respectively) to Kaluza–Klein $U(1)_{\text{KK}}$ and $U(1)$ factors belonging to the free abelian part of the F-theory gauge group.

In this Appendix, we describe how to convert between the gauge and geometric bases. The change of basis from the geometric basis to the gauge basis is given by (see Appendix B in [39])

$$\hat{D}_{\bar{I}} = \sigma_{\bar{I}}^J \hat{D}_J \tag{A.1}$$

where in the case of the $(\text{SU}(3) \times \text{SU}(2) \times \text{U}(1))/\mathbb{Z}_6$ model, the matrix elements $\sigma_{\bar{I}}^J$ are:

$$\begin{aligned} \sigma_{\bar{0}}^I &= (1, 0, -\frac{1}{2}K^\alpha, 0, 0, 0)^I \\ \sigma_{\bar{1}}^I &= (-1, 1, K^\alpha - Y^\alpha, \frac{1}{2}, \frac{1}{3}, \frac{2}{3})^I \\ \sigma_{\bar{J}}^I &= \delta_{\bar{J}}^I, \quad \bar{J} \neq 0, 1. \end{aligned} \tag{A.2}$$

Note that $\hat{D}_{\bar{1}} = \sigma_{\bar{1}}^I \hat{D}_I$ is the image of the Shioda map described in [61]. Using

$$\begin{aligned} (\sigma^{-1})_{\bar{0}}^{\bar{I}} &= (1, 0, \frac{1}{2}K^\alpha, 0, 0, 0)^{\bar{I}} \\ (\sigma^{-1})_{\bar{1}}^{\bar{I}} &= (1, 1, -\frac{1}{2}K^\alpha + Y^\alpha, -\frac{1}{2}, -\frac{1}{3}, -\frac{2}{3})^{\bar{I}} \\ (\sigma^{-1})_{\bar{J}}^{\bar{I}} &= \delta_{\bar{J}}^{\bar{I}} \quad \text{for } J \neq 0, 1, \end{aligned} \tag{A.3}$$

one can invert the above linear transformation:

$$(\sigma^{-1})^{\bar{I}}_J \sigma^{\bar{K}}_I = \delta^{\bar{K}}_J, \quad \sigma^J_{\bar{K}} (\sigma^{-1})^{\bar{I}}_J = \delta^{\bar{I}}_{\bar{K}}. \quad (\text{A.4})$$

Thus, e.g., the change of basis from geometric fluxes Θ_{IJ} to gauge basis fluxes $\Theta_{\bar{I}\bar{J}}$ relevant for computing the image of the nullspace of M in the constrained sublattice $\Lambda_C \subset \Lambda$ is

$$\begin{aligned} \Theta_{\bar{1}I} &= \sigma^J_{\bar{1}} \Theta_{JI} = -\Theta_{0I} + \Theta_{1I} + \frac{\Theta_{3I}}{2} + \frac{\Theta_{4I}}{3} + \frac{2\Theta_{5I}}{3}, \quad I \neq 1 \\ \Theta_{\bar{1}\bar{1}} &= \sigma^J_{\bar{1}} \sigma^{\bar{K}}_1 \Theta_{JK} = \Theta_{00} - 2\Theta_{01} - \Theta_{03} + \Theta_{11} + \Theta_{13} + \frac{2\Theta_{14}}{3} + \frac{4\Theta_{15}}{3} \\ &\quad + \frac{\Theta_{33}}{4} + \frac{\Theta_{34}}{3} + \frac{2\Theta_{35}}{3} + \frac{\Theta_{44}}{9} + \frac{4\Theta_{45}}{9} + \frac{4\Theta_{55}}{9} - \frac{2\Theta_{04}}{3} - \frac{4\Theta_{05}}{3}. \end{aligned} \quad (\text{A.5})$$

Note that $\Theta_{I\bar{0}} = \Theta_{I0}$ on the constrained sublattice, hence one can freely exchange the indices 0 and $\bar{0}$.

References

- [1] M. Cvetič, J. Halverson, G. Shiu and W. Taylor, *Snowmass White Paper: String Theory and Particle Physics*, [2204.01742](#).
- [2] N. Raghuram, W. Taylor and A. P. Turner, *General F-theory models with tuned $(\text{SU}(3) \times \text{SU}(2) \times \text{U}(1))/\mathbb{Z}_6$ symmetry*, *JHEP* **04** (2020) 008 [[1912.10991](#)].
- [3] C. Vafa, *The String landscape and the swampland*, [[hep-th/0509212](#)].
- [4] H. Ooguri and C. Vafa, *On the Geometry of the String Landscape and the Swampland*, *Nucl. Phys.* **B766** (2007) 21 [[hep-th/0605264](#)].
- [5] C. Vafa, *Evidence for F theory*, *Nucl. Phys.* **B469** (1996) 403 [[hep-th/9602022](#)].
- [6] D. R. Morrison and C. Vafa, *Compactifications of F theory on Calabi–Yau threefolds — I*, *Nucl. Phys.* **B473** (1996) 74 [[hep-th/9602114](#)].
- [7] D. R. Morrison and C. Vafa, *Compactifications of F theory on Calabi–Yau threefolds — II*, *Nucl. Phys.* **B476** (1996) 437 [[hep-th/9603161](#)].
- [8] W. Taylor and Y.-N. Wang, *A Monte Carlo exploration of threefold base geometries for 4d F-theory vacua*, *JHEP* **01** (2016) 137 [[1510.04978](#)].
- [9] J. Halverson, C. Long and B. Sung, *Algorithmic universality in F-theory compactifications*, *Phys. Rev.* **D96** (2017) 126006 [[1706.02299](#)].
- [10] W. Taylor and Y.-N. Wang, *Scanning the skeleton of the 4D F-theory landscape*, *JHEP* **01** (2018) 111 [[1710.11235](#)].
- [11] W. Taylor and Y.-N. Wang, *The F-theory geometry with most flux vacua*, *JHEP* **12** (2015) 164 [[1511.03209](#)].
- [12] R. Donagi and M. Wijnholt, *Model Building with F-Theory*, *Adv. Theor. Math. Phys.* **15** (2011) 1237 [[0802.2969](#)].
- [13] C. Beasley, J. J. Heckman and C. Vafa, *GUTs and Exceptional Branes in F-theory - I*, *JHEP* **01** (2009) 058 [[0802.3391](#)].

- [14] C. Beasley, J. J. Heckman and C. Vafa, *GUTs and Exceptional Branes in F-theory - II: Experimental Predictions*, *JHEP* **01** (2009) 059 [[0806.0102](#)].
- [15] R. Donagi and M. Wijnholt, *Breaking GUT Groups in F-Theory*, *Adv. Theor. Math. Phys.* **15** (2011) 1523 [[0808.2223](#)].
- [16] C.-M. Chen and Y.-C. Chung, *A Note on Local GUT Models in F-Theory*, *Nucl. Phys. B* **824** (2010) 273 [[0903.3009](#)].
- [17] J. J. Heckman, A. Tavanfar and C. Vafa, *The Point of $E(8)$ in F-theory GUTs*, *JHEP* **08** (2010) 040 [[0906.0581](#)].
- [18] R. Blumenhagen, T. W. Grimm, B. Jurke and T. Weigand, *Global F-theory GUTs*, *Nucl. Phys. B* **829** (2010) 325 [[0908.1784](#)].
- [19] E. Dudas and E. Palti, *Froggatt-Nielsen models from $E(8)$ in F-theory GUTs*, *JHEP* **01** (2010) 127 [[0912.0853](#)].
- [20] T. W. Grimm, S. Krause and T. Weigand, *F-Theory GUT Vacua on Compact Calabi-Yau Fourfolds*, *JHEP* **07** (2010) 037 [[0912.3524](#)].
- [21] J. Marsano, N. Saulina and S. Schafer-Nameki, *Compact F-theory GUTs with $U(1)$ (PQ)*, *JHEP* **04** (2010) 095 [[0912.0272](#)].
- [22] G. K. Leontaris, *Aspects of F-Theory GUTs*, *PoS CORFU2011* (2011) 095 [[1203.6277](#)].
- [23] J. C. Callaghan and S. F. King, *$E6$ Models from F-theory*, *JHEP* **04** (2013) 034 [[1210.6913](#)].
- [24] C. Mayrhofer, E. Palti and T. Weigand, *Hypercharge Flux in IIB and F-theory: Anomalies and Gauge Coupling Unification*, *JHEP* **09** (2013) 082 [[1303.3589](#)].
- [25] J. C. Callaghan, S. F. King and G. K. Leontaris, *Gauge coupling unification in E_6 F-theory GUTs with matter and bulk exotics from flux breaking*, *JHEP* **12** (2013) 037 [[1307.4593](#)].
- [26] A. P. Braun, A. Collinucci and R. Valandro, *Hypercharge flux in F-theory and the stable Sen limit*, *JHEP* **07** (2014) 121 [[1402.4096](#)].
- [27] S. Y. Li and W. Taylor, *Natural F-theory constructions of Standard Model structure from E_7 flux breaking*, [2112.03947](#).
- [28] S. Y. Li and W. Taylor, *Gauge symmetry breaking with fluxes and natural Standard Model structure from exceptional GUTs in F-theory*, [2207.14319](#).
- [29] J. J. Heckman, *Particle Physics Implications of F-theory*, *Ann. Rev. Nucl. Part. Sci.* **60** (2010) 237 [[1001.0577](#)].
- [30] A. Grassi, J. Halverson, J. Shaneson and W. Taylor, *Non-Higgsable QCD and the Standard Model Spectrum in F-theory*, *JHEP* **01** (2015) 086 [[1409.8295](#)].
- [31] W. Taylor and A. P. Turner, *Generic matter representations in 6D supergravity theories*, *JHEP* **05** (2019) 081 [[1901.02012](#)].
- [32] D. Klevers, D. K. Mayorga Pena, P.-K. Oehlmann, H. Piragua and J. Reuter, *F-Theory on all Toric Hypersurface Fibrations and its Higgs Branches*, *JHEP* **01** (2015) 142 [[1408.4808](#)].
- [33] M. Cvetič, D. Klevers, D. K. M. Peña, P.-K. Oehlmann and J. Reuter, *Three-Family Particle Physics Models from Global F-theory Compactifications*, *JHEP* **08** (2015) 087 [[1503.02068](#)].

- [34] M. Cvetič, J. Halverson, L. Lin, M. Liu and J. Tian, *Quadrillion F-Theory Compactifications with the Exact Chiral Spectrum of the Standard Model*, *Phys. Rev. Lett.* **123** (2019) 101601 [[1903.00009](#)].
- [35] M. Bies, C. Mayrhofer, C. Pehle and T. Weigand, *Chow groups, Deligne cohomology and massless matter in F-theory*, [1402.5144](#).
- [36] M. Bies, M. Cvetič, R. Donagi, M. Liu and M. Ong, *Root Bundles and Towards Exact Matter Spectra of F-theory MSSMs*, [2102.10115](#).
- [37] M. Bies, M. Cvetič and M. Liu, *Statistics of Limit Root Bundles Relevant for Exact Matter Spectra of F-Theory MSSMs*, [2104.08297](#).
- [38] M. Bies, M. Cvetič, R. Donagi and M. Ong, *Brill-Noether-general Limit Root Bundles: Absence of vector-like Exotics in F-theory Standard Models*, [2205.00008](#).
- [39] P. Jefferson, W. Taylor and A. P. Turner, *Chiral matter multiplicities and resolution-independent structure in 4D F-theory models*, [2108.07810](#).
- [40] T. W. Grimm, A. Kapfer and J. Keitel, *Effective action of 6D F-Theory with U(1) factors: Rational sections make Chern-Simons terms jump*, *JHEP* **07** (2013) 115 [[1305.1929](#)].
- [41] C. Lawrie, S. Schafer-Nameki and J.-M. Wong, *F-theory and All Things Rational: Surveying U(1) Symmetries with Rational Sections*, *JHEP* **09** (2015) 144 [[1504.05593](#)].
- [42] T. Weigand, *TASI Lectures on F-theory*, [[1806.01854](#)].
- [43] J. Marsano and S. Schäfer-Nameki, *Yukawas, g-flux, and spectral covers from resolved calabi-yau's*, *Journal of High Energy Physics* **2011** (2011) [[1108.1794](#)].
- [44] M. Kuntzler and S. Schafer-Nameki, *G-flux and Spectral Divisors*, *JHEP* **11** (2012) 025 [[1205.5688](#)].
- [45] M. Cvetič, A. Grassi, D. Klevers and H. Piragua, *Chiral four-dimensional f-theory compactifications with su(5) and multiple u(1)-factors*, *Journal of High Energy Physics* **2014** (2014) [[1306.3987](#)].
- [46] L. Lin and T. Weigand, *G₄-flux and standard model vacua in F-theory*, *Nucl. Phys.* **B913** (2016) 209 [[1604.04292](#)].
- [47] A. Grassi, J. Halverson, C. Long, J. L. Shaneson and J. Tian, *Non-simply-laced Symmetry Algebras in F-theory on Singular Spaces*, *JHEP* **09** (2018) 129 [[1805.06949](#)].
- [48] A. Grassi, J. Halverson, C. Long, J. L. Shaneson, B. Sung and J. Tian, *6D Anomaly-Free Matter Spectrum in F-theory on Singular Spaces*, [2110.06943](#).
- [49] S. Katz and W. Taylor, *Dimensional Reduction of B-Fields in F-theory*, [2204.13146](#).
- [50] M. Bies, C. Mayrhofer and T. Weigand, *Algebraic cycles and local anomalies in f-theory*, *Journal of High Energy Physics* **2017** (2017) [[1706.08528](#)].
- [51] P. Corvilain, T. W. Grimm and D. Regalado, *Chiral anomalies on a circle and their cancellation in F-theory*, *JHEP* **04** (2018) 020 [[1710.07626](#)].
- [52] P. Cheng, R. Minasian and S. Theisen, *Anomalies as Obstructions: from Dimensional Lifts to Swampland*, [2106.14912](#).

- [53] N. Raghuram, *Abelian F-theory Models with Charge-3 and Charge-4 Matter*, *JHEP* **05** (2018) 050 [[1711.03210](#)].
- [54] M. Cvetič, D. Klevers and H. Piragua, *F-Theory Compactifications with Multiple U(1)-Factors: Constructing Elliptic Fibrations with Rational Sections*, *JHEP* **06** (2013) 067 [[1303.6970](#)].
- [55] M. Cvetič, D. Klevers, H. Piragua and W. Taylor, *General U(1) x U(1) F-theory compactifications and beyond: geometry of unHiggsings and novel matter structure*, *JHEP* **11** (2015) 204 [[1507.05954](#)].
- [56] P. S. Aspinwall, S. H. Katz and D. R. Morrison, *Lie groups, Calabi-Yau threefolds, and F theory*, *Adv. Theor. Math. Phys.* **4** (2000) 95 [[hep-th/0002012](#)].
- [57] P. S. Aspinwall and D. R. Morrison, *Nonsimply connected gauge groups and rational points on elliptic curves*, *JHEP* **07** (1998) 012 [[hep-th/9805206](#)].
- [58] T. W. Grimm and T. Weigand, *On Abelian Gauge Symmetries and Proton Decay in Global F-theory GUTs*, *Phys. Rev. D* **82** (2010) 086009 [[1006.0226](#)].
- [59] S. Katz, D. R. Morrison, S. Schafer-Nameki and J. Sully, *Tate’s algorithm and F-theory*, *JHEP* **08** (2011) 094 [[1106.3854](#)].
- [60] M. Cvetič, T. W. Grimm and D. Klevers, *Anomaly Cancellation And Abelian Gauge Symmetries In F-theory*, *JHEP* **02** (2013) 101 [[1210.6034](#)].
- [61] D. R. Morrison and D. S. Park, *F-Theory and the Mordell–Weil Group of Elliptically-Fibered Calabi–Yau Threefolds*, *JHEP* **10** (2012) 128 [[1208.2695](#)].
- [62] M. Esole, P. Jefferson and M. J. Kang, *Euler Characteristics of Crepant Resolutions of Weierstrass Models*, *Commun. Math. Phys.* **371** (2019) 99 [[1703.00905](#)].
- [63] P. Jefferson and A. P. Turner, *Generating functions for intersection products of divisors in resolved F-theory models*, [2206.11527](#).
- [64] E. Witten, *On flux quantization in M theory and the effective action*, *J. Geom. Phys.* **22** (1997) 1 [[hep-th/9609122](#)].
- [65] B. R. Greene, D. R. Morrison and M. Plesser, *Mirror manifolds in higher dimension*, *Commun. Math. Phys.* **173** (1995) 559 [[hep-th/9402119](#)].
- [66] A. P. Braun and T. Watari, *The Vertical, the Horizontal and the Rest: anatomy of the middle cohomology of Calabi-Yau fourfolds and F-theory applications*, *JHEP* **01** (2015) 047 [[1408.6167](#)].
- [67] K. Dasgupta, G. Rajesh and S. Sethi, *M theory, orientifolds and G - flux*, *JHEP* **08** (1999) 023 [[hep-th/9908088](#)].
- [68] A. Collinucci and R. Savelli, *On Flux Quantization in F-Theory*, *JHEP* **02** (2012) 015 [[1011.6388](#)].
- [69] T. W. Grimm and H. Hayashi, *F-theory fluxes, Chirality and Chern-Simons theories*, *JHEP* **03** (2012) 027 [[1111.1232](#)].
- [70] T. W. Grimm and R. Savelli, *Gravitational Instantons and Fluxes from M/F-theory on Calabi-Yau fourfolds*, *Phys. Rev. D* **85** (2012) 026003 [[1109.3191](#)].

- [71] N. Raghuram, W. Taylor and A. P. Turner, *Automatic enhancement in 6D supergravity and F-theory models*, *JHEP* **07** (2021) 048 [[2012.01437](#)].